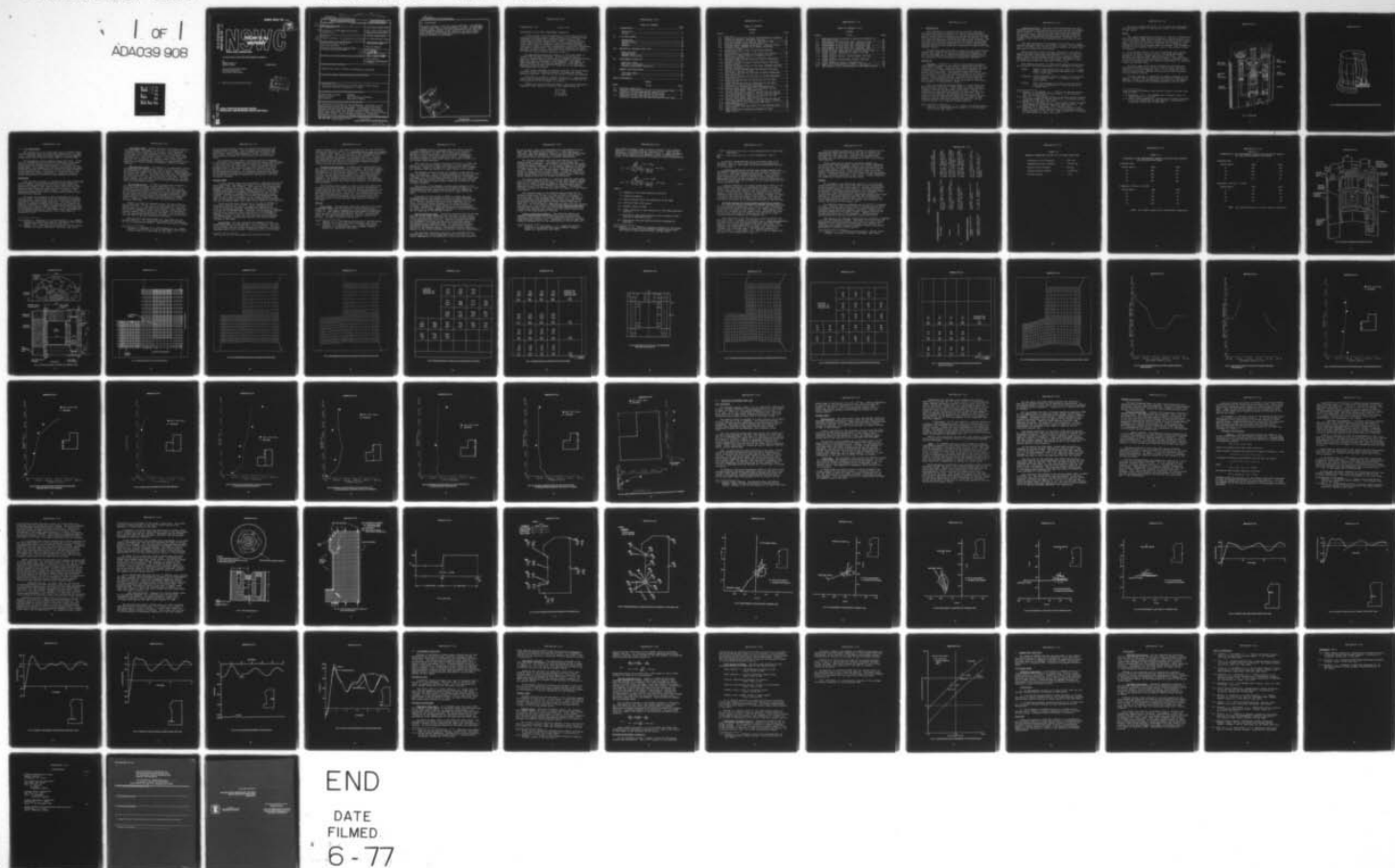


AD-A039 908

NAVAL SURFACE WEAPONS CENTER WHITE OAK LAB SILVER SP--ETC F/G 11/2
EVALUATION OF GCFR PCRV CONTAINMENT CAPABILITY.(U)
APR 77 J G CONNOR, M E GILTRUD
NSWC/WOI/TD-77-42

UNCLASSIFIED

1 OF 1
AD-A039 908



END

DATE
FILMED
6-77

NSWC/WOL/TR 77-42

AD A 039908
NSWC/WOL/TR 77-42

NSWC

TECHNICAL REPORT

WHITE OAK LABORATORY

EVALUATION OF GCFR PCRV CONTAINMENT CAPABILITY

BY
Joseph G. Connor, Jr.
Michael E. Giltrud

15 APRIL 1977

NAVAL SURFACE WEAPONS CENTER
WHITE OAK LABORATORY
SILVER SPRING, Maryland 20910

- Approved for public release; distribution unlimited.



NAVAL SURFACE WEAPONS CENTER
WHITE OAK, SILVER SPRING, MARYLAND 20910

DDC FILE COPY

UNCLASSIFIED

SECURITY CLASSIFICATION OF THIS PAGE (When Data Entered)

REPORT DOCUMENTATION PAGE		READ INSTRUCTIONS BEFORE COMPLETING FORM
1. REPORT NUMBER 14 NSWC/WOL/TR-77-42 ✓	2. GOVT ACCESSION NO.	3. RECIPIENT'S CATALOG NUMBER
4. TITLE (and Subtitle) 6 Evaluation of GCFR PCRV Containment Capability.		5. TYPE OF REPORT & PERIOD COVERED Final: July 1974-June '76
7. AUTHOR(s) 10 Joseph G./Connor, Jr. & Michael E./Giltrud		6. PERFORMING ORG. REPORT NUMBER
9. PERFORMING ORGANIZATION NAME AND ADDRESS Naval Surface Weapons Center ✓ White Oak Laboratory White Oak, Silver Spring, Maryland 20910		8. CONTRACT OR GRANT NUMBER(s) AT (49-24)-0103, Mod 16
11. CONTROLLING OFFICE NAME AND ADDRESS	10. PROGRAM ELEMENT, PROJECT, TASK AREA & WORK UNIT NUMBERS ERDA; 0; 0; WR6107	
14. MONITORING AGENCY NAME & ADDRESS (if different from Controlling Office)	12. REPORT DATE 11 15 Apr 1977	
	13. NUMBER OF PAGES 79 12850	
16. DISTRIBUTION STATEMENT (of this Report) Approved for public release; distribution unlimited	15. SECURITY CLASS. (of this report) Unclassified	
	15a. DECLASSIFICATION/DOWNGRADING SCHEDULE	
17. DISTRIBUTION STATEMENT (of the abstract entered in Block 20, if different from Report)		
18. SUPPLEMENTARY NOTES This report was sponsored by the Special Projects Branch, Nuclear Regulatory Commission, Washington, D. C. 20555.		
19. KEY WORDS (Continue on reverse side if necessary and identify by block number) Prestressed concrete NASTRAN Reactor Vessel Core Disruptive Accident Containment Explosive Loading		
20. ABSTRACT (Continue on reverse side if necessary and identify by block number) An analytical evaluation of the containment capability of the Prestressed Concrete Reactor Vessel for the Gas Cooled Fast Breeder Reactor has been conducted. Displacement and stress predictions were made from NASTRAN finite element calculations which were consistent with static hydraulic loading tests of 1/20 scale PCRV models. This favorable comparison strengthens confidence in the results of NASTRAN calculations for static and		

DD FORM 1 JAN 73 1473

EDITION OF 1 NOV 65 IS OBSOLETE
S/N 0102-014-6601

UNCLASSIFIED

SECURITY CLASSIFICATION OF THIS PAGE (When Data Entered)

391596

UNCLASSIFIED

SECURITY CLASSIFICATION OF THIS PAGE(When Data Entered)

20. (Continued)

transient loading of the full scale GCFR-PCRV. The NASTRAN results imply that a Core Disassembly Accident of 4000 MWsec thermal energy release should be contained by the PCRV with only moderate cracking at the inside of the lower haunch. This value should be substantiated by experiment before further analysis is performed.

SECTION 10	White Section	<input checked="" type="checkbox"/>
100	Blue Section	<input type="checkbox"/>
101	Red Section	<input type="checkbox"/>
102	Green Section	<input type="checkbox"/>
103	Yellow Section	<input type="checkbox"/>
104	Orange Section	<input type="checkbox"/>
105	Purple Section	<input type="checkbox"/>
106	Brown Section	<input type="checkbox"/>
107	Pink Section	<input type="checkbox"/>
108	Grey Section	<input type="checkbox"/>
109	Black Section	<input type="checkbox"/>
110	White Section	<input type="checkbox"/>
111	Blue Section	<input type="checkbox"/>
112	Red Section	<input type="checkbox"/>
113	Green Section	<input type="checkbox"/>
114	Yellow Section	<input type="checkbox"/>
115	Orange Section	<input type="checkbox"/>
116	Purple Section	<input type="checkbox"/>
117	Brown Section	<input type="checkbox"/>
118	Pink Section	<input type="checkbox"/>
119	Grey Section	<input type="checkbox"/>
120	Black Section	<input type="checkbox"/>
121	White Section	<input type="checkbox"/>
122	Blue Section	<input type="checkbox"/>
123	Red Section	<input type="checkbox"/>
124	Green Section	<input type="checkbox"/>
125	Yellow Section	<input type="checkbox"/>
126	Orange Section	<input type="checkbox"/>
127	Purple Section	<input type="checkbox"/>
128	Brown Section	<input type="checkbox"/>
129	Pink Section	<input type="checkbox"/>
130	Grey Section	<input type="checkbox"/>
131	Black Section	<input type="checkbox"/>
132	White Section	<input type="checkbox"/>
133	Blue Section	<input type="checkbox"/>
134	Red Section	<input type="checkbox"/>
135	Green Section	<input type="checkbox"/>
136	Yellow Section	<input type="checkbox"/>
137	Orange Section	<input type="checkbox"/>
138	Purple Section	<input type="checkbox"/>
139	Brown Section	<input type="checkbox"/>
140	Pink Section	<input type="checkbox"/>
141	Grey Section	<input type="checkbox"/>
142	Black Section	<input type="checkbox"/>
143	White Section	<input type="checkbox"/>
144	Blue Section	<input type="checkbox"/>
145	Red Section	<input type="checkbox"/>
146	Green Section	<input type="checkbox"/>
147	Yellow Section	<input type="checkbox"/>
148	Orange Section	<input type="checkbox"/>
149	Purple Section	<input type="checkbox"/>
150	Brown Section	<input type="checkbox"/>
151	Pink Section	<input type="checkbox"/>
152	Grey Section	<input type="checkbox"/>
153	Black Section	<input type="checkbox"/>
154	White Section	<input type="checkbox"/>
155	Blue Section	<input type="checkbox"/>
156	Red Section	<input type="checkbox"/>
157	Green Section	<input type="checkbox"/>
158	Yellow Section	<input type="checkbox"/>
159	Orange Section	<input type="checkbox"/>
160	Purple Section	<input type="checkbox"/>
161	Brown Section	<input type="checkbox"/>
162	Pink Section	<input type="checkbox"/>
163	Grey Section	<input type="checkbox"/>
164	Black Section	<input type="checkbox"/>
165	White Section	<input type="checkbox"/>
166	Blue Section	<input type="checkbox"/>
167	Red Section	<input type="checkbox"/>
168	Green Section	<input type="checkbox"/>
169	Yellow Section	<input type="checkbox"/>
170	Orange Section	<input type="checkbox"/>
171	Purple Section	<input type="checkbox"/>
172	Brown Section	<input type="checkbox"/>
173	Pink Section	<input type="checkbox"/>
174	Grey Section	<input type="checkbox"/>
175	Black Section	<input type="checkbox"/>
176	White Section	<input type="checkbox"/>
177	Blue Section	<input type="checkbox"/>
178	Red Section	<input type="checkbox"/>
179	Green Section	<input type="checkbox"/>
180	Yellow Section	<input type="checkbox"/>
181	Orange Section	<input type="checkbox"/>
182	Purple Section	<input type="checkbox"/>
183	Brown Section	<input type="checkbox"/>
184	Pink Section	<input type="checkbox"/>
185	Grey Section	<input type="checkbox"/>
186	Black Section	<input type="checkbox"/>
187	White Section	<input type="checkbox"/>
188	Blue Section	<input type="checkbox"/>
189	Red Section	<input type="checkbox"/>
190	Green Section	<input type="checkbox"/>
191	Yellow Section	<input type="checkbox"/>
192	Orange Section	<input type="checkbox"/>
193	Purple Section	<input type="checkbox"/>
194	Brown Section	<input type="checkbox"/>
195	Pink Section	<input type="checkbox"/>
196	Grey Section	<input type="checkbox"/>
197	Black Section	<input type="checkbox"/>
198	White Section	<input type="checkbox"/>
199	Blue Section	<input type="checkbox"/>
200	Red Section	<input type="checkbox"/>
201	Green Section	<input type="checkbox"/>
202	Yellow Section	<input type="checkbox"/>
203	Orange Section	<input type="checkbox"/>
204	Purple Section	<input type="checkbox"/>
205	Brown Section	<input type="checkbox"/>
206	Pink Section	<input type="checkbox"/>
207	Grey Section	<input type="checkbox"/>
208	Black Section	<input type="checkbox"/>
209	White Section	<input type="checkbox"/>
210	Blue Section	<input type="checkbox"/>
211	Red Section	<input type="checkbox"/>
212	Green Section	<input type="checkbox"/>
213	Yellow Section	<input type="checkbox"/>
214	Orange Section	<input type="checkbox"/>
215	Purple Section	<input type="checkbox"/>
216	Brown Section	<input type="checkbox"/>
217	Pink Section	<input type="checkbox"/>
218	Grey Section	<input type="checkbox"/>
219	Black Section	<input type="checkbox"/>
220	White Section	<input type="checkbox"/>
221	Blue Section	<input type="checkbox"/>
222	Red Section	<input type="checkbox"/>
223	Green Section	<input type="checkbox"/>
224	Yellow Section	<input type="checkbox"/>
225	Orange Section	<input type="checkbox"/>
226	Purple Section	<input type="checkbox"/>
227	Brown Section	<input type="checkbox"/>
228	Pink Section	<input type="checkbox"/>
229	Grey Section	<input type="checkbox"/>
230	Black Section	<input type="checkbox"/>
231	White Section	<input type="checkbox"/>
232	Blue Section	<input type="checkbox"/>
233	Red Section	<input type="checkbox"/>
234	Green Section	<input type="checkbox"/>
235	Yellow Section	<input type="checkbox"/>
236	Orange Section	<input type="checkbox"/>
237	Purple Section	<input type="checkbox"/>
238	Brown Section	<input type="checkbox"/>
239	Pink Section	<input type="checkbox"/>
240	Grey Section	<input type="checkbox"/>
241	Black Section	<input type="checkbox"/>
242	White Section	<input type="checkbox"/>
243	Blue Section	<input type="checkbox"/>
244	Red Section	<input type="checkbox"/>
245	Green Section	<input type="checkbox"/>
246	Yellow Section	<input type="checkbox"/>
247	Orange Section	<input type="checkbox"/>
248	Purple Section	<input type="checkbox"/>
249	Brown Section	<input type="checkbox"/>
250	Pink Section	<input type="checkbox"/>
251	Grey Section	<input type="checkbox"/>
252	Black Section	<input type="checkbox"/>
253	White Section	<input type="checkbox"/>
254	Blue Section	<input type="checkbox"/>
255	Red Section	<input type="checkbox"/>
256	Green Section	<input type="checkbox"/>
257	Yellow Section	<input type="checkbox"/>
258	Orange Section	<input type="checkbox"/>
259	Purple Section	<input type="checkbox"/>
260	Brown Section	<input type="checkbox"/>
261	Pink Section	<input type="checkbox"/>
262	Grey Section	<input type="checkbox"/>
263	Black Section	<input type="checkbox"/>
264	White Section	<input type="checkbox"/>
265	Blue Section	<input type="checkbox"/>
266	Red Section	<input type="checkbox"/>
267	Green Section	<input type="checkbox"/>
268	Yellow Section	<input type="checkbox"/>
269	Orange Section	<input type="checkbox"/>
270	Purple Section	<input type="checkbox"/>
271	Brown Section	<input type="checkbox"/>
272	Pink Section	<input type="checkbox"/>
273	Grey Section	<input type="checkbox"/>
274	Black Section	<input type="checkbox"/>
275	White Section	<input type="checkbox"/>
276	Blue Section	<input type="checkbox"/>
277	Red Section	<input type="checkbox"/>
278	Green Section	<input type="checkbox"/>
279	Yellow Section	<input type="checkbox"/>
280	Orange Section	<input type="checkbox"/>
281	Purple Section	<input type="checkbox"/>
282	Brown Section	<input type="checkbox"/>
283	Pink Section	<input type="checkbox"/>
284	Grey Section	<input type="checkbox"/>
285	Black Section	<input type="checkbox"/>
286	White Section	<input type="checkbox"/>
287	Blue Section	<input type="checkbox"/>
288	Red Section	<input type="checkbox"/>
289	Green Section	<input type="checkbox"/>
290	Yellow Section	<input type="checkbox"/>
291	Orange Section	<input type="checkbox"/>
292	Purple Section	<input type="checkbox"/>
293	Brown Section	<input type="checkbox"/>
294	Pink Section	<input type="checkbox"/>
295	Grey Section	<input type="checkbox"/>
296	Black Section	<input type="checkbox"/>
297	White Section	<input type="checkbox"/>
298	Blue Section	<input type="checkbox"/>
299	Red Section	<input type="checkbox"/>
300	Green Section	<input type="checkbox"/>
301	Yellow Section	<input type="checkbox"/>
302	Orange Section	<input type="checkbox"/>
303	Purple Section	<input type="checkbox"/>
304	Brown Section	<input type="checkbox"/>
305	Pink Section	<input type="checkbox"/>
306	Grey Section	<input type="checkbox"/>
307	Black Section	<input type="checkbox"/>
308	White Section	<input type="checkbox"/>
309	Blue Section	<input type="checkbox"/>
310	Red Section	<input type="checkbox"/>
311	Green Section	<input type="checkbox"/>
312	Yellow Section	<input type="checkbox"/>
313	Orange Section	<input type="checkbox"/>
314	Purple Section	<input type="checkbox"/>
315	Brown Section	<input type="checkbox"/>
316	Pink Section	<input type="checkbox"/>
317	Grey Section	<input type="checkbox"/>
318	Black Section	<input type="checkbox"/>
319	White Section	<input type="checkbox"/>
320	Blue Section	<input type="checkbox"/>
321	Red Section	<input type="checkbox"/>
322	Green Section	<input type="checkbox"/>
323	Yellow Section	<input type="checkbox"/>
324	Orange Section	<input type="checkbox"/>
325	Purple Section	<input type="checkbox"/>
326	Brown Section	<input type="checkbox"/>
327	Pink Section	<input type="checkbox"/>
328	Grey Section	<input type="checkbox"/>
329	Black Section	<input type="checkbox"/>
330	White Section	<input type="checkbox"/>
331	Blue Section	<input type="checkbox"/>
332	Red Section	<input type="checkbox"/>
333	Green Section	<input type="checkbox"/>
334	Yellow Section	<input type="checkbox"/>
335	Orange Section	<input type="checkbox"/>
336	Purple Section	<input type="checkbox"/>
337	Brown Section	<input type="checkbox"/>
338	Pink Section	<input type="checkbox"/>
339	Grey Section	<input type="checkbox"/>
340	Black Section	<input type="checkbox"/>
341	White Section	<input type="checkbox"/>
342	Blue Section	<input type="checkbox"/>
343	Red Section	<input type="checkbox"/>
344	Green Section	<input type="checkbox"/>
345	Yellow Section	<input type="checkbox"/>
346	Orange Section	<input type="checkbox"/>
347	Purple Section	<input type="checkbox"/>
348	Brown Section	<input type="checkbox"/>
349	Pink Section	<input type="checkbox"/>
350	Grey Section	<input type="checkbox"/>
351	Black Section	<input type="checkbox"/>
352	White Section	<input type="checkbox"/>
353	Blue Section	<input type="checkbox"/>
354	Red Section	<input type="checkbox"/>
355	Green Section	<input type="checkbox"/>
356	Yellow Section	<input type="checkbox"/>
357	Orange Section	<input type="checkbox"/>
358	Purple Section	<input type="checkbox"/>
359	Brown Section	<input type="checkbox"/>
360	Pink Section	<input type="checkbox"/>
361	Grey Section	<input type="checkbox"/>
362	Black Section	<input type="checkbox"/>
363	White Section	<input type="checkbox"/>
364	Blue Section	<input type="checkbox"/>
365	Red Section	<input type="checkbox"/>
366	Green Section	<input type="checkbox"/>
367	Yellow Section	<input type="checkbox"/>
368	Orange Section	<input type="checkbox"/>
369	Purple Section	<input type="checkbox"/>
370	Brown Section	<input type="checkbox"/>
371	Pink Section	<input type="checkbox"/>
372	Grey Section	<input type="checkbox"/>
373	Black Section	<input type="checkbox"/>
374	White Section	<input type="checkbox"/>
375	Blue Section	<input type="checkbox"/>
376	Red Section	<input type="checkbox"/>
377	Green Section	<input type="checkbox"/>
378	Yellow Section	<input type="checkbox"/>
379	Orange Section	<input type="checkbox"/>
380	Purple Section	<input type="checkbox"/>
381	Brown Section	<input type="checkbox"/>
382	Pink Section	<input type="checkbox"/>
383	Grey Section	<input type="checkbox"/>
384	Black Section	<input type="checkbox"/>
385	White Section	<input type="checkbox"/>
386	Blue Section	<input type="checkbox"/>
387	Red Section	<input type="checkbox"/>
388	Green Section	<input type="checkbox"/>
389	Yellow Section	<input type="checkbox"/>
390	Orange Section	<input type="checkbox"/>
391	Purple Section	<input type="checkbox"/>
392	Brown Section	<input type="checkbox"/>
393	Pink Section	<input type="checkbox"/>
394	Grey Section	<input type="checkbox"/>
395	Black Section	<input type="checkbox"/>
396	White Section	<input type="checkbox"/>
397	Blue Section	<input type="checkbox"/>
398	Red Section	<input type="checkbox"/>
399	Green Section	<input type="checkbox"/>
400	Yellow Section	<input type="checkbox"/>
401	Orange Section	<input type="checkbox"/>
402	Purple Section	<input type="checkbox"/>
403	Brown Section	<input type="checkbox"/>
404	Pink Section	<input type="checkbox"/>
405	Grey Section	<input type="checkbox"/>
406	Black Section	<input type="checkbox"/>
407	White Section	<input type="checkbox"/>
408	Blue Section	<input type="checkbox"/>
409	Red Section	<input type="checkbox"/>
410	Green Section	<input type="checkbox"/>
411	Yellow Section	<input type="checkbox"/>
412	Orange Section	<input type="checkbox"/>
413	Purple Section	<input type="checkbox"/>
414	Brown Section	<input type="checkbox"/>
415	Pink Section	<input type="checkbox"/>
416	Grey Section	<input type="checkbox"/>
417	Black Section	<input type="checkbox"/>
418	White Section	<input type="checkbox"/>
419	Blue Section	<input type="checkbox"/>
420	Red Section	<input type="checkbox"/>
421	Green Section	<input type="checkbox"/>
422	Yellow Section	<input type="checkbox"/>
423	Orange Section	<input type="checkbox"/>
424	Purple Section	<input type="checkbox"/>
425	Brown Section	<input type="checkbox"/>
426	Pink Section	<input type="checkbox"/>
427	Grey Section	<input type="checkbox"/>
428	Black Section	<input type="checkbox"/>
429	White Section	<input type="checkbox"/>
430	Blue Section	<input type="checkbox"/>
431	Red Section	<input type="checkbox"/>
432	Green Section	<input type="checkbox"/>
433	Yellow Section	<input type="checkbox"/>
434	Orange Section	<input type="checkbox"/>
435	Purple Section	<input type="checkbox"/>
436	Brown Section	<input type="checkbox"/>
437	Pink Section	<input type="checkbox"/>
438	Grey Section	<input type="checkbox"/>
439	Black Section	<input type="checkbox"/>
440	White Section	<input type="checkbox"/>
441	Blue Section	<input type="checkbox"/>
442	Red Section	<input type="checkbox"/>
443	Green Section	<input type="checkbox"/>
444	Yellow Section	<input type="checkbox"/>
445	Orange Section	<input type="checkbox"/>
446	Purple Section	<input type="checkbox"/>
447	Brown Section	<input type="checkbox"/>
448	Pink Section	<input type="checkbox"/>
449	Grey Section	<input type="checkbox"/>
450	Black Section	<input type="checkbox"/>
451	White Section	<input type="checkbox"/>
452	Blue Section	<input type="checkbox"/>
453	Red Section	<input type="checkbox"/>
454	Green Section	<input type="checkbox"/>
455	Yellow Section	<input type="checkbox"/>
456	Orange Section	<input type="checkbox"/>
457	Purple Section	<input type="checkbox"/>
458	Brown Section	<input type="checkbox"/>
459	Pink Section	<input type="checkbox"/>
460	Grey Section	<input type="checkbox"/>
461	Black Section	<input type="checkbox"/>
462	White Section	<input type="checkbox"/>
463	Blue Section	<input type="checkbox"/>
464	Red Section	<input type="checkbox"/>
465	Green Section	<input type="checkbox"/>
466	Yellow Section	<input type="checkbox"/>
467	Orange Section	<input type="checkbox"/>
468	Purple Section	<input type="checkbox"/>
469	Brown Section	<input type="checkbox"/>
470	Pink Section	<input type="checkbox"/>
471	Grey Section	<input type="checkbox"/>
472	Black Section	<input type="checkbox"/>
473	White Section	<input type="checkbox"/>
474	Blue Section	<input type="checkbox"/>
475	Red Section	<input type="checkbox"/>
476	Green Section	<input type="checkbox"/>
477	Yellow Section	<input type="checkbox"/>
478	Orange Section	<input type="checkbox"/>
479	Purple Section	<input type="checkbox"/>
480	Brown Section	<input type="checkbox"/>
481	Pink Section	<input type="checkbox"/>
482	Grey Section	<input type="checkbox"/>
483	Black Section	<input type="checkbox"/>
484	White Section	<input type="checkbox"/>
485	Blue Section	<input type="checkbox"/>
486	Red Section	<input type="checkbox"/>
487	Green Section	<input type="checkbox"/>
488	Yellow Section	<input type="checkbox"/>
489	Orange Section	<input type="checkbox"/>
490	Purple Section	<input type="checkbox"/>
491	Brown Section	<input type="checkbox"/>
492	Pink Section	<input type="checkbox"/>
493	Grey Section	<input type="checkbox"/>
494	Black Section	<input type="checkbox"/>
495	White Section	<input type="checkbox"/>
496	Blue Section	<input type="checkbox"/>
497	Red Section	<input type="checkbox"/>
498	Green Section	<input type="checkbox"/>
499	Yellow Section	<input type="checkbox"/>
500	Orange Section	<input type="checkbox"/>

UNCLASSIFIED

SECURITY CLASSIFICATION OF THIS PAGE(When Data Entered)

NSWC/WOL/TR 77-42

15 April 1977

EVALUATION OF GCFR PCRV CONTAINMENT CAPABILITY

In the course of the NRC Regulatory Staff review of the Gas Cooled Fast Breeder Reactor (GCFR) concept, this laboratory was requested to estimate the containment capabilities of the Prestressed Concrete Reactor Vessel (PCRV). An energy release in the reactor cavity following a Core Disassembly Accident (CDA) could cause an accidental overpressure load which must be contained in order to prevent contamination of the area surrounding the reactor installation. The containment capability has been examined, though no clear definition of the magnitude or severity of a CDA for these reactors presently exists.

An experimental/analytical study of a 1/20 scale model of another PCRV has been evaluated. Calculations and static hydraulic measurements on this model are compared with computations made with similar approximation techniques using the NASA STRuctural ANALysis computer system (NASTRAN). The purpose of this comparison was to establish NASTRAN as a valid tool for examining proposed GCFR PCRV's for which few or no experimental measurements are available.

This report addresses the general question: can the proposed structure contain a pressure excursion to double the normal operating pressure? Both static and dynamic loading are examined.

The study is primarily a safety evaluation --- local details within the structure are passed over in favor of determining the gross behavior of the structure as a whole.

Support for this work was provided by the Nuclear Regulatory Commission under Contract AT(49-24)-0103, Modification 16.

J. W. Enig
J. W. ENIG
By direction

TABLE OF CONTENTS

	Page
I. INTRODUCTION.....	5
Background.....	5
Precis.....	7
II. 1/20 SCALE MODEL.....	10
Background.....	10
NASTRAN Models.....	12
Results.....	13
Summary.....	18
III. ANALYSIS OF PROPOSED GCFR PCRV.....	45
PCRV Prototype.....	45
NASTRAN Model.....	46
NASTRAN Calculations.....	49
IV. CONTAINMENT CAPABILITY.....	70
Explosion Loads.....	70
Explosion Containment.....	70
Accident Containment Capability.....	72
V. SUMMARY AND CONCLUSIONS.....	76
1/20 Scale Model.....	76
GCFR PCRV.....	76
LIST OF REFERENCES.....	78

TABLES

Table	Title	Page
2.1	Prestress Quantities.....	19
2.2	Material Properties for the GA 1/20 Scale Model PCRV.....	20
2.3	Comparison of the Experimental Results with Analytical Results for the Solid PCRV Model.....	21
2.4	Comparison of the Experimental Results with Analytical Results for the Modified Modulus PCRV Model...	22

TABLE OF CONTENTS

FIGURES

Figure	Title	Page
1.1	GCFR Core.....	8
1.2	Schematic Drawing of Cracking and Deformation Patterns...	9
2.1	General Arrangement 1000 MW(e) Reactor.....	23
2.2	1/20 Scale Model of GA PCRV for 1000 MW(e) HTGR.....	24
2.3	Modified Modulus Finite Element Model.....	25
2.4	Deformed Shape: NASTRAN Solid Model; Prestress Alone.....	26
2.5	Deformed Shape: NASTRAN Solid Model; Prestress + 650 psi (1 MCP).....	27
2.6	Maximum Principal Stress in the Haunch Region; Solid Model.....	28
2.7	Maximum Principal Stress in the Head; Solid Model.....	29
2.8	Positions of Strain Gages for Comparison with Analytical Results.....	30
2.9	Deformed Shape: NASTRAN Modified Modulus Technique; Prestress alone.....	31
2.10	Maximum Principal Stress in Haunch Region; Modified Modulus Method.....	32
2.11	Maximum Principal Stress in the Head: NASTRAN Modified Modulus Technique.....	33
2.12	Deformed Shape: NASTRAN Modified Modulus Technique; Prestress + 650 psi (1 MCP).....	34
2.13	Hoop Stress Between the Cavities at Barrel Midheight; Prestress Only.....	35
2.14	Hoop Stress Through the Cavities at Barrel Midheight; Prestress Only.....	36
2.15	Radial Strain Through the Centerline of the Head; Prestress Only.....	37
2.16	Radial Strain Through the Centerline of the Head; Prestress + 650 psi Cavity Pressure.....	38
2.17	Radial Strain Through the Head; Prestress Only.....	39
2.18	Internal Hoop Strain Next to the Cavities for the GA 1/20 Scale Model; Prestress Only.....	40
2.19	Internal Hoop Strain next to the Cavities for the GA 1/20 Scale Model; Prestress + 650 psi Cavity Pressure....	41
2.20	External Hoop Strain Next to the Cavities for the GA 1/20 Scale Model; Prestress Only.....	42
2.21	External Hoop Strain Next to the Cavities for the GA 1/20 Scale Model; Prestress + 650 psi Cavity Pressure....	43
2.22	Displacements in GA's 1/20 Scale PCRV Test.....	44
3.1	PCRv Configuration.....	54
3.2	Finite Element Grid and Loads for PCRv NASTRAN Model.....	55
3.3	Step Load.....	56
3.4	Static Stresses in Sensitive Elements of PCRv Model (psi).....	57

TABLE OF CONTENTS (Cont.)

FIGURES

Figure	Title	Page
3.5	Maximum Principal Stresses in Sensitive Elements of PCRVR Model (psi).....	58
3.6	Displacement of Grid Point 3001; Transient Load.....	59
3.7	Displacement of Grid Point 692; Transient Load.....	60
3.8	Displacement of Grid Point 165; Transient Load.....	61
3.9	Displacement of Grid Point 501; Transient Load.....	62
3.10	Displacement of Grid Point 519; Transient Load.....	63
3.11	Stress vs Time: Upper Haunch; 1250 psi 'Step' Load.....	64
3.12	Stress vs Time: Midheight of Barrel; 1250 psi 'Step' Load.....	65
3.13	Stress vs Time: Barrel, Bottom Haunch; 1250 psi 'Step' Load.....	66
3.14	Stress vs Time: Bottom Head, Haunch; 1250 psi 'Step' Load.....	67
3.15	Axial and Radial Stress in Element 433.....	68
3.16	Radial and Circumferential Stress in Element 2.....	69
4.1	Peak Reactor Cavity Overpressure vs TNT Charge Weight....	75

I. INTRODUCTION

Heat generated in a reactor core by nuclear reactions is extracted and used to produce steam, which in turn operates electricity generating turbines. In the Gas Cooled Fast Breeder Reactor (GCFR), heat is transferred between the reactor core and the steam generators by flowing helium gas at high pressure. The core and heat exchangers for this proposed reactor (illustrated in Figure 1.1) are to be contained by a monolithic Prestressed Concrete Reactor Vessel (PCRV) which will provide the necessary radiation shielding and mechanical restraints to confine the high pressure helium.

No PCRVs have been designed to operate at the pressures and temperatures proposed for the device under consideration. The goal of this study is to examine the mechanical properties of the proposed PCRV and to study the containment capabilities of the particular PCRV configuration proposed for the GCFR.

BACKGROUND

Concrete. Concrete is a brittle visco-elastic material whose tensile strength is one order of magnitude less than its compressive strength. Local cracking appears wherever concrete is placed in a state of moderate tension; the function of reinforcing bars (rebar) is to contain these cracks and to prevent their spreading. Prestressing creates an initial state of compression in a concrete structure which will be called upon to sustain tensile loading. Creation and propagation of cracks is thus minimized by the addition of rebar, and the tensile load carrying capacity of the structure is enhanced by the presence of a prestressing system.

Tests on reinforced concrete beams (1.1) have shown that, after the first load cycle, beams exhibit a linear relation between stress and strain. Local cracks occur with the first (tensile) load and are contained by the rebar. Pieces of aggregate pull away from one another and the rebar; when the first load is released, the aggregate returns to new and slightly different equilibrium locations. Successive tensile loads, as long as they do not exceed tensile yield, do not seriously disturb these new equilibrium locations, and the concrete behaves as a linearly elastic material.

-
- (1.1) Penzien, J. and Hansen, R. J., "Static and Dynamic Elastic Behavior of Reinforced Concrete Beams," J. Am. Concrete Inst. 25 545 (Mar 1954).

Cracking Patterns. Concrete failure mechanisms have been observed in tests, but results have not been reduced to accepted design formulas. Beams and beam-like structures are discussed in (1.1) and (1.2). Because of this lack of design formation, the behavior under load of adequate sized PCRV models and prototypes must be established by experimental investigations to reinforce the results of the evaluation detailed later in this report.

The PCRV configuration considered in this study is a right circular cylinder with flat end plates, or heads. The cylindrical wall is the barrel; the reentrant corner between the barrel and each head is referred to as a haunch.

Static hydraulic tests have been performed on cylindrical vessels similar to the type considered here (1.2, 1.3, and 1.4). These tests have established the patterns of cracks produced by static loads. Major cracking occurs at the haunches, at the mid height of the barrel, and in the heads. The general types of cracks which occur are indicated in Figure 1.2.

The location and types of cracks which appear and which grow as the static load level increases can be classified as follows:

- Heads: Radial cracks appear like the spokes in a bicycle wheel; a concave outward dome peels off --- much like a large spall.
- Haunches: Cracks propagate radially through the concrete at the reentrant corner --- as though a cap were being removed.
- Barrel: Axial cracks appear at regular intervals around the outer circumference --- like the splits in a banana skin.

-
- (1.1) Penzien, J. and Hansen, R. J., "Static and Dynamic Elastic Behavior of Reinforced Concrete Beams," J. Am. Concrete Inst. 25 545 (Mar 1954).
 - (1.2) Tan, C. P., "Prestressed Concrete in Nuclear Reactor Vessels: A Critical Review of Current Literature," Oak Ridge National Laboratory, ORNL 4227 (May 1968).
 - (1.3) Corum, J. M. and Smith, J. E., "Use of Small Models in Design and Analysis of Prestressed Concrete Reactor Vessels," Oak Ridge National Laboratory, ORNL 4346 (May 1970).
 - (1.4) Karlsson, B. I. and Sozen, M. A., "Shear Strength of End Slabs with and without Penetrations in Prestressed Concrete Reactor Vessels," Univ. of Ill., ORNL Contract No. W-7405-eng-26, Subcontract No. 2906, (Jul 1971).

The tests on which the above list is based were performed on laboratory-scale models of the type of vessel to be considered in this report.

PRECIS

This report summarizes the results of a series of calculations made with NASTRAN (NASA STructural ANalysis computer system) (1.5), a large general purpose linear elastic structural analysis computer code. This code can be used to determine the response of a large complex structure to static and transient loads; responses are determined for a finite element model constructed from axisymmetric constant strain elements which are a part of the program library of elements.

In an earlier report (1.6) it was estimated that the GCFR PCRVR would be able to contain safely a CDA (Core Disassembly Accident)* of energy release approaching 4000 MWsec. This estimate was based on static load calculations. The objective of the effort reported here has been to obtain knowledge of PCRVR response to dynamic loads and, from this information, to establish a more reliable CDA limit.

The first step was to compare NASTRAN calculations with experimental results obtained in a series of static hydraulic tests on a 1/20 scale model of PCRVR. It was found that, with certain modifications, NASTRAN calculations reliably reproduce the experimental results.

The next step was to determine the dynamic response of the model of the GCFR PCRVR by Exercising the transient capability of NASTRAN. Finally, the peak dynamic responses output by NASTRAN were used to estimate the containment capability of the PCRVR.

*Core Disassembly Accident: uncontrolled release of energy from reactor core.

- (1.5) McCormick, C. W., "The NASTRAN User's Manual, Level 15", NASA SP-222(01) (Jun 1972).
- (1.6) Atomic Energy Commission, "Preapplication Safety Evaluation of the Gas Cooled Fast Breeder Reactor", Directorate of Licensing, Project 456 (1 Aug 1974).

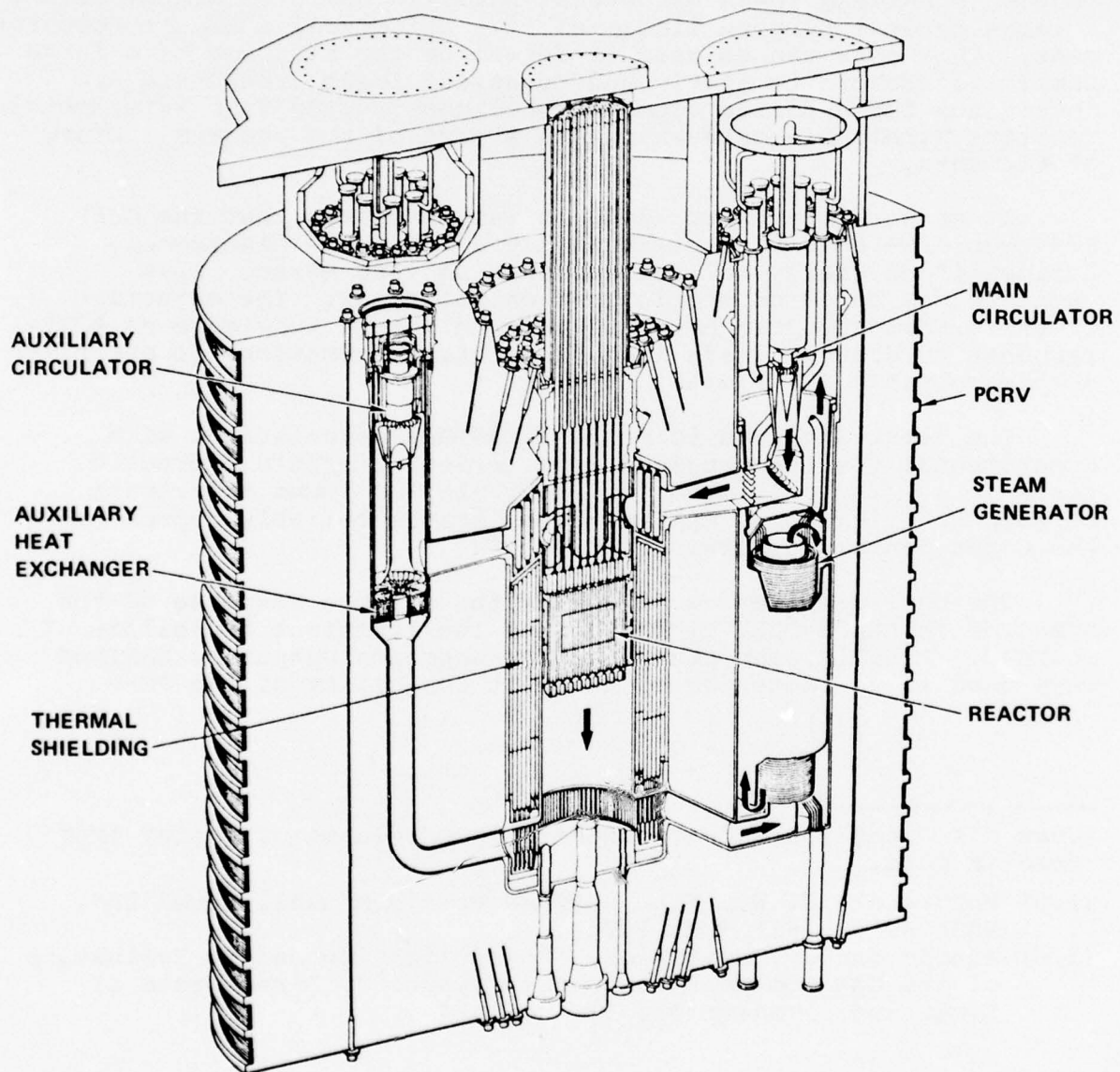


FIG. 1.1 GCFR CORE.

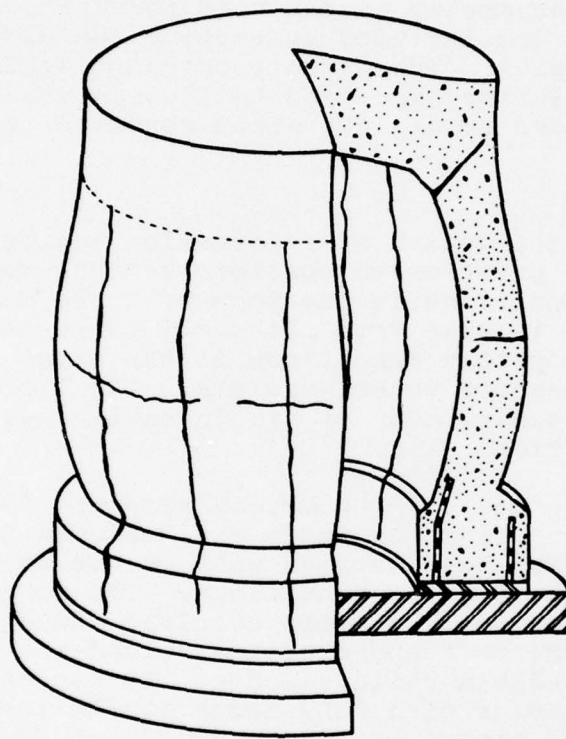


FIG. 1.2 SCHEMATIC DRAWING OF CRACKING AND DEFORMATION PATTERNS.

II. 1/20 SCALE MODEL

The response of a 1/20 scale model PCRV to several static internal pressure loads was determined experimentally in 1969 (2.1). Data from these tests were compared to static NASTRAN calculations using a finite element model of the GCFR PCRV.

Two axisymmetric finite element models were used. In one model no attempt was made to model the asymmetry of the head penetrations and steam generator cavities. The material properties for this model were assumed to be uniform. In the second model, the asymmetry of the head penetrations and steam generator cavities was included by varying the elastic modulus in the affected region. The results of calculations on the second model were further modified to include the effect of stress concentrations around the steam generator cavities.

BACKGROUND

Over the years a wealth of information has been accumulated on the response of prestressed concrete reactor vessels to various loading conditions in the form of scale model tests. Models have ranged in size from the small table top size constructed under laboratory conditions to the large 1/4 scale models of entire reactor vessel systems. Similarly, the experimental models have been of single cavity design as well as multi-cavity design.

The tests were designed to obtain response data in two loading realms. One class of tests was designed to determine the response of vessel elements as well as the overall vessel response to credible loading conditions. The other class of tests was designed to estimate the overload and ultimate load behavior of the PCRV to support ultimate load analysis as well as establishing credible failure modes. It was concluded that the structural behavior of a PCRV under static load conditions can be demonstrated experimentally with a high degree of reliability (2.2).

-
- (2.1) Davies, I., Franklin, R. N. and Gotschall, H. L., "Model Studies of a Multicavity PCRV for 1000 MW(e) HTGR System," General Atomic Co., CA-P-1002-33 (Feb 1970).
 - (2.2) Cheung, K. C., "PCRV Design Verification," General Atomic Company, San Diego, GA-A-12821 (GA-LTR-8) (Mar 1974).

Hartlepool Model. Several extensive experimental efforts have been made. An example of this was a 1/10 scale model of a complete PCRV constructed and tested by Taylor Woodrow Construction Ltd. (TWC), England in 1968. The Tests of the scale model for the Hartlepool PCRV was the first model study undertaken for a multi-cavity vessel. The primary object of the tests was to observe the complete range of the vessel behavior, to evaluate design techniques, to demonstrate failure modes and to firmly establish an adequate reserve of vessel strength.

Ohbayashi-Gumi Model. An example of an experimental effort encompassing both single cavity as well as multi-cavity PCRVs was undertaken by Ohbayashi-Gumi Ltd. of Japan. Ohbayashi-Gumi constructed and tested 1/20 scale model PCRVs for high temperature gas reactor use (HTGR). The models were adequately instrumented to record deflection and strain data during the test. General Atomic Company (GA) analyzed the overload response of the vessel under internal pressure using their own finite element computer code with satisfactory results.

GA 1/20 Scale Test. In 1969 GA constructed and tested a 1/20 scale model of a multi-cavity HTGR PCRV (2.1). In construction of the model, close attention was given to the achieving accurate scaling of dimensions, physical properties of the concrete and steel liner as well as the prestress loads. The prototype upon which the model was based contained a large central cavity for the nuclear core assembly and six smaller steam generator cavities equally spaced around the central cavity. Figure 2.1 shows an artists representation of the prototype HTGR PCRV.

Figure 2.2 shows the geometry of the 1/20 scale model of the GA HTGR PCRV. The height of the model was 49.2 in. with a diameter of 53.4 in. The model was constructed in 3 sections; the top head, the bottom head and the barrel. Slip planes were originally introduced to allow radial slipping of the barrel without inducing radial tension in the heads. It was believed that the slip planes would prevent vertical cracks from running into the head at the head and barrel interface.

The model PCRV was prestressed both longitudinally and circumferentially. The longitudinal prestress was achieved by the use of prestressing tendons. There were two sets of tendons,

-
- (2.1) Davies, I., Franklin, R. N. and Gotschall, H. L., "Model Studies of a Multicavity PCRV for 1000 MW(e) HTGR System", General Atomic Co., GA-P-1002-33 (Feb 1970).

one set around the main cavity and another around each of the steam generator cavities. The circumferential prestress was effected by wire wrapping both the heads and the barrel with steel cable. Table I from reference 2 shows a comparison of the prestressing loads for the prototype and the 1/20 scale model.

The response of the vessel to pressurization was examined in four tests. The pressure for each test was applied hydraulically. It was found that the model behaved essentially elastically up to a pressure of 800 psi. which was 1.2 times the maximum cavity pressure (MCP).^{*} The model was observed to behave as a solid structure up to that point. Inclusion of the slip plane was deemed unnecessary since it was recognized that when the vessel was subjected to overpressure, progressive cracking originating at the haunch would lead to substantial separation at the head and barrel juncture.

NASTRAN MODEL

A finite element model was constructed to represent the GA 1/20 scale model PCRV. The model consisted of 615 nodes and 560 solid axisymmetric four node elements. Each node has two translational degrees of freedom, axial and radial, except for those degrees of freedom constrained to satisfy boundary conditions. The other translational degree of freedom, circumferential, and the three rotational degrees of freedom must be constrained out of the problem. Only the bottom half of the PCRV was modeled because there exists a plane of symmetry at the vessel midheight. The mesh was adjusted so that there were more elements of a smaller size in the regions where there high stress gradients were expected.

There were two major limitations in the use of NASTRAN to perform the analysis of the PCRV. First, NASTRAN does not allow the mixing of thin shell axisymmetric elements with solid of revolution elements, therefore the PCRV liner was not included in the NASTRAN model. Secondly, two dimensional elements, such as bars, cannot be used in conjunction with axisymmetric elements. This meant that the rebar could not be included in the NASTRAN model. It was felt that the gross vessel response could be obtained satisfactorily without the liner and rebar included in the model.

Solid Model. For this analysis the asymmetry of the penetrations and the steam generator cavities were not included. It was assumed that the vessel was a solid structure. That is, the slip plane was not included because the results of the tests indicated that it did not play a significant part in the overall

^{*}MCP for the CA 1/20 scale model was defined as 650 psi.

vessel response (2.2). The material properties for the reinforced concrete are shown in Table 2.2. The prestressing loads were applied as constant value loads. The circumferential prestress was applied as a radial load. The total load due to the longitudinal prestressing tendons was applied as a concentrated load. That is, the total applied longitudinal prestressing load at any radius was computed and applied as a concentrated load at that radius. Figure 2.3 shows the grid point and element numbering scheme used as well as the prestressing loads.

Modified Modulus Model. A second finite element model of the GA 1/20 scale model PCRV was formulated. The overall geometry was identical to the previous model; however, there were several modifications to the material properties. There was an attempt to model the influence of the asymmetry of the steam generator cavities and the head penetrations on the overall structural response. The asymmetry was modeled by modifying the elastic modulus in the regions affected by the asymmetry. The modified modulus method enabled the gross vessel response to be predicted more accurately.

The modified modulus model of the GA 1/20 scale model PCRV is shown in Figure 2.3 illustrating the regions in which the elastic modulus was modified to account for the penetrations and steam generator cavities. The value of the elastic modulus in the steam generator cavity region (E^*) was determined by scaling the unmodified modulus (E) by the ratio of the solid concrete perimeter to the total perimeter in the affected region (2.3). Again as before the liner and the rebar were not included in the model.

RESULTS

Solid Model. The prestress loads were applied to the solid homogeneous model with the resultant deformed shape shown in Figure 2.4. The radial compression at the vessel midheight was 0.0032 in. The internal pressure was then applied to the main cavity as well as the steam generator cavities. The deformed shape for the prestress loads plus an internal pressure of 650 psi. (1.0 MCP) is shown in Figure 2.5.

- (2.2) Cheung, K. C., "PCRV Design Verification," General Atomic Company, San Diego, GA-A-12821 (GA-LTR-8) (Mar 1974).
- (2.3) Wistrom, J. D. and Bisset, J. R., "Simplified Elastic Analysis of Cylindrical Multicavity PCRVs," General Atomic Co., GA-B-12171 (Oct 1973).

The NASTRAN analysis indicated that the vessel overcame prestress compression in the haunch region at an internal pressure of 300 psi (.46 MCP). At an internal pressure of 650 psi (1.0 MCP) there were high enough tensile stresses in the haunch region to cause cracking to occur. The maximum principle stresses in the haunch region are shown in Figure 2.6 for various load conditions.

Note that for an internal pressure of 650 psi (1.0 MCP) the region of high tensile stress is limited to a few elements in the corner. There is no doubt that cracking will occur, however the cracking would be limited to a small region in the haunch.

The maximum principal stress for elements in the head is shown in Figure 2.7. For an internal pressure of 650 psi (1.0 MCP) there was noticeable doming of the head which was illustrated in Figure 2.5. At an internal pressure of 800 psi (1.2 MCP) there were high enough tensile stresses in the head to cause cracking. However, the region of high tensile stress was confined to the outermost elements.

The results of the NASTRAN analysis were compared to the experimental data and the results are compared in Table 2.3. Four circumferential strain gages were chosen for the comparison. Figure 2.8 shows the location of the strain gages within the PCRV.

Inspection of the results in Table 2.3 shows very poor agreement between the analytical values of strain predicted by NASTRAN for the solid model and the experimental strain gage data. Further research into the problem indicated that the strain gages were located adjacent to the steam generator cavities. Therefore the steam generator cavities were acting as stress intensifiers. Since the analysis was axisymmetric, the effect of the steam generator cavities as stress intensifiers was not apparent in the NASTRAN analysis.

Modified Modulus Model. Intuition indicated that the regions adjacent to the steam generators were the most critical ones. That is, cracks would occur first in the haunch region adjacent to the steam generator cavities. Therefore a method was found that attempted to account for the loss of stiffness because of the presence of the steam generators and head penetrations. A modified modulus method was used. As previously discussed, the method accounts for the cavities by varying the elastic modulus in the effected region. The method, however, does not account for the stress intensifying effect of the head penetrations.

The prestress loads were applied to the modified modulus NASTRAN model with the deformed shape shown in Figure 2.9. The radial compression of the midheight of the barrel was 0.0040 in.

As can be seen, there was considerably more deformation in this model than the previous one (Figure 2.4). This agrees with intuition, the steam generator cavities and the head penetrations cause the vessel to respond in a much less rigid manner than the previous solid one resulting in larger deformations.

The internal pressure loads were then applied to the finite element model of the PCRV. The response of the vessel was determined using NASTRAN. The analysis indicated that the vessel overcame prestress compression in the haunch region at an internal pressure of 400 psi (.6 MCP). At an internal pressure of 650 psi (1.0 MCP) there were high enough tensile stresses in the haunch region to cause cracking to occur there. The maximum principal stress for elements in the haunch region is shown in Figure 2.10. Though cracks would have occurred in the haunch region, the gross vessel response would not be altered significantly.

The vessel head remained in a state of prestress compression until a static pressure of 650 psi (1.0 MCP) was reached. Though there was a region of tensile stress in the head, those stresses were not of a large enough magnitude to cause cracking until a pressure of over 1000 psi (1.5 MCP) was reached. The maximum principal stresses in the head are shown in Figure 2.11 for various load states.

The deformed shape of the modified modulus model for an internal pressure of 650 psi (1.0 MCP) is shown in Figure 2.12. As can be seen, there is much more distortion in this model than there was in the previous model (Figure 2.5). The results of the modified modulus NASTRAN analysis were compared to the experimental strain gage data with those results tabulated in Table 2.4. As can be seen by comparing the table with the previous one (Table 2.3), the results of the modified modulus method were somewhat more accurate, but still not within experimental error. A method was required that accounts for the stress intensifying effect of the steam generator cavities.

Stress Intensifying Effects. The modified modulus axisymmetric results were further modified using the following formulae to incorporate the stress intensifying effect of the steam generator cavities (2.3). Equations 2.1 and 2.2 were used primarily because they are the same equations that GA used with

-
- (2.3) Wistrom, J. D. and Bisset, J. R., "Simplified Elastic Analysis of Cylindrical Multicavity PCRVs," General Atomic Co., GA-B-12171 (Oct 1973).

their SAFE-2D computer code to obtain stresses in the elements adjacent to the Steam Generator Cavities (2.4). Since GA has experience in designing and analyzing PCRVs, it seems reasonable to use their equations with NASTRAN in order to determine the effect of the steam generators as sources of stress concentration.

$$\sigma_{\theta} = \sigma'_{\theta} + \frac{\sum_{r_s-d/2}^{R_s} \sigma' \Delta r + d p d_2}{2(R_s - r)^2 \left(2 - \frac{d}{R_s - R_i}\right)} \quad \text{for } r < R_s \quad (2.1)$$

$$\sigma_{\theta} = \sigma'_{\theta} + \frac{\sum_{r_s-d/2}^{R_s} \sigma' \Delta r + \alpha p d^2}{2(r - R_s)^2 \left(2 - \frac{d}{R_o - R_s}\right)} \quad \text{for } r > R_s \quad (2.2)$$

Where:

d = diameter of the steam generator cavities.

p = internal pressure.

r = radial distance from the centerline of the PCRv.

R_i = radius of PCRv core cavity.

R_o = outside radius of PCRv.

R_s = radial distance to the centerline of the steam generator cavities.

α = fraction of the steam generator cavity pressure force carried by membrane action.

σ'_{θ} = hoop stress from the modified modulus axisymmetric analysis.

(2.4) Cornell, D. C., "SAFE-2D: A Computer Program for the Stress Analysis of Plane and Axisymmetric Composite Structures," Gulf General Atomic Report GA-9076 (12 Feb 1969).

$\alpha P d^2$ = free body force due to the pressurization of the steam generators.

$\sum_1^2 \sigma \Delta r$ = area under the σ vs r curve bounded by 1 and 2.

In effect, these formulae allow the stress state to be determined along a radial line through the steam generator cavities. That is, the stress state may be determined adjacent to the cavities.

A computer program was written that further modified the axisymmetric NASTRAN results by the above formulae (Equation (2.1) and (2.2)). Both the circumferential stress and the circumferential strain were modified appropriately. The results of such a modification is shown in Figure 2.13 and Figure 2.14. Examination of the figures emphasize the fact that Equations (2.1) and (2.2) indeed model the influence of the steam generators as stress concentrations.

A typical example of the stress intensifying effect of the steam generator cavities is illustrated by Figure 2.13 and Figure 2.14. The steam generator cavity caused a 27% increase in the circumferential stress at the inner surface of the main cavity. At the outside surface, the increase in the circumferential stress was 18%. The most noticeable increase in stress occurred at the steam generator cavity surface. There was an increase of 103% at that surface. As can be seen the method does allow the stress to be determined adjacent to the cavities.

Modified Modulus Method with Stress Intensifying Effects.

The modified modulus axisymmetric NASTRAN results which were further modified by Equations (2.1) and (2.2) were compared to the experimental strain gage results. The comparison is shown graphically in Figure 2.15 to Figure 2.21. There appears to be quite good agreement for the radial stress throughout the head for prestress alone and for prestress and 650 psi (1.0 MCP) internal pressure (Figure 2.15 to Figure 2.17).

The comparison of the hoop strains is more favorable than previously shown in (Table 2.3 and Table 2.4). There was acceptable agreement between the analytical results and the experimental data for the internal hoop strains for both load cases. The comparison was made graphically in Figure 2.18 and Figure 2.19. Likewise, the comparison for the external hoop strains was favorable for both load cases. The graphical comparison is made in Figure 2.20 and Figure 2.21. This tends to support the validity of using Equations 2.1 and 2.2.

The displacements predicted by NASTRAN are compared to the experimental values obtained during the test in Figure 2.22. Unfortunately there are only a few experimental data points available for the comparison. However, the comparison was favorable for both the head displacements as well as the barrel displacements.

Though there was not absolute agreement between the analytical and the experimental results, the general agreement was quite good. The agreement found by this investigation was of the same order of magnitude as that which has been found by other investigators (2.2). There typically seem to be less accurate results obtained in the head region than in the barrel region. A probable reason for this is that the head penetrations and plugs alter the stiffness in that region. Better agreement was found for the data in the barrel region.

SUMMARY

An axisymmetric two dimensional analysis of a statically loaded multi-cavity PCRV scale model does not provide reliable detailed results in high stress regions. However, modification of the elastic modulus in the regions of high stress permits determination of overall vessel response to a reasonable degree of accuracy. With further modification of the results to account for stress concentrations, reasonable stresses and strains adjacent to the steam generator cavities can be determined. Even better results in these regions could be obtained with a three dimensional analysis of a 30° wedge; this, however, was beyond the purview of the present task.

The modified parameter technique can be used for a transient analysis. However, local modification of the mass matrix would be necessary to exclude the mass of the concrete which would otherwise occupy the steam generator cavities. Effects of the parameter modification on overall vessel response would not be as well defined as in a static analysis. Comparison with experimental data would be impossible, since none exists.

This phase of the task has established the viability of NASTRAN as a tool for analysis of PCRVs. Exclusion of the cavities and penetrations limits applicability such that only gross overall behavior of the vessel will be described; this, however, is sufficient for a safety analysis performed without confirmatory experimental evidence to check against.

(2.2) Cheung, K. C., "PCRV Design Verification", General Atomic Company, San Diego, GA-A-12821 (GA-LTR-8) (Mar 1974).

TABLE 2.1 PRESTRESS QUANTITIES

		1000 MW(e) PCRV at End of Life Conditions
<u>Circumferential Prestressing</u>		
	<u>Model</u>	
Top Heads	44 1/2 turns of number 8 gage wire at 3000 lb tension - 530 psi.	4 bands of 445 turns each of 0.6-in. diameter strand, at 29 kips each, corresponds to 520 psi.
Barrel	165 1/4 turns of number 8 gage wire at 2700 lb. tension = 550 psi.	14 bands of 445 turns each of 0.6-in. diameter strand at 26.8 kips each, corresponds to 514 psi.
Bottom Head	43 1/2 turns of number 8 gage wire at 3000 lb. tension = 520 psi.	4 bands of 445 turns each of 0.6-in. diameter strand, at 29 kips each, corresponds to 520 psi.
<u>Longitudinal Prestress</u>		
Tendons Around Core Cavity	13 number 8 gage wires at 2860 lb. tension.	13 - 168 wire (A = 8.25 in. ²) tendons at 1100 kips tension.
Tendons Around Steam Generator Cavities	8 - 1/4 in. diameter wires at 6000 lb. tension	20-168 wire (A=8.25 in. ²) Tendons at 1100 kips tension

TABLE 2.2

MATERIAL PROPERTIES FOR THE GA 1/20 SCALE MODEL PCRV

Compressive Yield Strength	=	6500 psi
Compressive Elastic Modulus	=	4.5×10^6 psi
Tensile Yield Strength	=	500 psi
Tensile Elastic Modulus	=	4.5×10^6 psi
Poisson's Ratio	=	0.167

TABLE 2.3

COMPARISON OF THE EXPERIMENTAL RESULTS WITH ANALYTICAL RESULTS
FOR THE SOLID PCRV MODEL

Prestress Only

Strain Gage #	$\epsilon_{\text{exp.}}$	$\epsilon_{\text{ana.}}$
13	360	195
14	480	215
15	176	95
16	315	120

Prestress + 650 psi (1.0 MCP)

Strain Gage #	$\epsilon_{\text{exp.}}$	$\epsilon_{\text{ana.}}$
13	45	80
14	165	75
15	68	78
16	162	90

NOTE: All strain values are in microstrain compression.

TABLE 2.4

COMPARISON OF THE EXPERIMENTAL RESULTS WITH ANALYTICAL RESULTS
FOR THE MODIFIED MODULUS PCRV MODEL

Prestress Only

Strain Gage #	$\epsilon_{\text{exp.}}$	$\epsilon_{\text{ana.}}$
13	360	234
14	480	268
15	176	131
16	315	151

Prestress + 650 psi (1.0 MCP)

Strain Gage #	$\epsilon_{\text{exp.}}$	$\epsilon_{\text{ana.}}$
13	45	128
14	165	115
15	68	98
16	162	105

NOTE: All strain values are in micro strain compression.

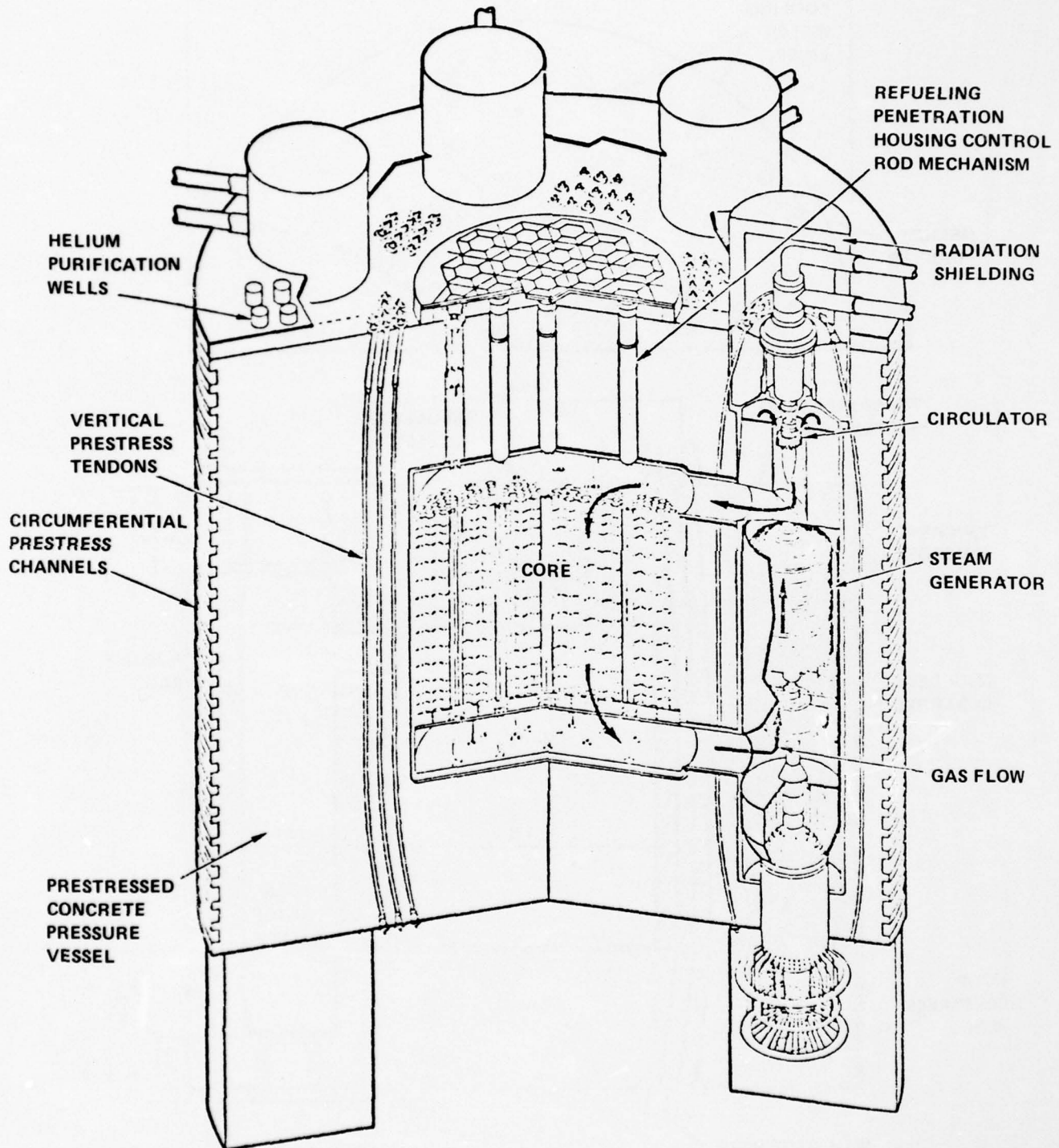


FIG. 2.1 GENERAL ARRANGEMENT 1000 MW(e) REACTOR

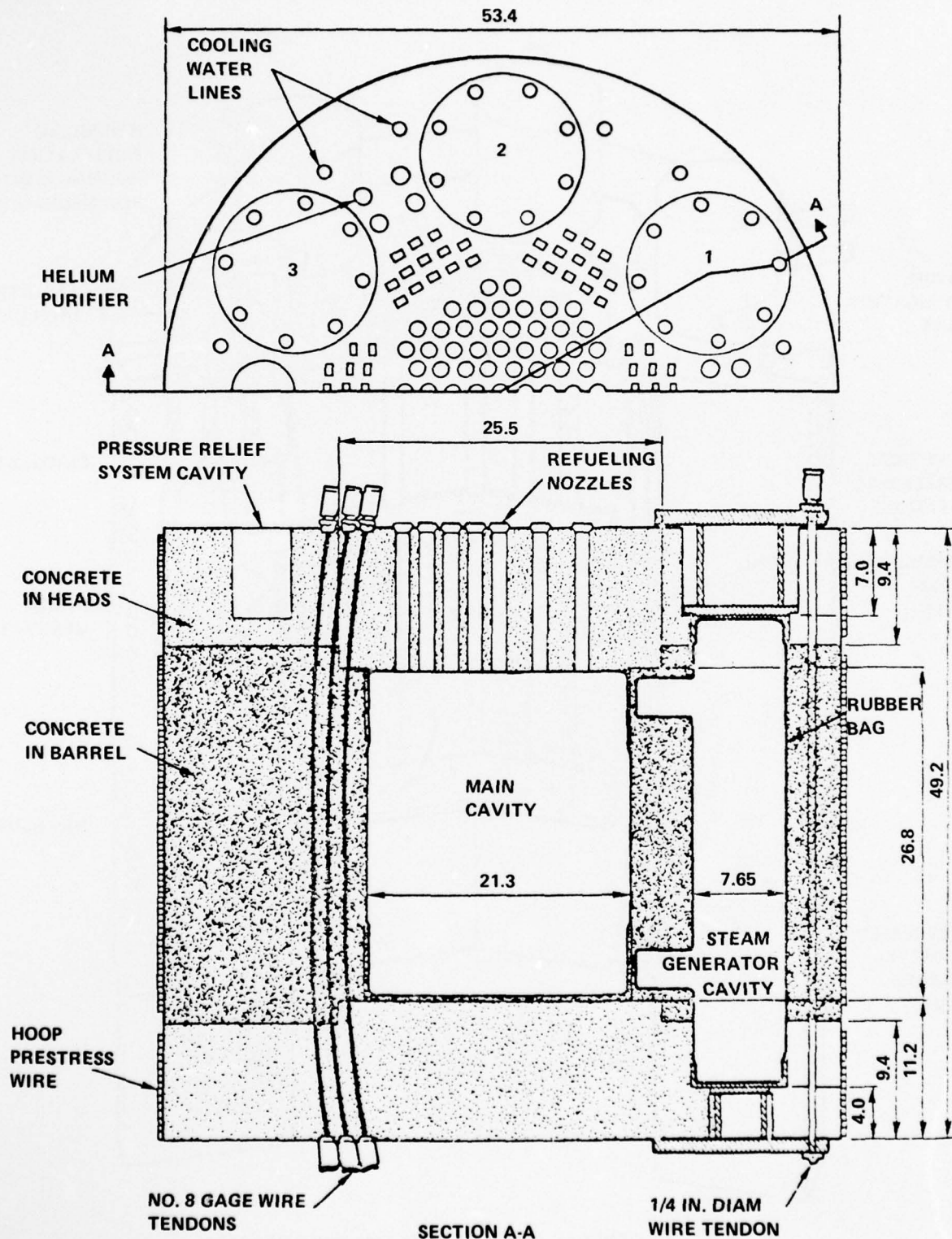


FIG. 2.2 1/20TH SCALE MODEL OF GA PCRV FOR 1000-MW(e) HTGR

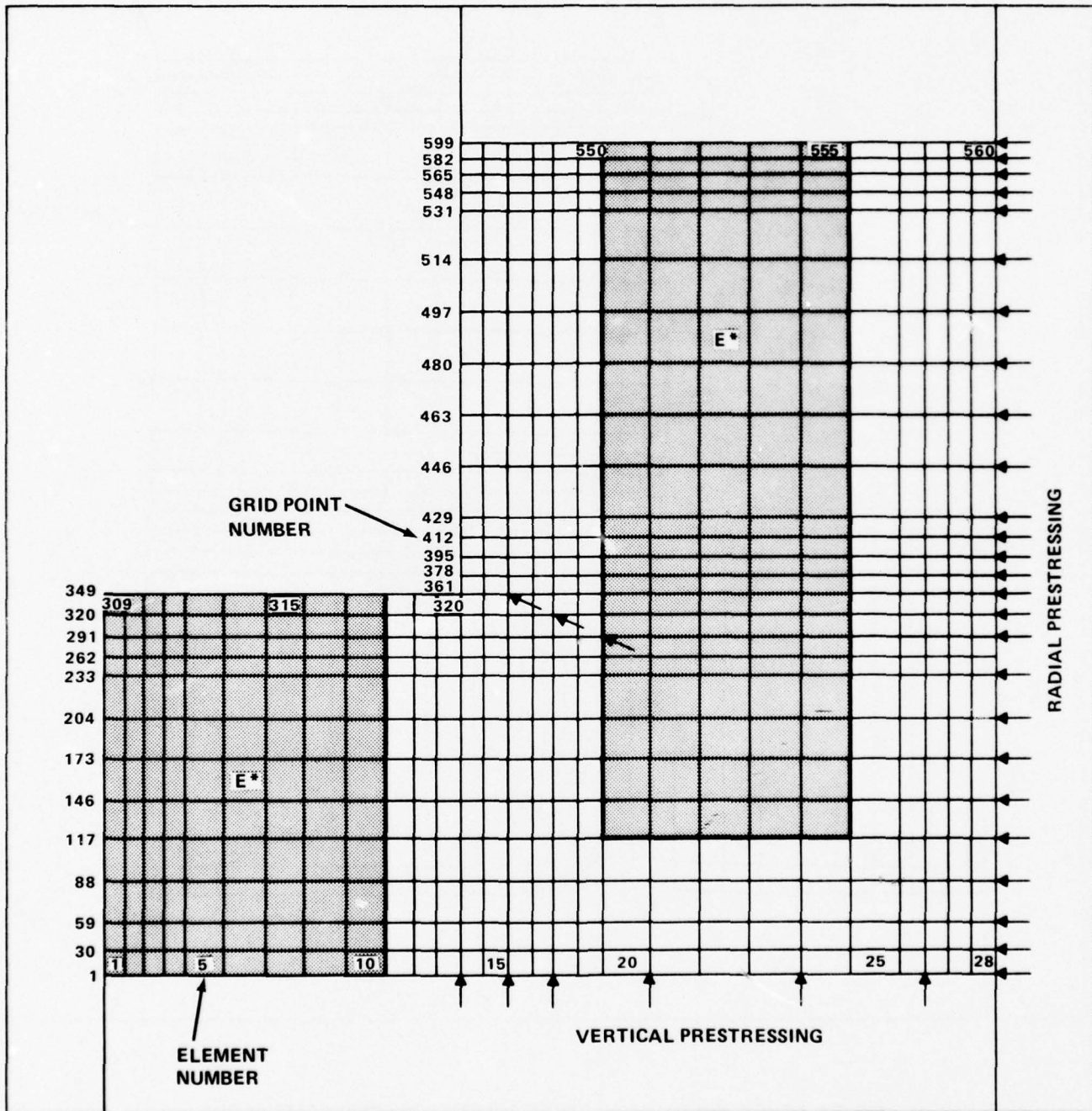


FIG. 2.3 MODIFIED MODULUS FINITE ELEMENT MODEL

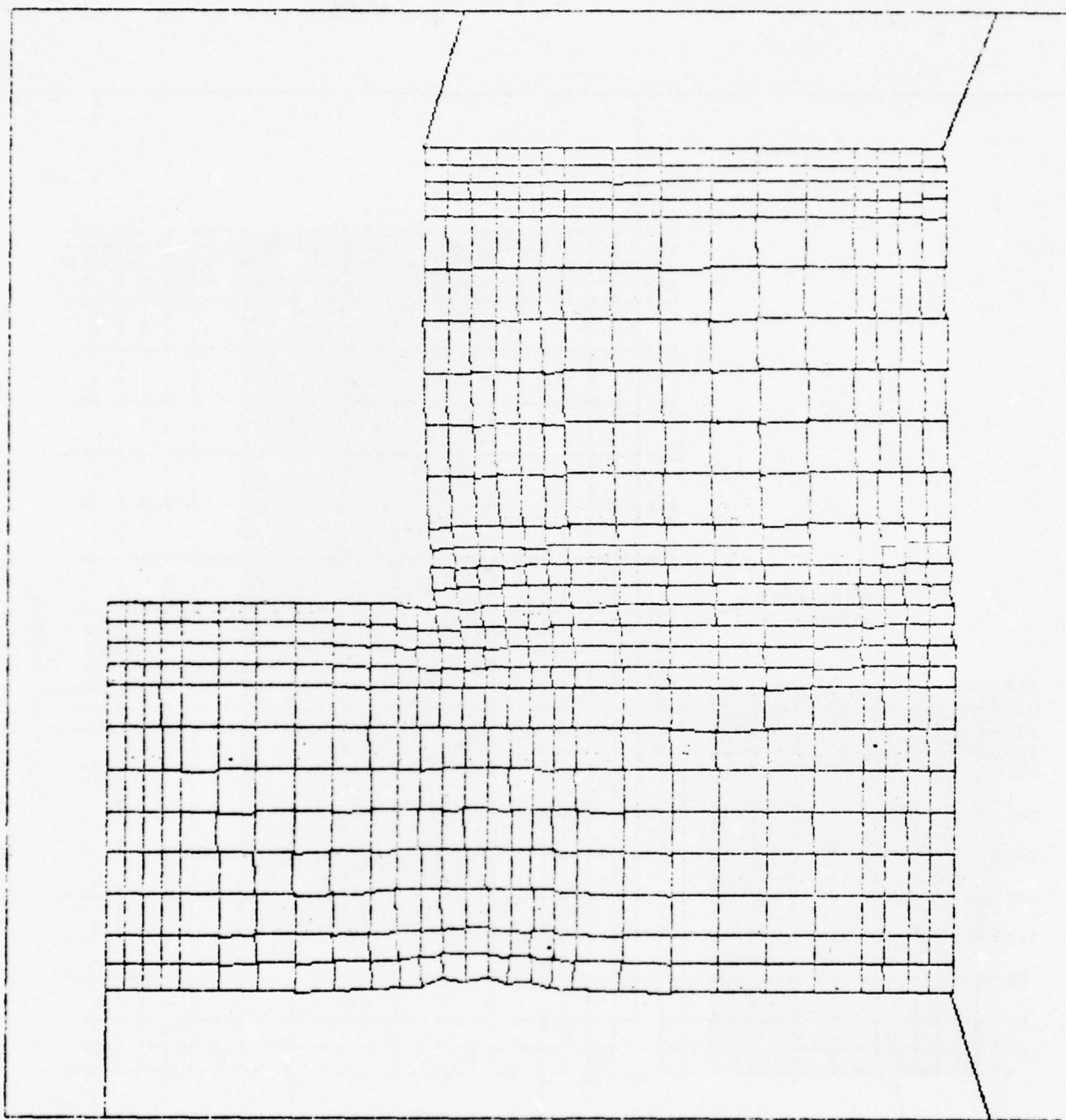


FIG. 2.4 DEFORMED SHAPE; NASTRAN SOLID MODEL, PRESTRESS ALONE

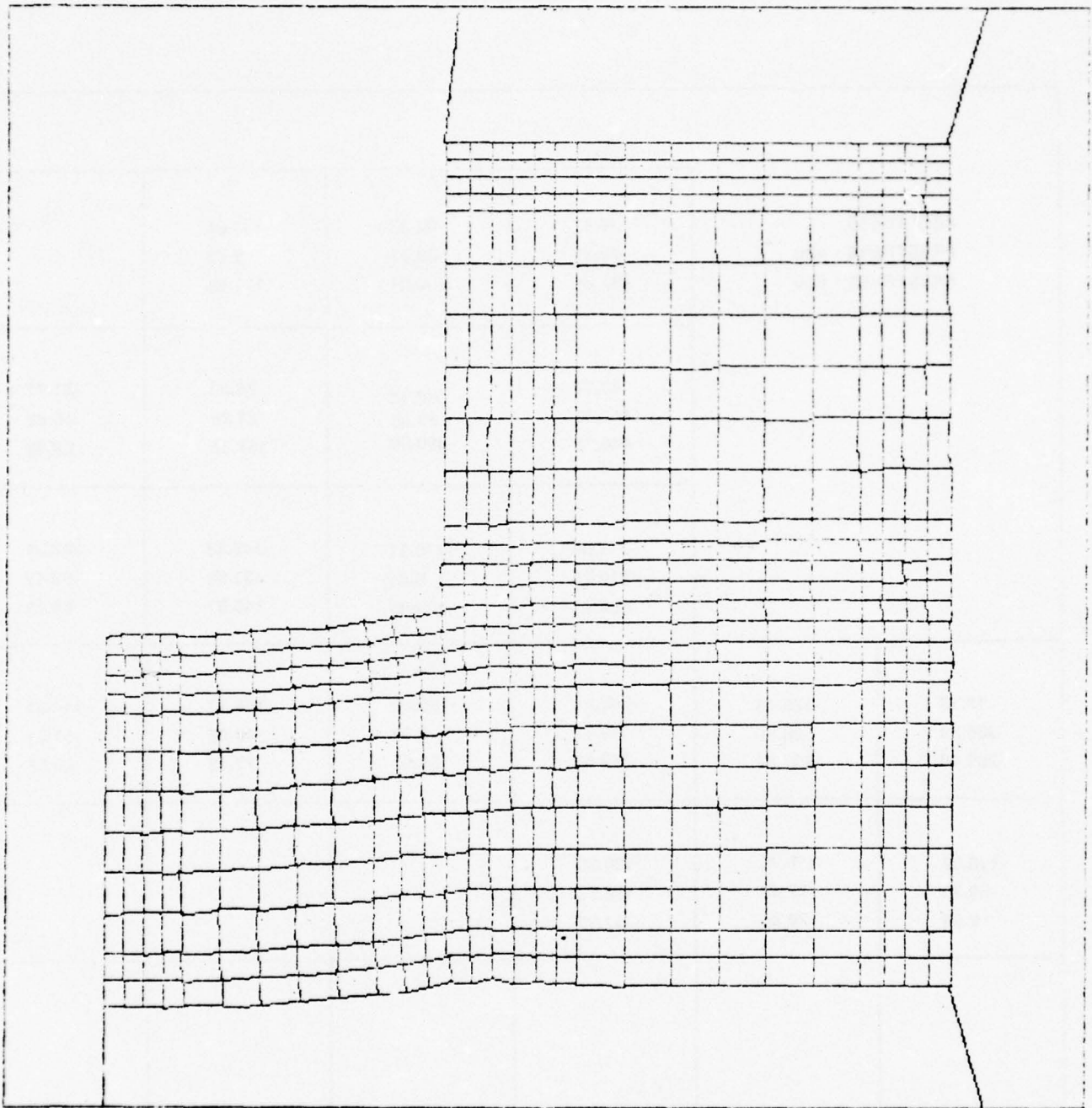


FIG. 2.5 DEFORMED SHAPE; NASTRAN SOLID MODEL PRESTRESS + 650 PSI (1 MCP)

PRESTRESS PRESTRESS + 400 PRESTRESS + 650		-16.47	-62.33	-133.64	
		72.91	39.92	5.33	
		197.24	200.04	157.63	
		-37.77	-69.13	-76.31	-81.92
		147.18	28.88	-21.26	-40.62
		446.78	300.00	158.18	89.98
		-271.04	-410.11	-348.33	-363.31
		210.29	-0.41	-31.98	-59.47
		802.21	249.89	145.97	55.21
-13.33	-225.84	-345.81	-162.22	-106.23	-114.84
-385.39	-88.80	19.42	-0.30	-40.02	-67.21
-261.48	537.85	389.83	184.97	77.40	28.97
-110.07	-115.78	-120.30			
-59.75	-77.45	-86.53			
8.90	-20.85	-37.89			

FIG. 2.6 MAXIMUM PRINCIPAL STRESS IN THE HAUNCH REGION, SOLID MODEL

14.35 -79.10 -139.29 85	18.27 -78.22 -133.96 86	17.14 -76.40 -124.06 87	15.32 -73.74 -108.64 88	PRESTRESS + 650 PRESTRESS + 400 PRESTRESS ALONE 89
11.84 -13.25 -62.85 57	11.61 -34.18 -59.53 58	11.16 -33.18 -53.34 59	10.43 -31.76 -45.50 60	61
5.16 -9.83 -18.04 29	5.10 -9.80 -16.57 30	5.05 -9.30 -13.14 31	4.86 -8.84 -9.17 32	33
1.34 -1.39 16.89 1	1.24 -1.69 10.48 2	1.27 -1.57 6.44 3	1.28 -1.07 3.95 4	5

NOTE: ☐ ELEMENT
NUMBER

FIG. 2.7 MAXIMUM PRINCIPAL STRESS IN THE HEAD, SOLID MODEL

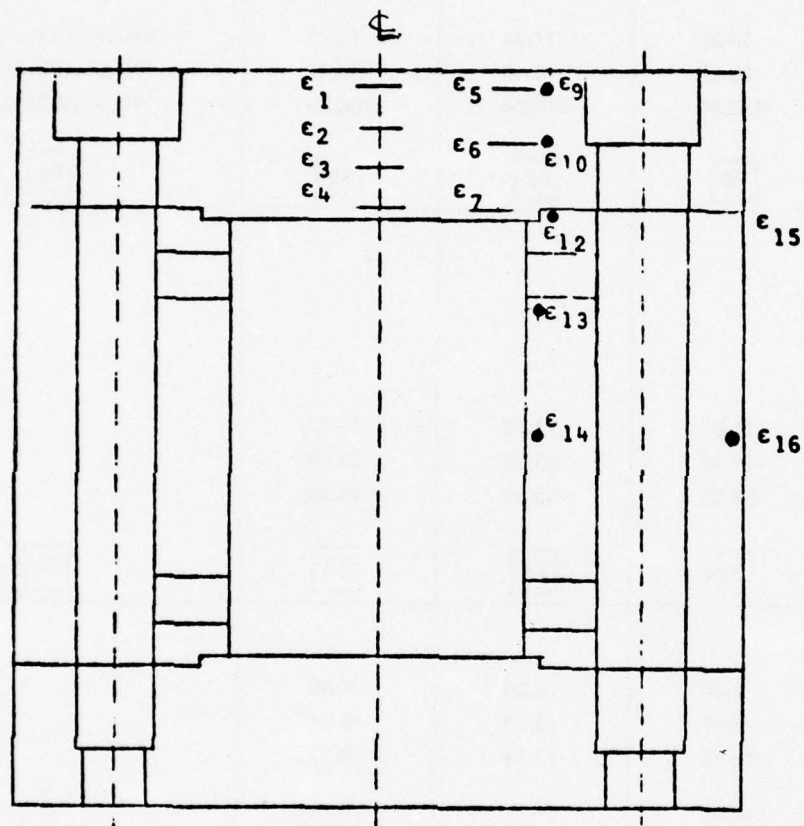


FIG. 2.8 POSITIONS OF STRAIN GAUGES. FOR COMPARISONS
WITH ANALYTICAL RESULTS

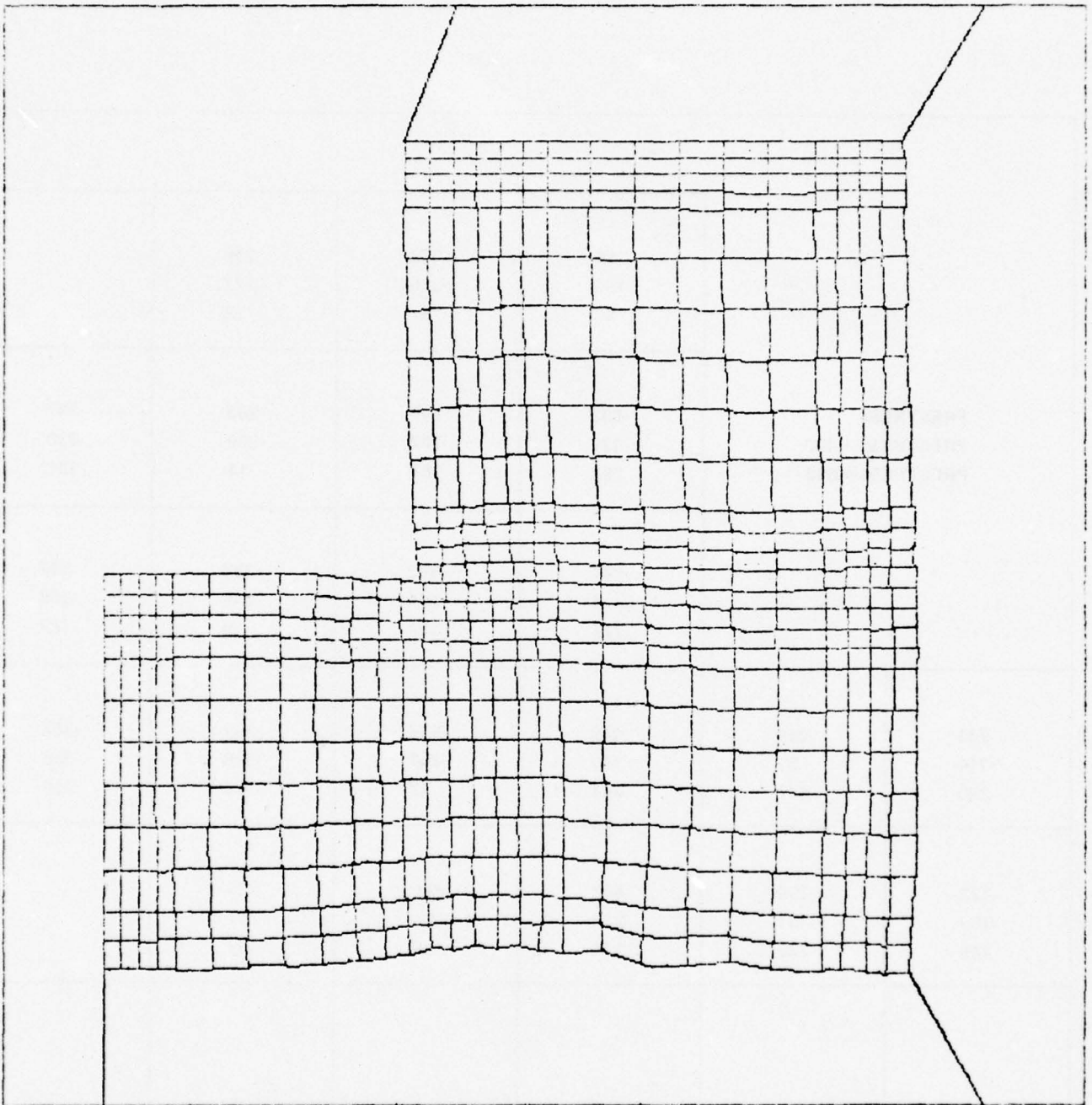


FIG. 2.9 DEFORMED SHAPE; NASTRAN MODIFIED MODULUS TECHNIQUE, PRESTRESS ALONE

PRESTRESS PRESTRESS + 400 PRESTRESS + 650		-56 -193 80	-138 -226 67	-216 -277 -23	
		-633 -127 283	-230 -202 183	-263 -280 -14	-297 -330 -131
		-294 -3 777	-363 -214 152	-322 -299 -5	-333 -352 -167
		-241 -114 236	-485 -137 361	-434 -261 12	-353 -326 -124
		-259 57 887			-362 -368 -210
		-442 -219 114	-468 -383 -55	-421 -331 -192	
		-122 -181 145	-250 -151 226		

FIG. 2.10 MAXIMUM PRINCIPAL STRESS IN HAUNCH REGION, MODIFIED MODULUS METHOD

12 169 57	18 170 58	27 174 59	37 177 60	PRESTRESS + 800 PRESTRESS + 1200 61	
110 313 29	108 309 30	105 299 31	100 284 32	33	
234 498 1	224 481 2	214 463 3	200 440 4	5	

NOTE: ELEMENT NUMBER

FIG. 2.11 MAXIMUM PRINCIPAL STRESS IN THE HEAD NASTRAN MODIFIED
MODULUS TECHNIQUE

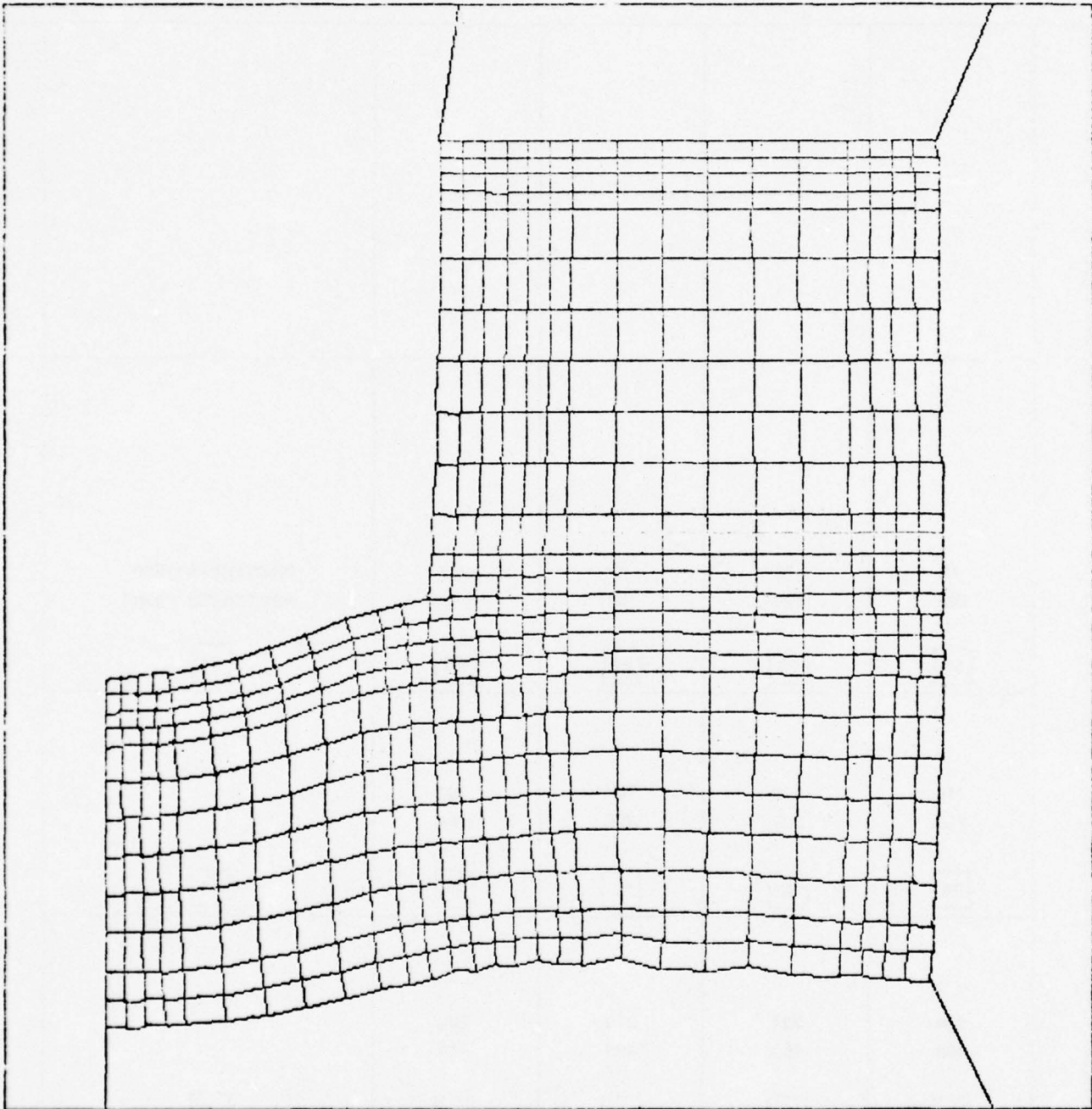


FIG. 2.12 DEFORMED SHAPE; NASTRAN MODIFIED MODULUS TECHNIQUE, PRESTRESS + 650 PSI (1 MCP)

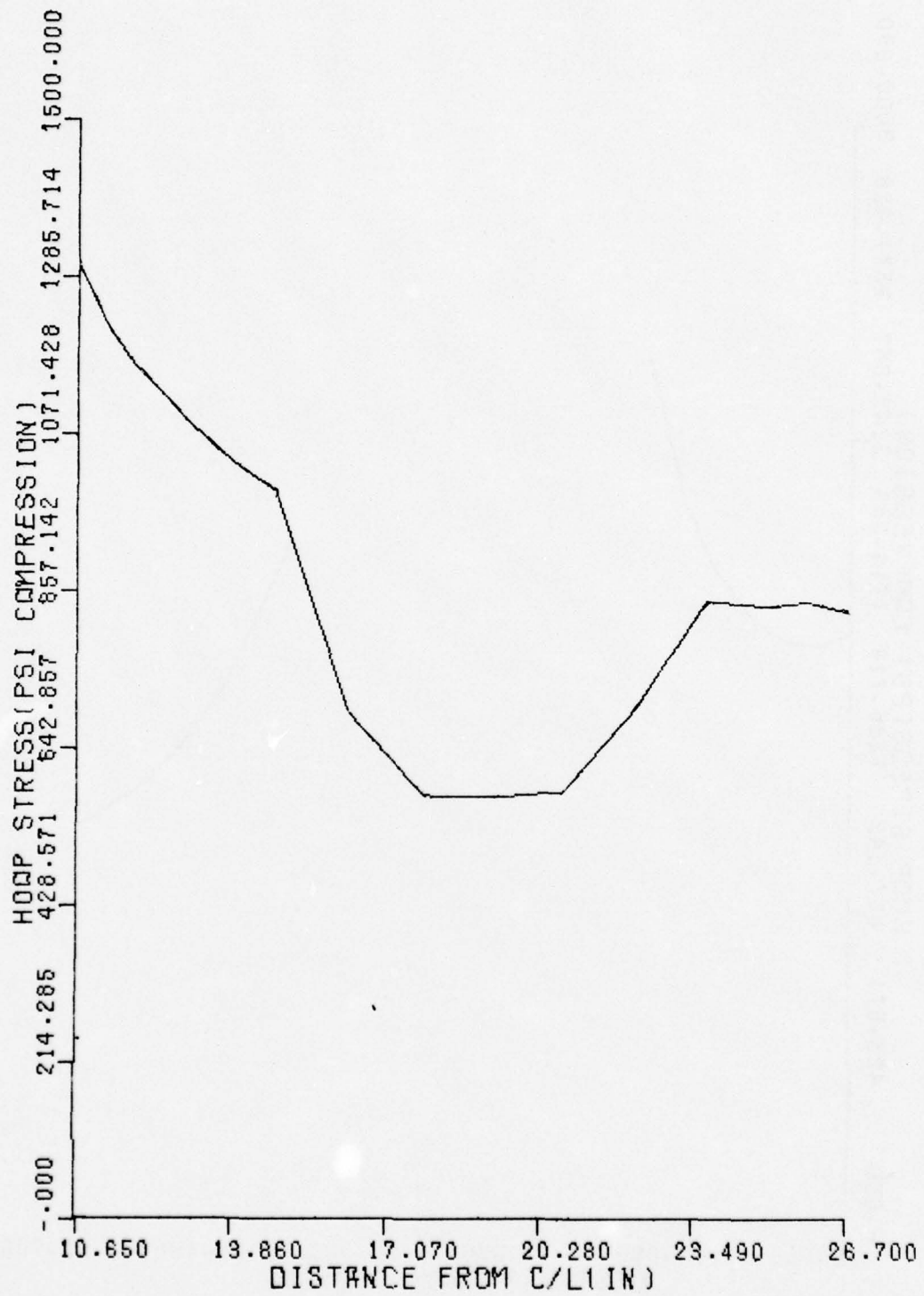


FIG. 2.13 HOOP STRESS BETWEEN THE CAVITIES AT BARREL MIDHEIGHT
PRESTRESS ONLY

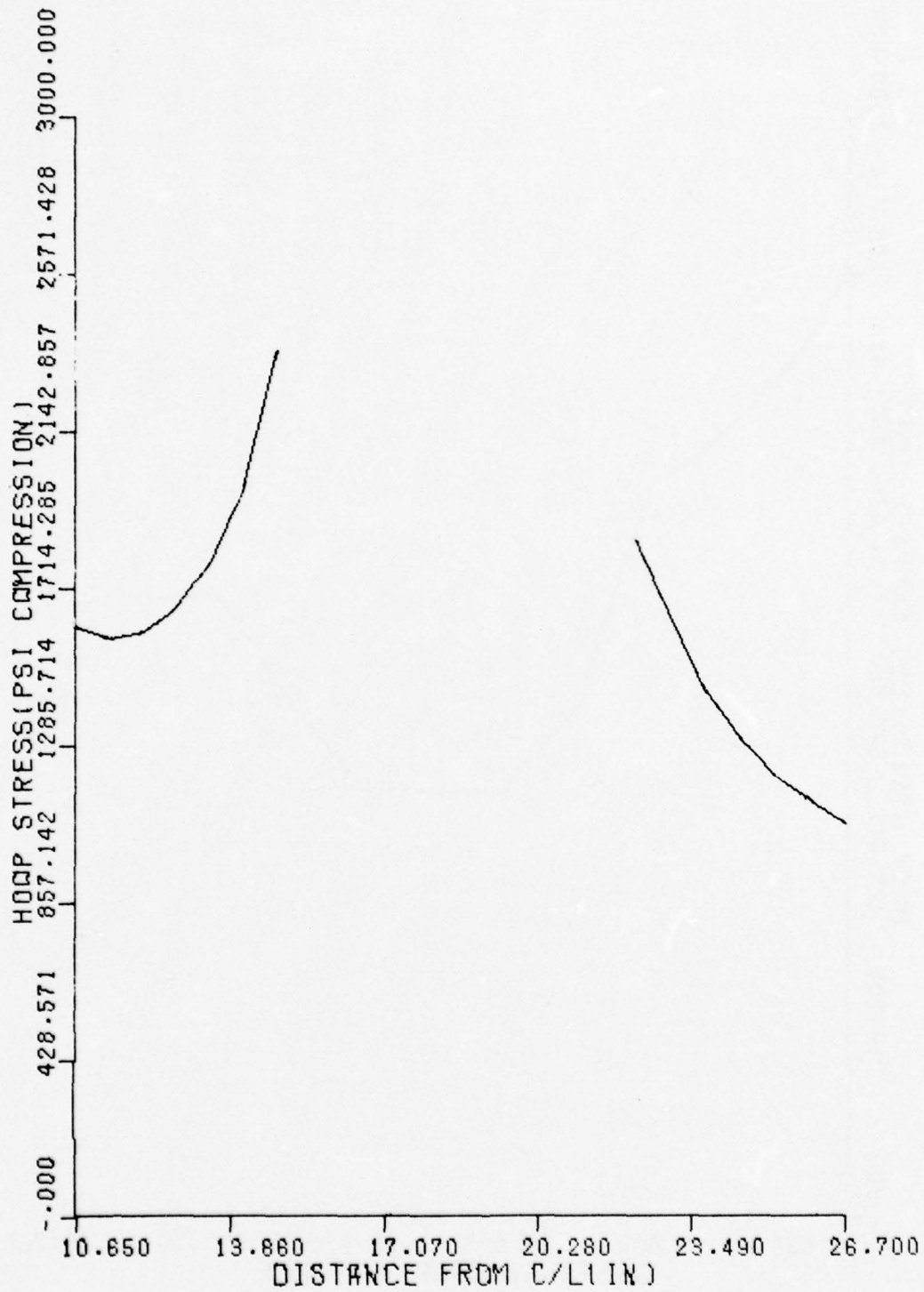


FIG. 2.14 HOOP STRESS THROUGH THE CAVITIES AT BARREL MID HEIGHT
PRESTRESS ONLY

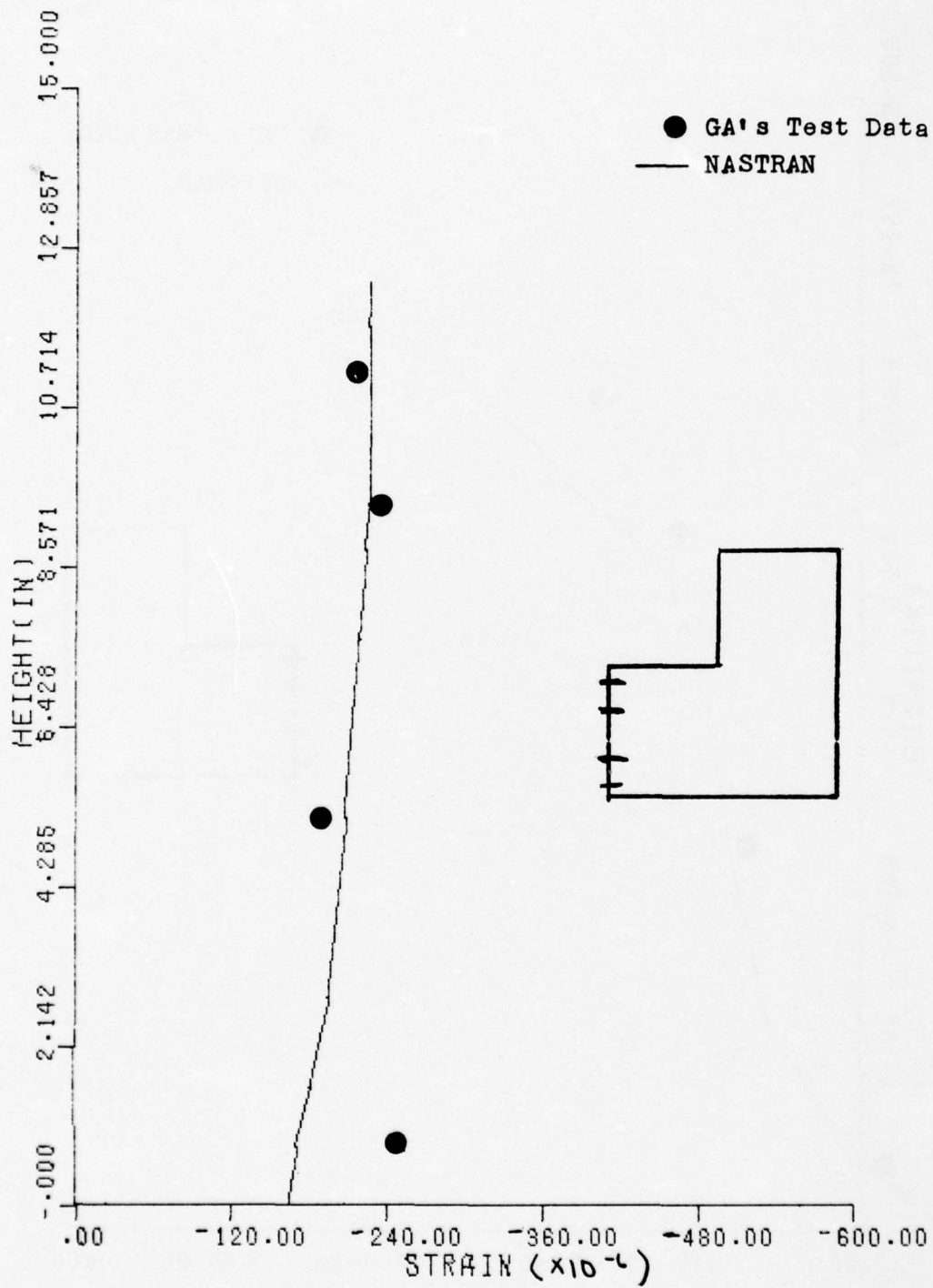


FIG. 2.15 RADIAL STRAIN THROUGH THE CENTERLINE OF THE HEAD, PRESTRESS ONLY

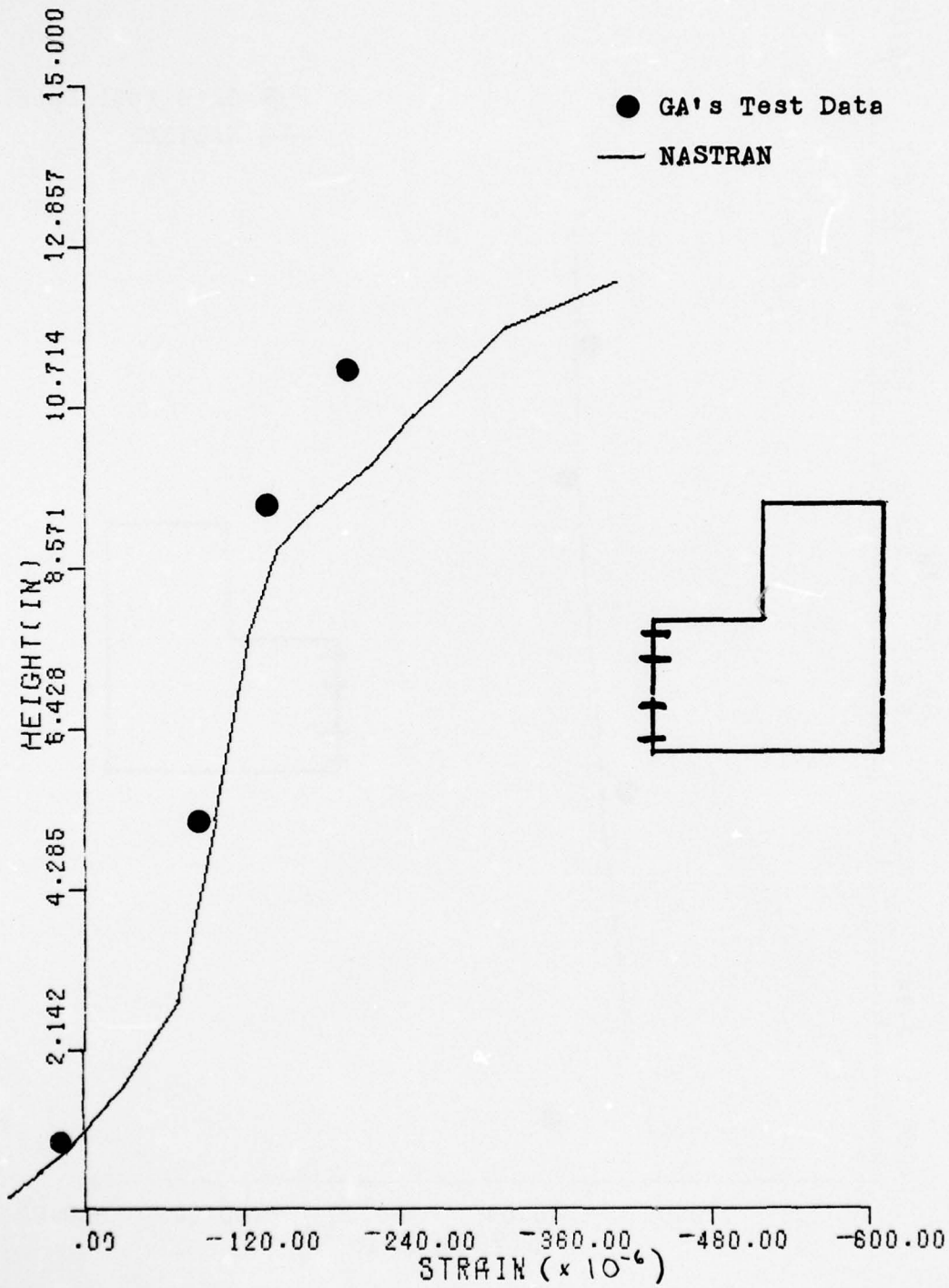


FIG. 2.16 RADIAL STRAIN THROUGH THE CENTERLINE OF THE HEAD,
PRESTRESS +850 PSI CAVITY PRESSURE



FIG. 2.17 RADIAL STRAIN THROUGH THE HEAD; PRESTRESS ONLY

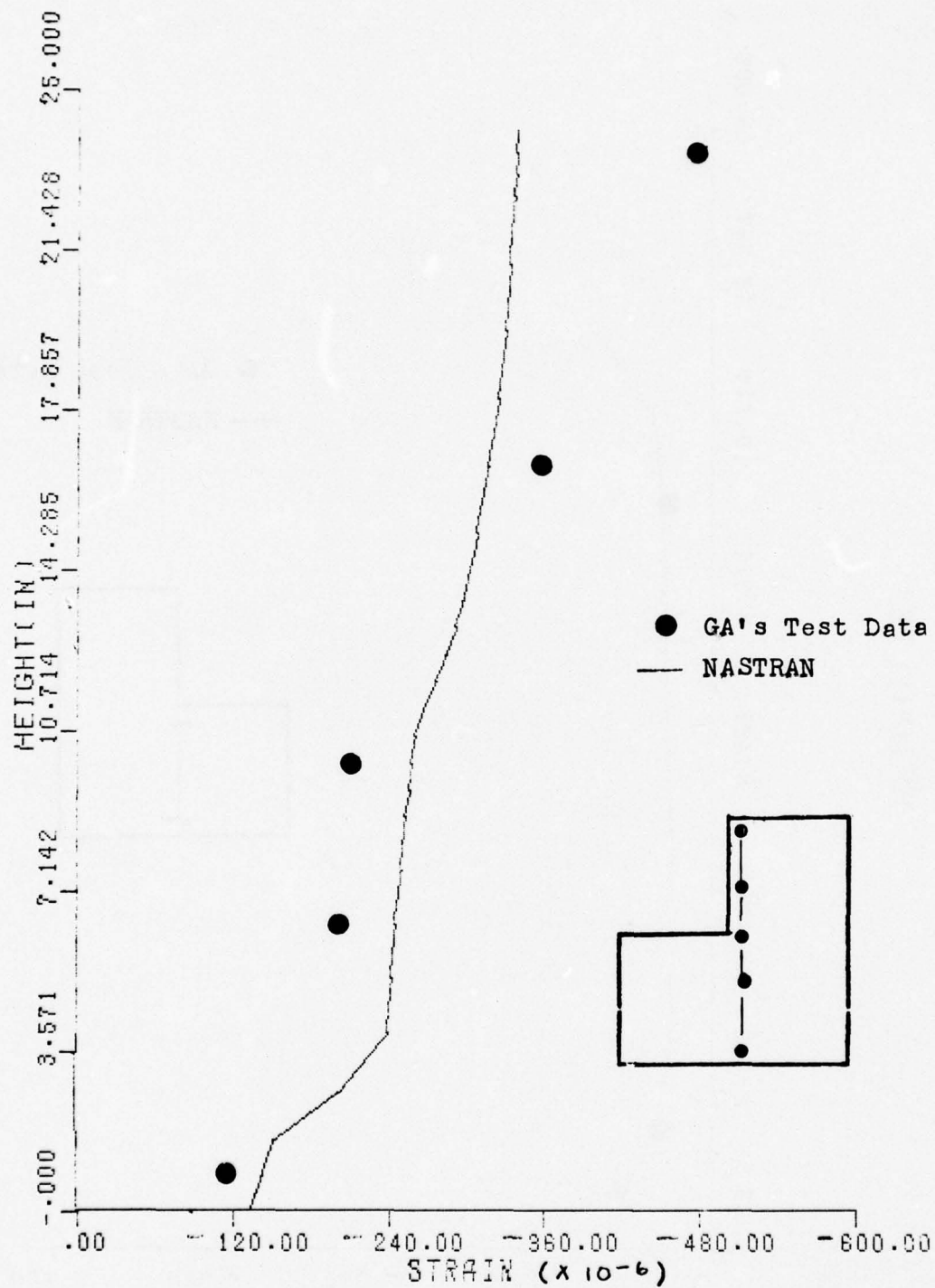


FIG. 2.18 INTERNAL HOOP STRAIN NEXT TO THE CAVITIES FOR THE GA 1/20 SCALE MODEL; PRESTRESS ONLY

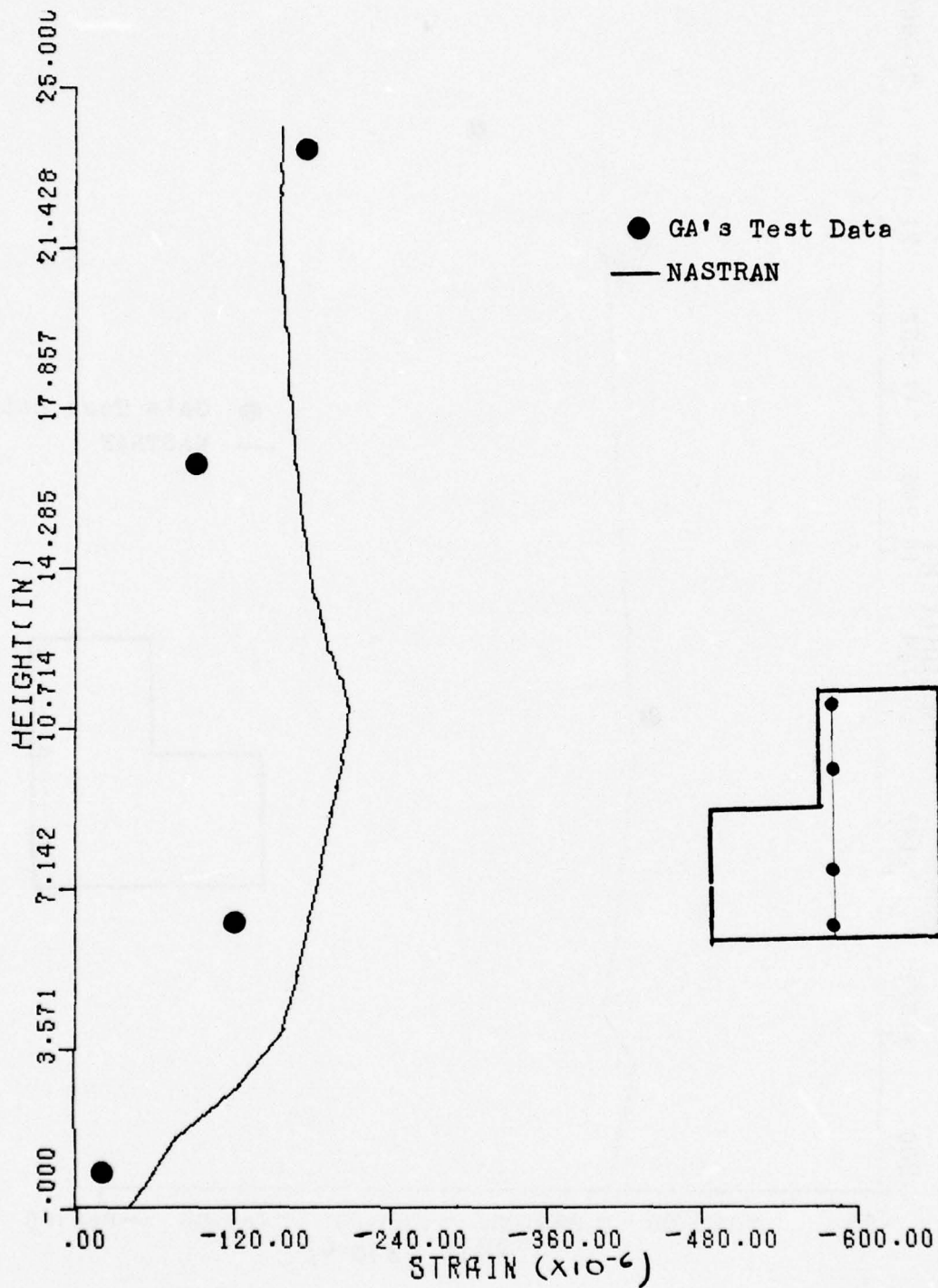


FIG. 2.19 INTERNAL HOOP STRAIN NEXT TO THE CAVITIES FOR THE
GA 1/20 SCALE MODEL; PRESTRESS + 650 PSI CAVITY PRESSURE

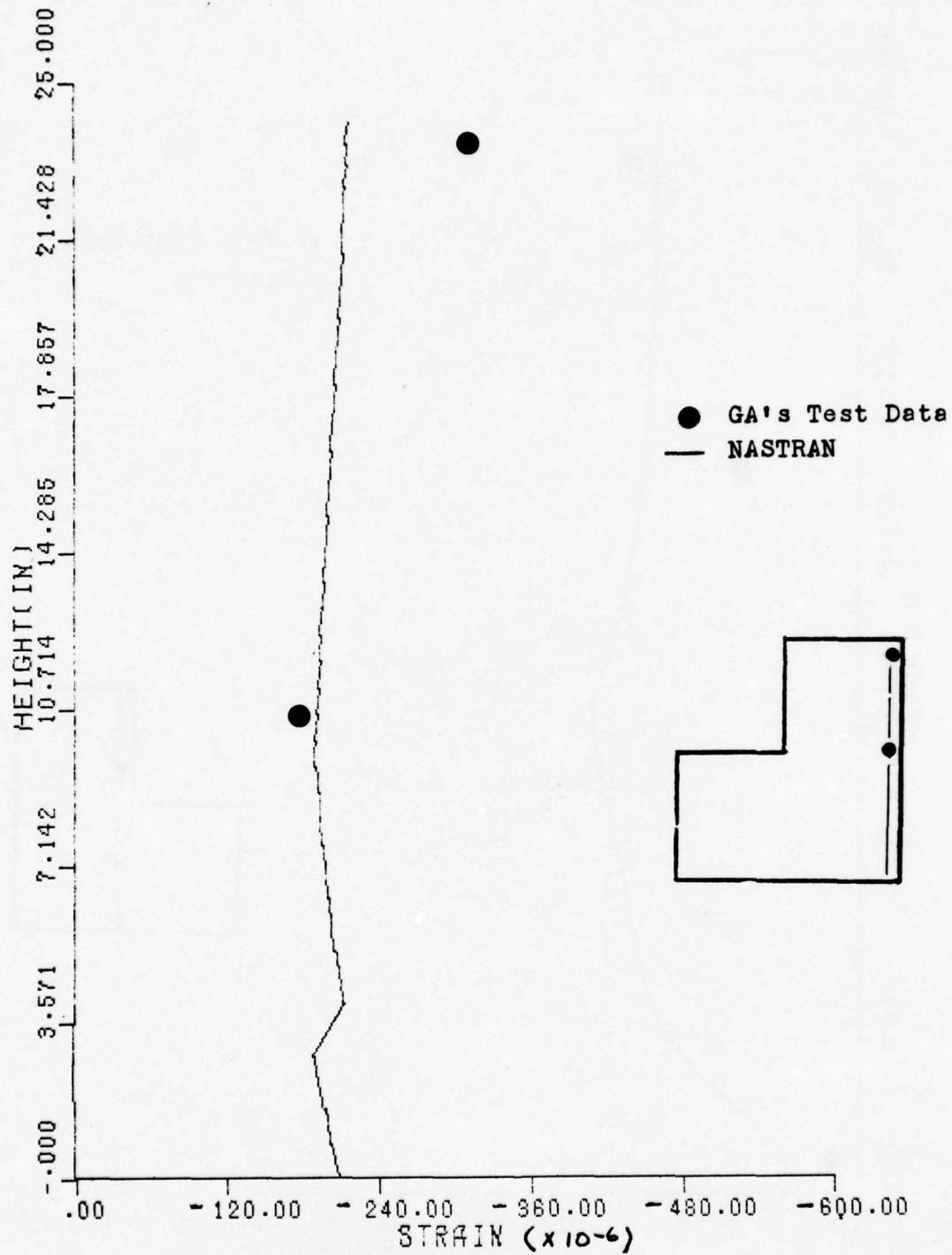


FIG. 2.20 EXTERNAL HOOP STRAIN NEXT TO THE CAVITIES FOR THE GA 1/20 SCALE MODEL; PRESTRESS ONLY

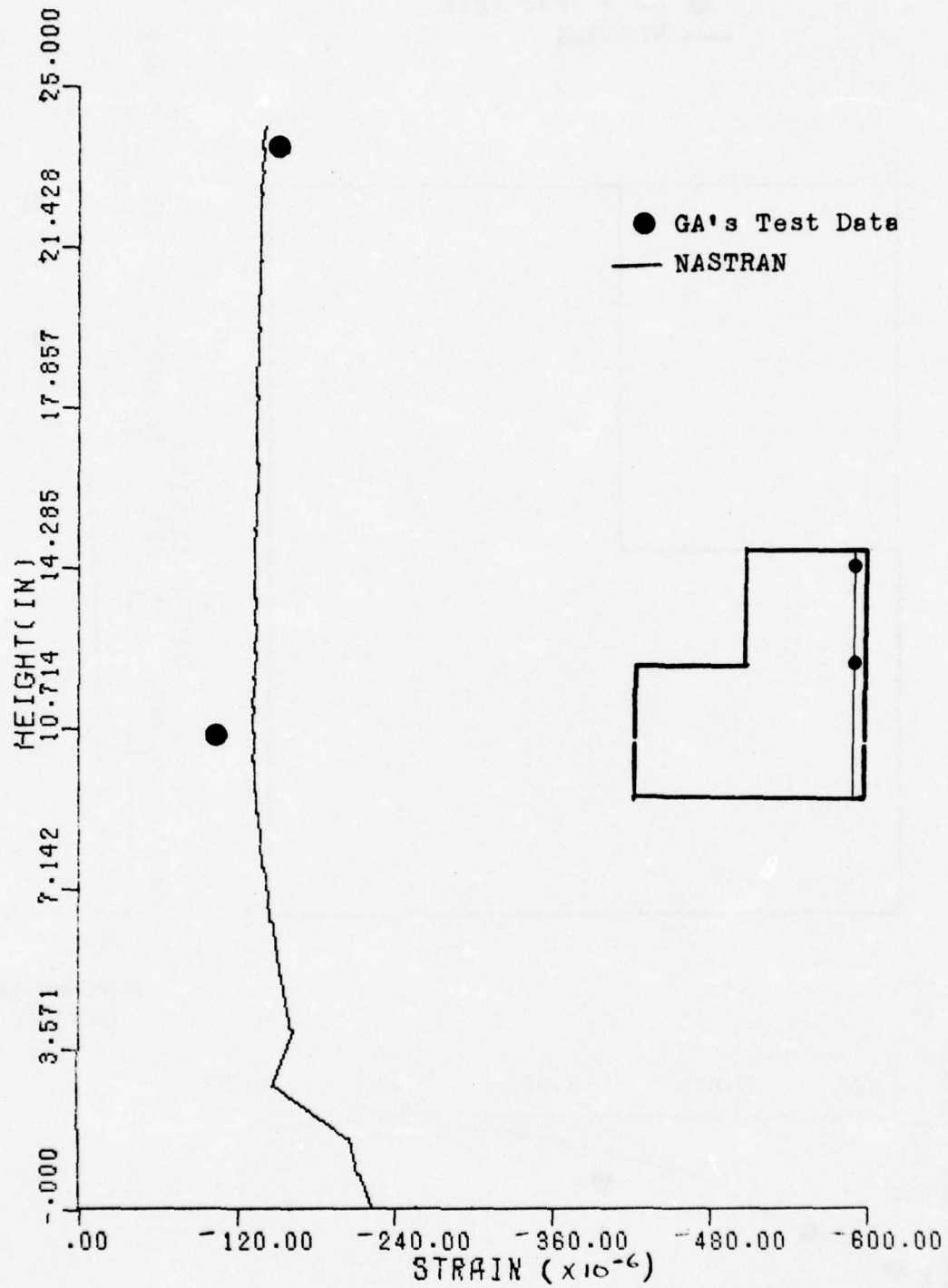


FIG. 2.21 EXTERNAL HOOP STRAIN NEXT TO THE CAVITIES FOR THE GA 1/20 SCALE MODEL; PRESTRESS + 650 PSI CAVITY PRESSURE

● GA's Test Data
— NASTRAN

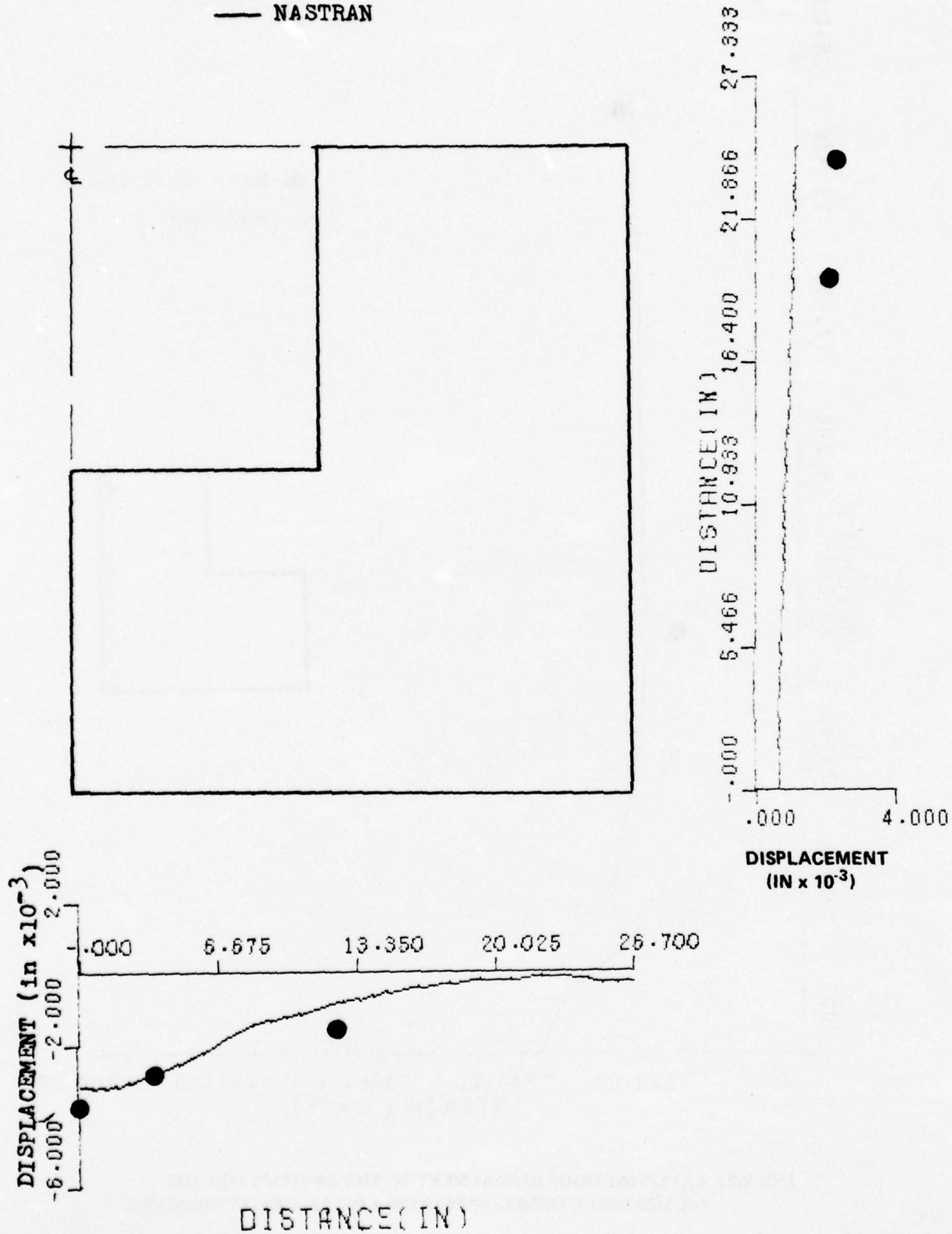


FIG. 2.22 DISPLACEMENTS IN GA'S 1/20 SCALE PCRV TEST; PRESTRESS + 650 PSI CAVITY PRESSURE

III. ANALYSIS OF PROPOSED GCFR PCR

PCR PROTOTYPE

The proposed reactor vessel (3.1) is a monolithic prestressed concrete cylinder weighing in the neighborhood of 50×10^6 pounds. As shown in Figure 3.1, its outside diameter is 81 ft and it is 71 ft high. It is not a solid mass of concrete since there are seven cavities of three sizes, numerous penetrations, and steel reinforcing which takes up about 0.5% of the total volume.

The reactor itself is located in a large central cavity which is 40 ft high and 20 ft in diameter. Six satellite cavities surround the main cavity; these contain gas circulators and heat exchangers. The three larger satellite cavities contain the primary steam generators; the three smaller ones, placed alternately around the circumference, are redundant backup units.

The side walls and bottom head will be cast as a single unit leaving a large opening at the top. The reactor core fuel rods are to be suspended from a plug which is inserted in this opening. The plug is a cylinder, roughly 12 ft in both diameter and height. It is held in place by a series of redundant locking devices, primary among which is a ring of toggles which transfer the cavity pressure load from the plug to the inner ring of prestress cables. Thus, this plug is a structural entity separate from the barrel and the bottom head.

Heat is generated by nuclear reactions in the core. Helium gas at an operating pressure of 1250 psi and a temperature of 1022°F flows over the core and back through the steam generator cavities. Water enters and steam leaves the cavities by way of penetrations in the cavity plugs. All the cavities are lined with a steel "membrane" of 3/4" plate to prevent leakage of the high pressure gas. In addition, the concrete is protected from the high temperature of the helium gas by this membrane which in turn is separated from the concrete by a thick layer of thermal insulation.

To maintain a state of compressive stress in the body of the concrete, vertical and radial prestress loads are applied by means of heavy steel cables in tension passing through and around the vessel. Six rings of vertical cables stretch from the top to the bottom heads; each ring consists of 20 to 30 multi-strand

(3.1) General Atomic Company, "Preliminary Safety Information Document (PSID) for the Gas Cooled Fast Breeder Reactor (GCFR)," Volumes I and II, San Diego, CA, Ga 10928 (Feb 1971).

cables under a tensile force of 1.29×10^6 lbs. Radial compression is supplied by wire cables wrapped on the outside cylindrical surface of the vessel. There will be enough layers under sufficient tension to exert an approximately uniform 1035 psi radial compressive stress on the cylindrical surface of the concrete barrel.

NASTRAN MODEL

Idealizations. The steel cavity liner and thermal insulation have been omitted from the structural model because they have only secondary structural strength. Rebar has also been omitted because its primary function is to retard or distribute local tension cracks; in addition, its cross sectional area is a small fraction of that of the concrete.

Further, exclusion of the circulator cavities from the model should not affect the gross behavior of the vessel since each is surrounded by prestress cables which tend to counter their weakening effect on the structure. Thus, the prestress cables around each of the cavities are also excluded from the model.

The top plug is not included as a structural entity in the model because it is connected to the barrel walls only at the innermost ring of prestress cables. However, an equivalent ring force applied to the cable anchors is a part of the loading on the model. The ring force is determined by multiplying the exposed bottom face area of the plug by the cavity pressure at a given load condition. This force is then distributed axisymmetrically about the ring of cable anchors. The plug is thus represented in the model by its effect on the top haunch.

PCRV Model. The structural model analyzed by NASTRAN consists of a large number of axisymmetric ring finite elements. It is a large hollow cylinder closed at the bottom and open at the top. The majority of the ring elements have a trapezoidal cross section, while a few elements of triangular cross section fill in at corners.

A large number of annular rings of various diameters are fitted together to form the structure. A vertical section of half the model is shown in Figure 3.2 which illustrates all of the 1007 grid points in the model and their connections by 944 ring elements. The grid points all lie in a plane which includes the symmetry axis of the PCRV.

Trapezoidal and triangular ring elements are uniquely specified by listing four (or three) points in counterclockwise order; NASTRAN internally attaches to these points inertial and elastic properties appropriate to a ring symmetric about the axis of the vessel. Only axial and radial displacements of the grid points are allowed with these elements, although circumferential (hoop) stress is calculated in addition to axial and radial stress at the centroid of the section of each element. The ring elements cannot be used in conjunction with any of the other elements in the NASTRAN library because the axisymmetry implied by the use of the ring elements is not compatible with the other elements.

Constraints. Of the six degrees of freedom available to a point in three dimensional space, only two translational displacements are available when the axisymmetric ring elements are used in a model. Radial and axial displacements are permitted; angular displacement and all three rotations must be constrained to zero. In addition, grid points on the axis of symmetry are permitted only axial displacement since the direction of positive radial displacement is ambiguous at $R = 0$.

When all the constraints are applied, 2004 degrees of freedom remain from which a stiffness matrix is constructed by NASTRAN for the PCRv model.

Loads. In a NASTRAN analysis using axisymmetric elements, loads must be applied to grid points; there is no provision for internal conversion of pressure loads to point loads. The loads must be axisymmetric and each must be supplied as a point force at one of the grid points shown in the vertical half section shown in Figure 3.2. The total force due to the cavity pressure or the circumferential prestress pressure on the surface of an element is shared equally by each of the neighboring grid points; that is, one half the pressure times the element surface area to which the pressure is applied is stated as a radial force, an axial force, or a combination of the two, on a grid point.

Axial prestress is supplied by six concentric rings of cables extending through the body of the concrete between the top and the bottom heads. There are thirty multi-strand cables in the inner rings and seventy in the outer rings. Each can be approximated by a force uniformly distributed along the circumference of the ring. Grid points were chosen so that each ring of axial prestress cable anchors coincides with a grid point. The cables in the inner two rings bend around the reactor cavity so that these cables apply forces to the PCRv at two points inside the concrete in addition to the forces applied at the top and bottom head anchor points.

For the static and normal modes analyses the forces are supplied as constant forces at the appropriate grid points. It is a simple matter to alter some or all of the forces to correspond to differing cavity pressures. A multiplier on a single card must be changed.

For the dynamic analysis a different method of supplying loads to the computer model is necessary since neither static forces nor negative times are recognized by the dynamic analysis formats in NASTRAN. The method is as follows. Normal operating cavity pressure and prestress loads are applied to the vessel as step loads at zero time. These are then constant magnitude time dependent forces for the duration of the calculation. After a long enough time for structural ringing to damp out, the cavity overpressure is increased to the value of interest for the particular problem case.

The dynamic equivalent to the static loads thus is applied as a step function at zero time, and the structure vibrates at its fundamental frequency. These loads are constant in time so that, after the ringing is damped out, other transient loads can be applied to what is, in effect, a statically preloaded structure. The time interval between application of the static preload forces and the desired transient load should be 10^5 to 10^6 times the natural period of the structure.

In the case of the PCRV model, normal mode calculations resulted in a lowest natural resonance of about 83 hertz, with a period of about 0.012 sec. The prestress loads were applied at $t = 0$ and the transient loads at $t = 3000$ sec; thus, the time interval is $(3000)/(0.012) = 2.5 \times 10^5$ times the natural period. Ringing was found to have died away when 1000 sec had elapsed.

The rise time of the transient load should not be zero -- this would lead to the same undesirable ringing observed when the prestress loads are applied. Yet, for the load to appear to the structure as a step load, its rise time should be less than one tenth of the first quarter period of the natural vibration, or $(0.1)(0.003) = 0.0003$ sec. The transient loads actually used in the calculations reported here had rise times of 0.00001 sec (one hundredth of a millisecond).

The transient load applied to the finite element model is shown in Figure 3.3. The figure shows only the pressure in the main cavity as a function of time. As described above, initial cavity pressure (1250 psi) was applied at $t = 0$; at $t = 3000$ sec the cavity pressure rose to 2500 psi in 10^{-5} sec and remained constant. Prestress cable loads were applied with the initial cavity pressure at $t = 0$ and were constant throughout the computation.

NASTRAN CALCULATIONS

The model described above has been used successfully for a number of static and transient analyses. Grid point displacements and element stresses were calculated for a number of static loads and one transient load. Results of these calculations are discussed in the following.

Static Calculations. Stresses and displacements produced by several static load combinations were computed; three cases are discussed here. The prestress loads produced a contraction of the vessel; this was then approximately balanced by application of the 1250 psi normal working pressure in the reactor cavity. The third case combined the prestress loads with twice normal working pressure in the reactor cavity: 2500 psi. Other cases were considered for pressure loads between the two mentioned; they served mainly to establish the linear nature of the solutions: i.e. displacements and stresses are proportional to the magnitude of the reactor cavity pressure load.

Static Stresses. The objective of the calculations is to find those regions of the PCRV in which tensile stress exceeds + 600 psi (the estimated tensile strength of concrete). These are the regions in which cracking would be expected to occur in the prototype vessel. At the other extreme, compressive failure occurs in regions in which compressive stresses exceed - 6000 psi; however, no such regions were found with the largest load used.

The static hydraulic tests described earlier produced longitudinal cracks in the test models at mid-height on the inner and outer surfaces of the barrel, in the top and bottom heads, and at both haunches. As shown in Figure 3.4 and 3.5, excessive tensile stresses were observed primarily at the haunches in the calculation model.

For the load magnitudes considered here, cracking will occur only near the surfaces of the PCRV. This is indicated by the principal stresses shown in Figure 3.5. The maximum, or most tensile, principal stresses are shown for several elements at each haunch. Compressive or low tensile stresses are observed in the second element into the body of the PCRV from each surface. Thus, the cracks which are implied by the high principal stresses in the surface elements do not propagate very deeply into the concrete and should be contained by the reinforcing bars in the neighborhood.

Tensile stresses calculated by NASTRAN at the top and bottom outside corners of the vessel did not exceed 25 psi. Since these were found in segments of the vessel far removed from the reactor cavity, they are considered unimportant to the integrity of the PCR. Cracks induced by such small tensile stresses in remote areas of the vessel can be contained easily by the rebar in that area of the vessel.

The elements in the barrel walls at each haunch exhibit large tensile stresses in the axial direction. At the bottom haunch, the element in the bottom head at the corner exhibits a large tensile stress. These observations are consistent with the notion that the heads and barrel walls bend away from each other at the haunches when the cavity pressure reaches high levels. Stresses calculated in various critical regions of the PCR are indicated in Figure 3.4.

Transient Calculations.

Damping. Uniform structural damping was added to the finite element model for the dynamic calculations. The following artifice is used to incorporate uniform damping into NASTRAN model calculations. Consider the equation of motion for a single degree of freedom oscillator:

$$m \ddot{x} + b \dot{x} + k x = P(t)$$

(where the symbols have their usual meanings.)

Assume harmonic stimulus and response at angular frequency ω ; then:

$$-m \omega^2 x + i \omega b x + k x = P(\omega).$$

A complex stiffness can be defined from the last two terms:

$$i \omega b x + k x = (1 + i g) k x$$

where

$$g k = \omega b, \text{ or, } b = (g/\omega)k.$$

Now rewrite the original equation of motion:

$$m \ddot{x} + (g/\omega)k \dot{x} + k x = P(t).$$

NASTRAN solves this equation with the damping coefficient expressed in terms of measured parameters for the given material. g is the loss factor appropriate to the structural material, and ω is taken (in NASTRAN) to be the radian frequency of the fundamental structural resonance.

Loss factor is the fraction of kinetic energy dissipated in each vibration cycle; it is also twice the fraction of critical damping in the structure. A value of g typical of concrete (and many other materials) (1.1; 1.2) is $g = 0.1$, or 5% critical damping. In the course of checking various aspects of the use of the NASTRAN transient analysis module on this problem, several values of g were used. The values ranged from 0.0005 to 0.1; i.e., from essentially zero up to the value taken to be typical of concrete. No more than minor differences in grid point displacements were detectable in the output.

Transient Displacements. Calculated grid point displacements at 1000, 2000 and 3000 seconds following application of the equivalent static base loads (prestressing plus 1250 psi cavity pressure) were consistent with those calculated for the static load using NASTRAN's static analysis module. Transient radial and axial displacements are shown in Figures 3.6 through 3.10 for several grid points during the 30 msec following application of the cavity pressure rise to 2500 psi at $t = 3000$ sec.

Figures 3.6 through 3.8 show the displacements of three grid points at which the innermost ring of prestress cables are in contact with the concrete. The next two figures (3.9 and 3.10) show the displacements at barrel mid-height on the inner and outer surfaces. These five points are of greater interest than those on the bottom of the PCRv, which will be fixed on a firm foundation when the PCRv is built.

Also shown on each of these five figures are the displacements produced by the two equivalent static loads: prestress forces plus 1250 psi cavity pressure and prestress forces plus 2500 psi cavity pressure.

It is obvious that, by 3000 seconds, structural ringing due to the step loads applied at $t = 0$ had died out: the displacements produced by the initial transient step loads agree with those produced by the 1250 psi static load. Calculations out to 30 msec following application of the second step load in the cavity indicate structural ringing; this same phenomenon must have occurred at $t = 0$, but it had damped out by 3000 seconds.

In each case the radial component of displacement settles into a lightly damped oscillation about the equivalent static load produced displacement. The axial displacement in all cases seems

-
- (1.1) Penzien, J. and Hansen, R. J., "Static and Dynamic Elastic Behavior of Reinforced Concrete Beams" J. Am. Concrete Inst. 25 545 (Mar 1954).
 - (1.2) Tan, C. P., "Prestressed Concrete in Nuclear Reactor Vessels: A Critical Review of Current Literature" Oak Ridge National Laboratory, ORNL4227 (May 1968).

to be drifting toward the static value; by 30 msec none have progressed very far toward this value though. The axial component at the prestress cable anchor points (Figures 3.6 through 3.8) oscillates about an upward drifting center point. Both radial and axial vibrations have a period of 11 to 13 msec, which corresponds to the lowest mode frequency of 83 hertz calculated for the structure by NASTRAN. This indicates degenerate modes of oscillation, though it is not obvious that the radial and axial directions are, in fact, the normal coordinates for the vibration.

It is estimated that several hundred msec would be required for the axial displacement to reach the magnitude of that produced by the equivalent static load of 2500 psi cavity pressure. It must be remembered that the load for this calculation was held constant at 2500 psi; an actual load would decay in time as the hot gases bleed from the main reactor cavity into the satellite cavities. Thus, less time would be required for the axial components of displacement to reach the values pertinent to the applied load at a given time. Once having reached this value, the axial displacement would decay at the same rate as the load.

Radial oscillations are apparently more readily initiated than the axial vibrations. For the axial modes, the PCRV can be viewed as an extremely large mass (the barrel walls) on the end of a short cantilever (the bottom head). This mass is set into vertical vibration primarily by the upward pressure forces exerted on the partial closure of the top head. Ringing occurs but the inertia of the massive walls retards the net upward motion of the walls. Radial oscillations, however, are more readily initiated because the resistance to the attendant deformations arises primarily from hoop stresses in the walls; no large mass must be accelerated. Gravitational forces are not a consideration in the relative behavior of the axial and radial vibrations simply because gravitation was excluded from the finite element model.

Transient Stresses. At 1000, 2000 and 3000 seconds following application of the equivalent static loads, the stresses in the dynamic problem were, like the grid point displacements, consistent with the stresses calculated for the purely static load case. At 3000 seconds a damped oscillation with a period of 11 - 13 msec began in all stresses. In each case the oscillations were centered on the stress level calculated for the static load consisting of prestress forces plus 2500 psi cavity pressure.

Stresses in several elements are illustrated in Figures 3.11 through 3.16 during the 30 msec following application of the transient step of cavity pressure from 1250 to 2500 psi. The elements shown are either those in which the largest stresses were observed, or they are those in regions of the PCRV where cracking was observed in static tests of similar PCRV's. Three components of stress were calculated by NASTRAN for each element; axial, radial and circumferential. The component shown in each

illustration is the largest of the three in each case. This tends to give a clearer picture of the type of crack failure to be expected in a given region of the PCRV.

In regions of the PCRV other than those shown, stresses either remain compressive or do not reach tensile levels of any significance (i.e., no more than 600 psi tensile). Throughout the entire PCRV, the greatest tensile stress was about +1600 psi, and the greatest compressive stress was -2500 psi.

In each illustration, the stresses which correspond to the static loads of prestress plus 1250 psi and prestress plus 2500 psi cavity pressure are indicated. The 1250 psi static load produces the same stress in each element that is produced by the dynamic load which is applied at $t = 0$ in the transient problem. The 2500 psi static load, for each element, produces a stress which is the center of stress oscillations in each element for at least 30 msec following application of the 1250 psi step pressure load at $t = 3000$ seconds.

In Figure 3.15 the axial and radial stresses near the outer surface of the barrel at mid height are shown. Circumferential stress falls between these two. Axial stress is by far the largest of the three, and it never becomes tensile - at least for the duration of the calculations. The interesting feature of this illustration is the radial stress: it holds virtually steady at 1060 psi. Recall that the circumferential prestress load applied by the encircling cables is 1035 psi; loading, transient or static, has little if any effect on this component of stress in elements far removed from the reactor cavity.

In the bottom head away from the axis of symmetry axial stresses are small. Radial and circumferential stresses are of approximately the same magnitude, with the radial component generally slightly the larger of the two. These two components exceed the tensile strength of concrete, indicating that cracking and perhaps spalling is to be expected on the outer surface of the bottom head. This phenomenon may have some influence on the type of support used under the PCRV. The radial and circumferential stresses in the lower head element in which the radial stress has the largest peak value are shown in Figure 3.16.

Peak Tensile Stress. Response of a finite element model of the proposed GCFR PCRV to a transient step load has been determined with NASTRAN. The load consists of a jump from operating pressure to twice operating pressure (2500 psi) in 0.1 msec; from then on the load is held constant in time.

The greatest peak tensile stress occurs at 6 msec following application of the transient step, and is found in an element at the lower haunch; it was + 1560 psi --- almost three times the estimated tensile strength of concrete. This figure will be used in the discussion of containment capability in the next chapter.

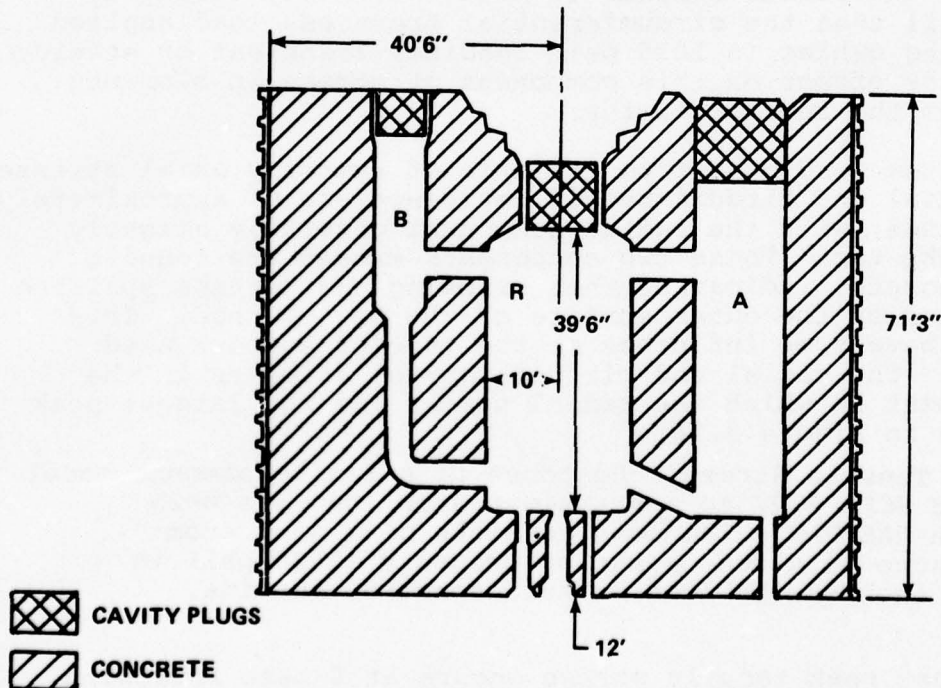
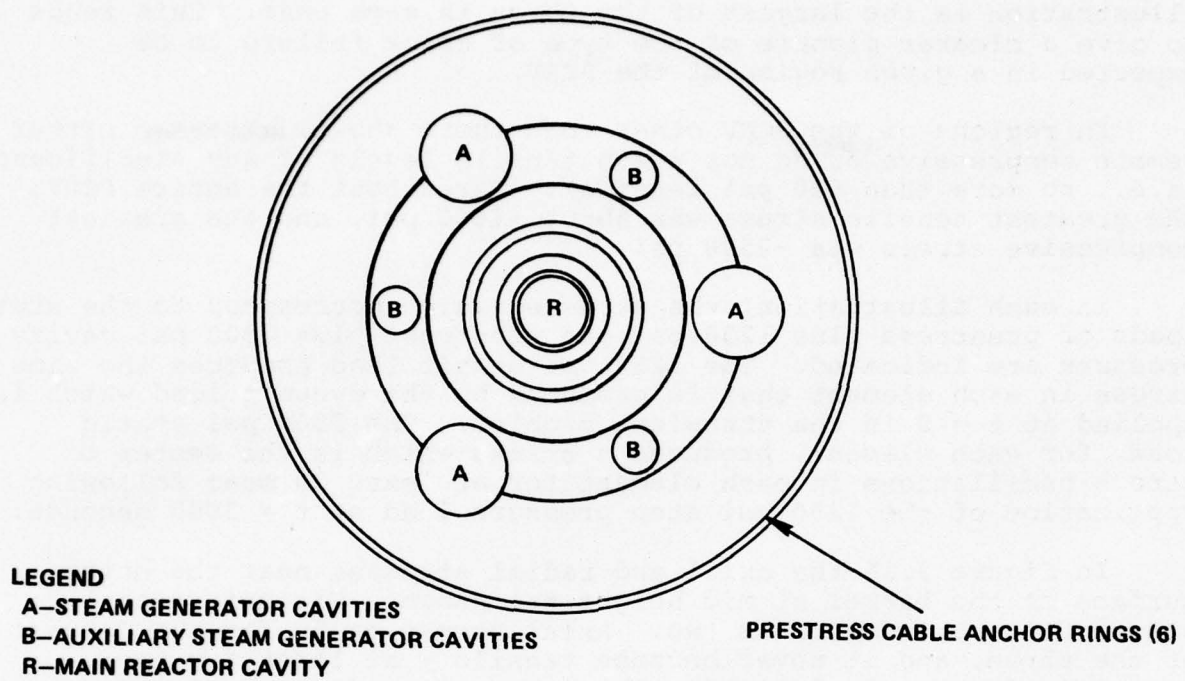


FIG. 3.1 PCRV CONFIGURATION

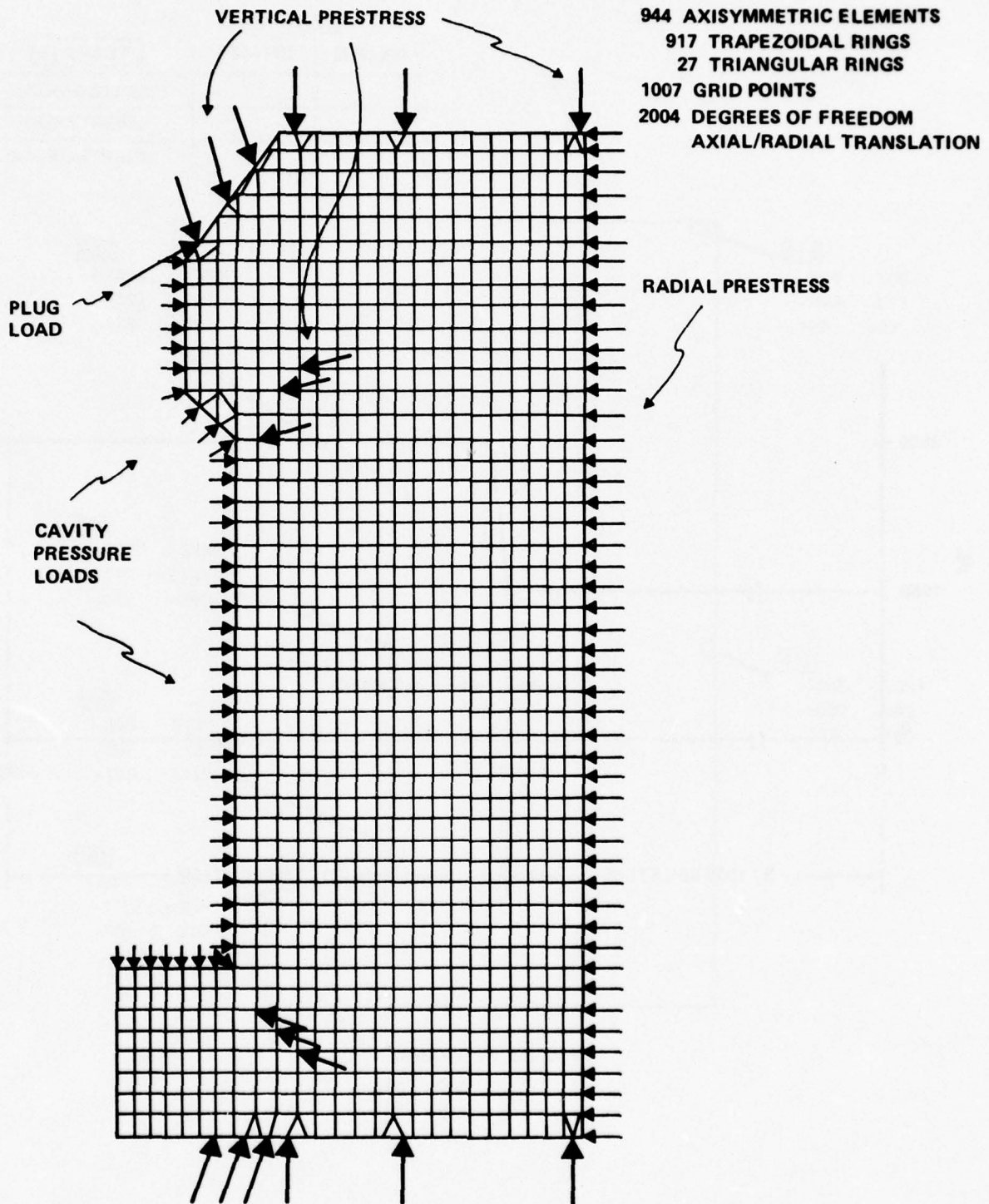


FIG. 3.2 FINITE ELEMENT GRID AND LOADS FOR PCRV NASTRAN MODEL.

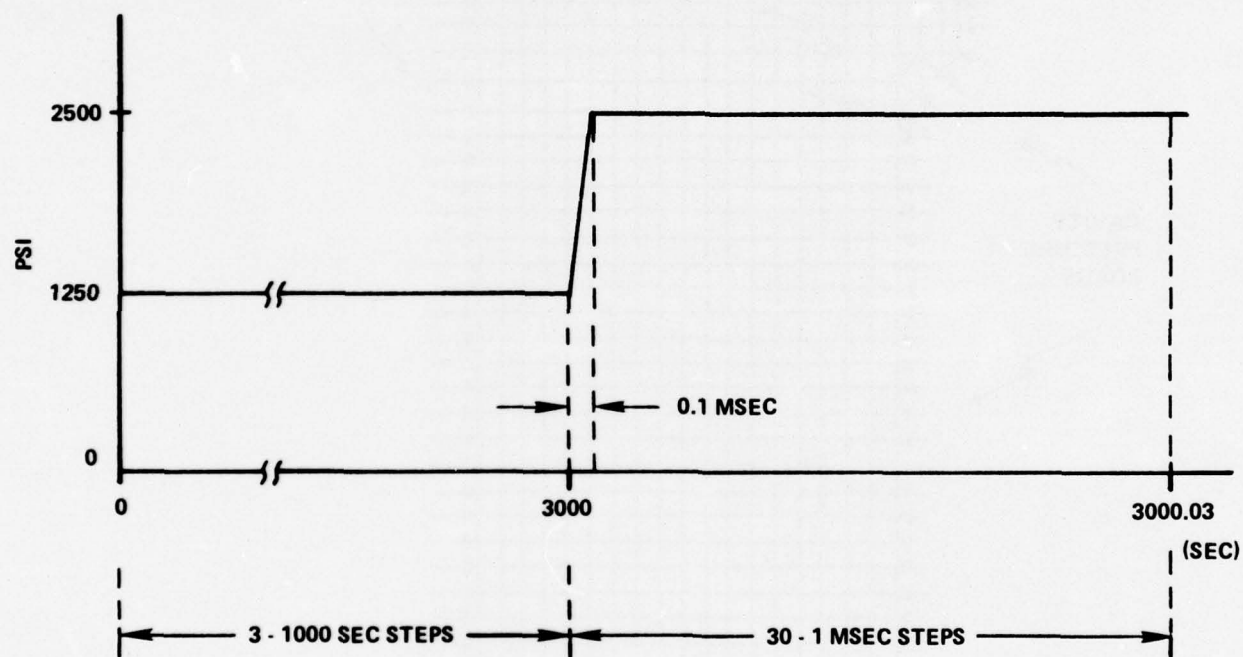


FIG. 3.3 STEP LOAD.

LEGEND

ELEMENT	LOAD	
	1250 PSI	2500 PSI
RADIAL STRESS:		
HOOP STRESS:		
AXIAL STRESS:		

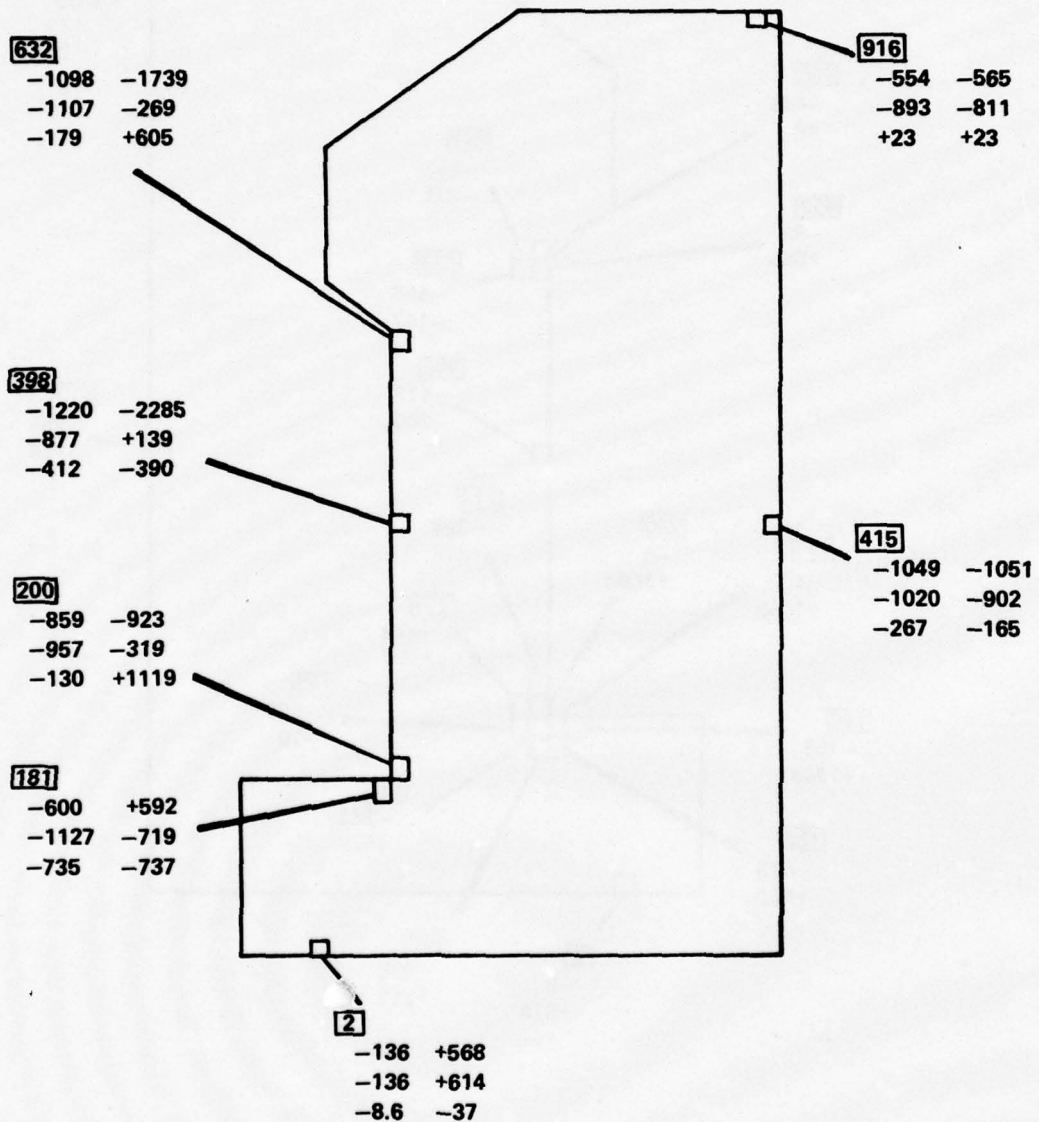


FIG. 3.4 STATIC STRESSES IN SENSITIVE ELEMENTS OF PCRV MODEL (PSI) .

LEGEND

ELEMENT

1250 PSI RESPONSE

2500 PSI RESPONSE

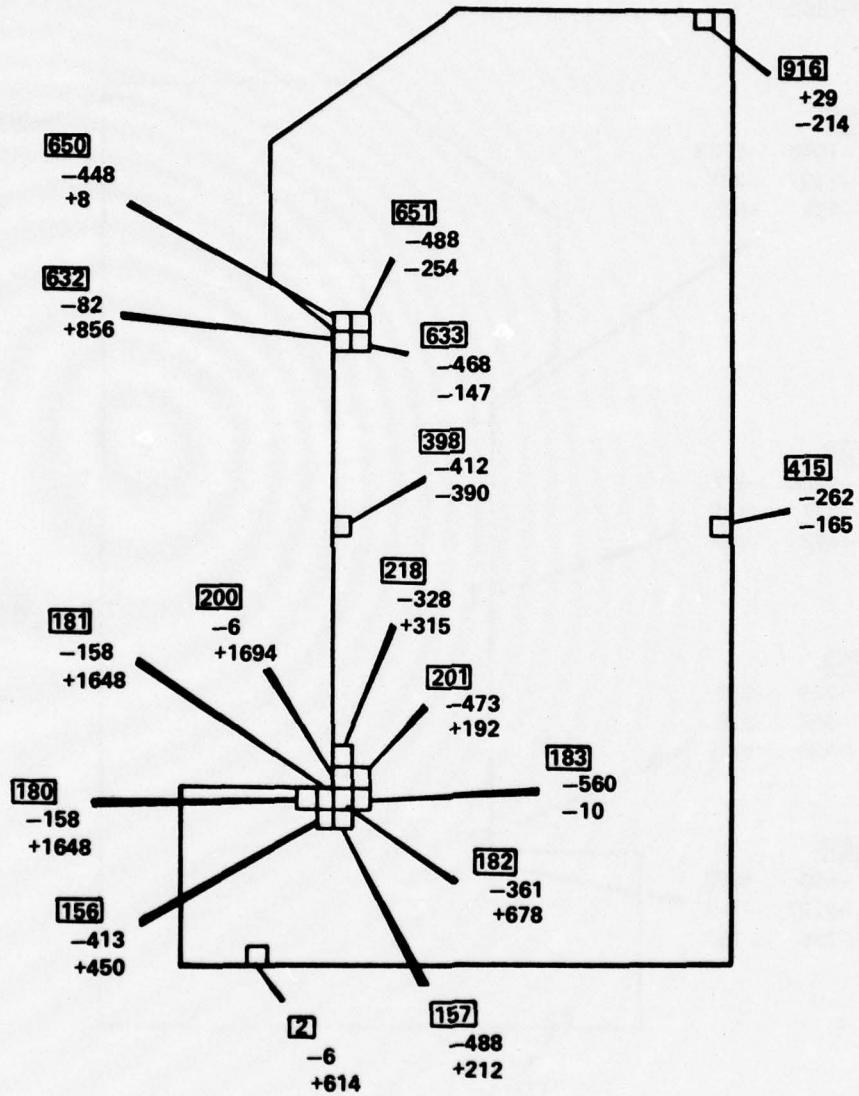


FIG. 3.5. MAXIMUM PRINCIPAL STRESSES IN SENSITIVE ELEMENTS OF PCRV MODEL (PSI).

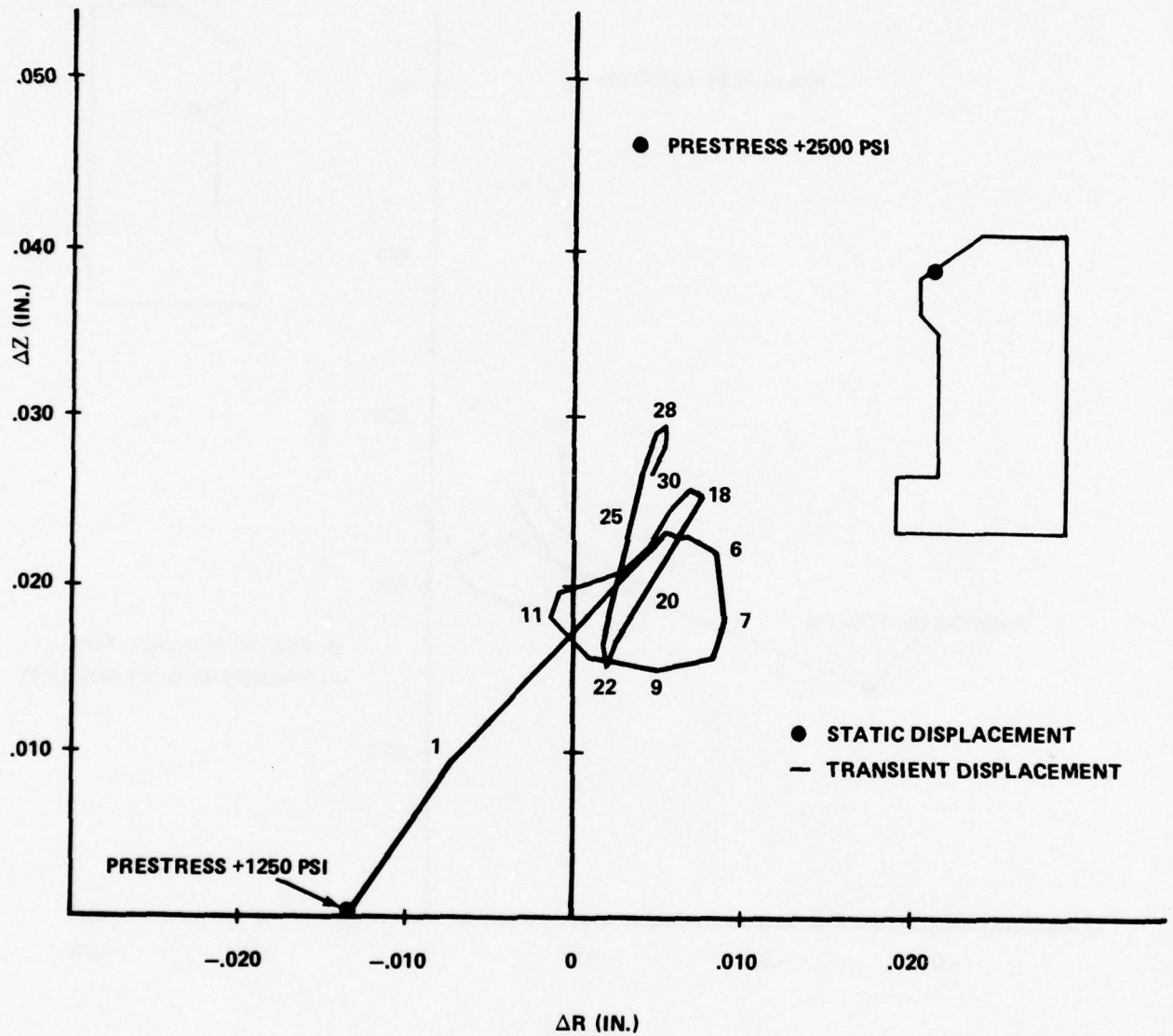


FIG. 3.6. DISPLACEMENT OF GRID POINT 3001; TRANSIENT LOAD.

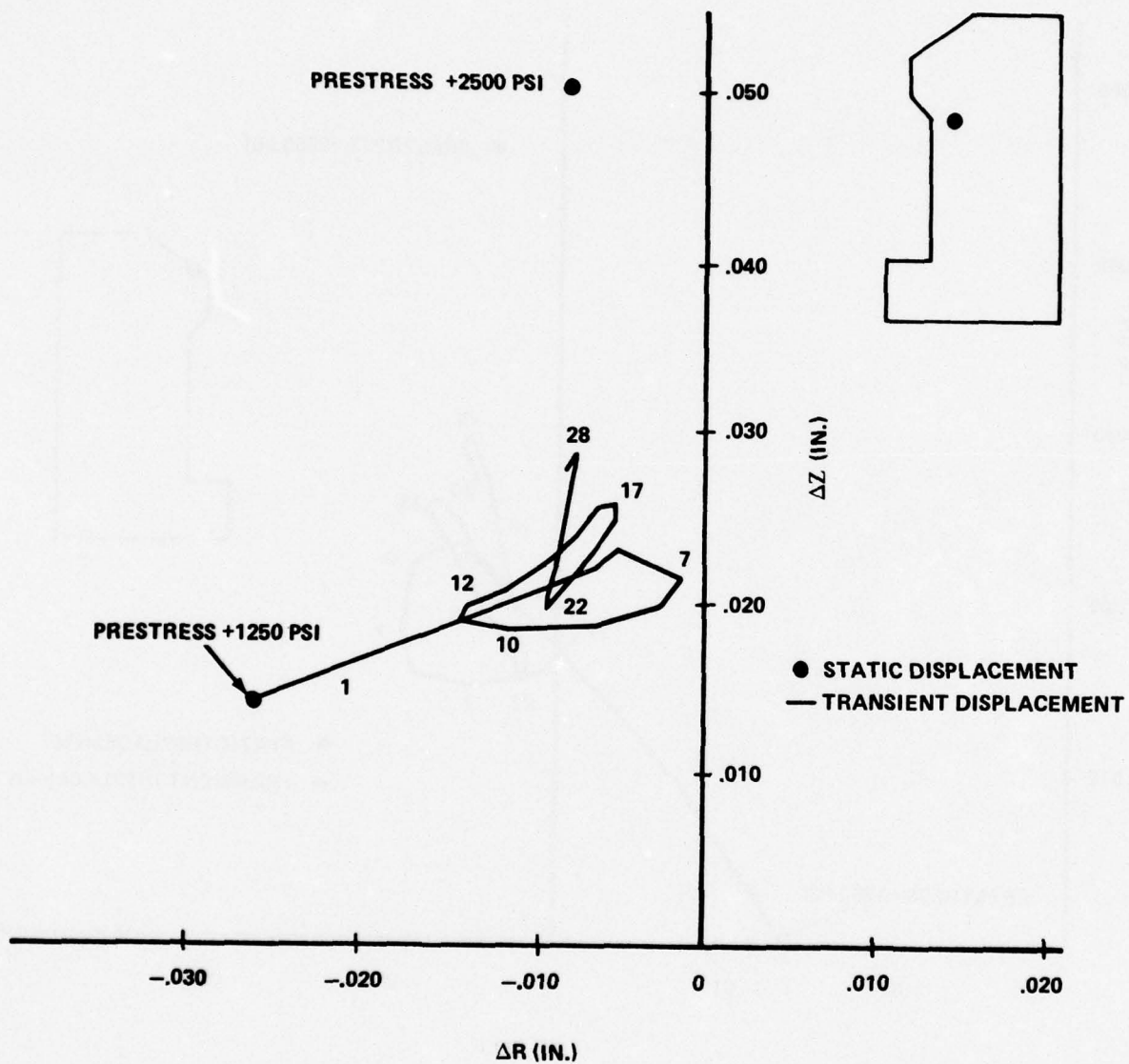


FIG. 3.7 DISPLACEMENT OF GRID POINT 692; TRANSIENT LOAD.

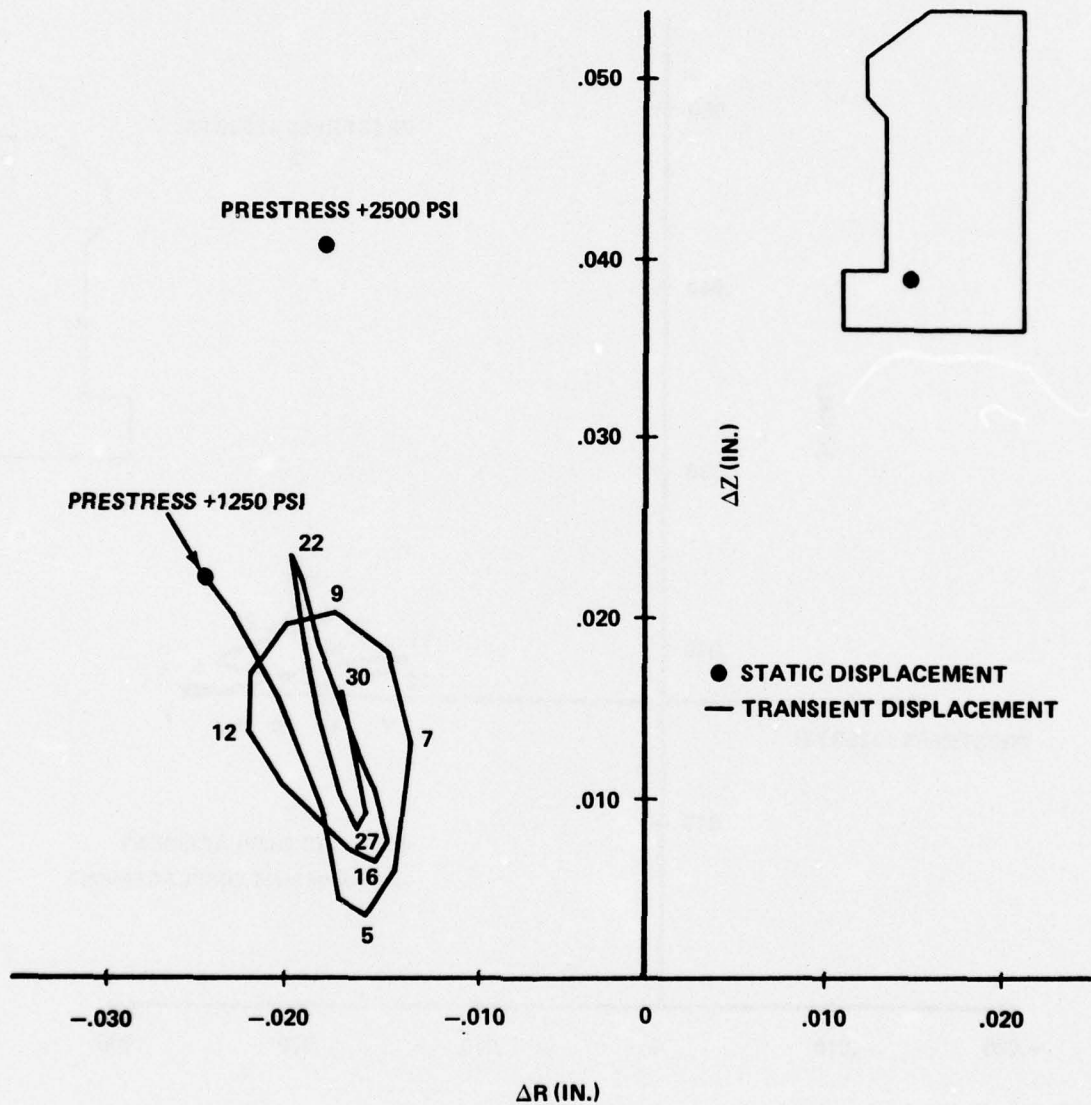


FIG. 3.8 DISPLACEMENT OF GRID POINT 165; TRANSIENT LOAD.

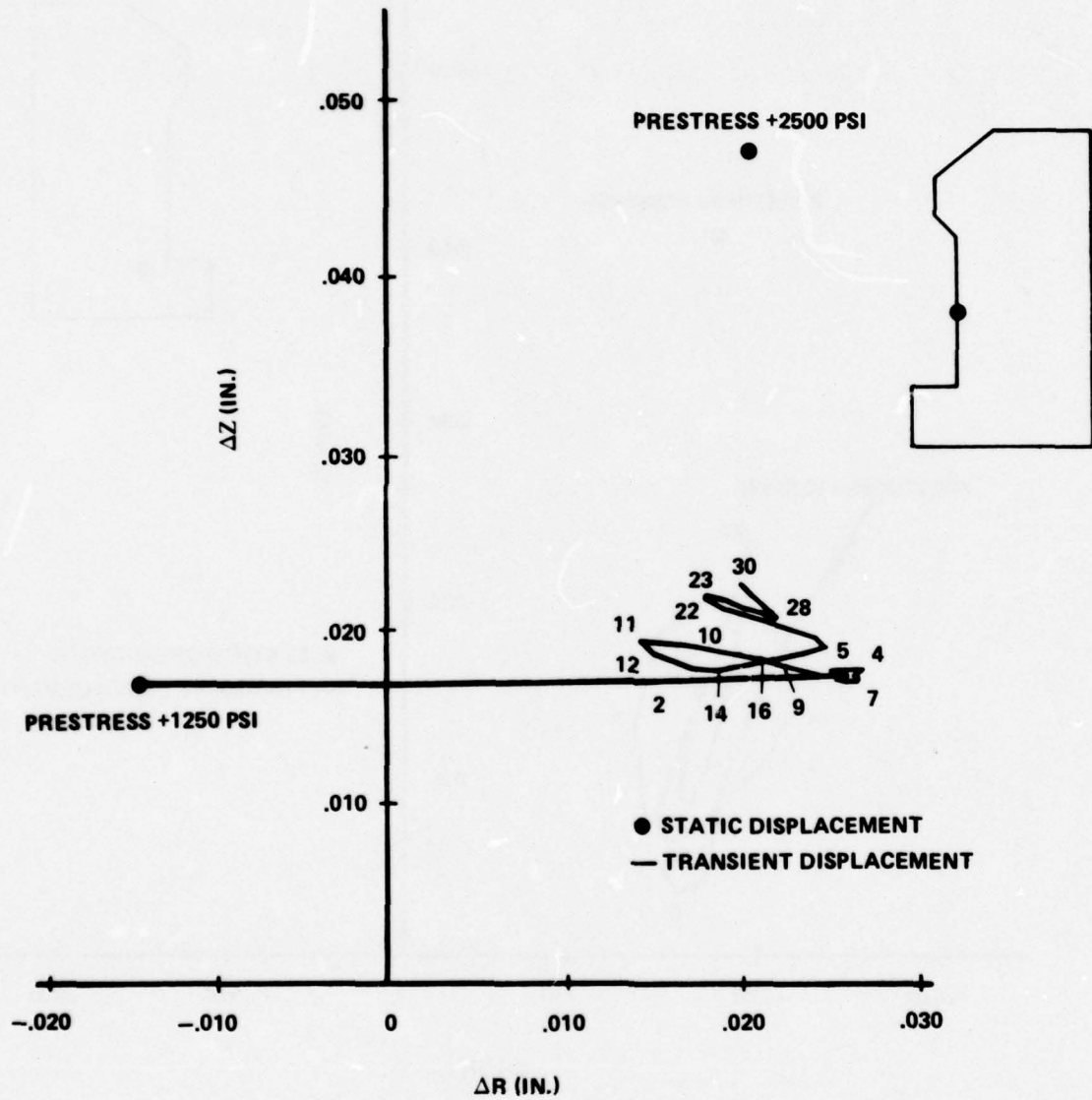


FIG. 3.9 DISPLACEMENT OF GRID POINT 501 UNDER TRANSIENT LOAD.

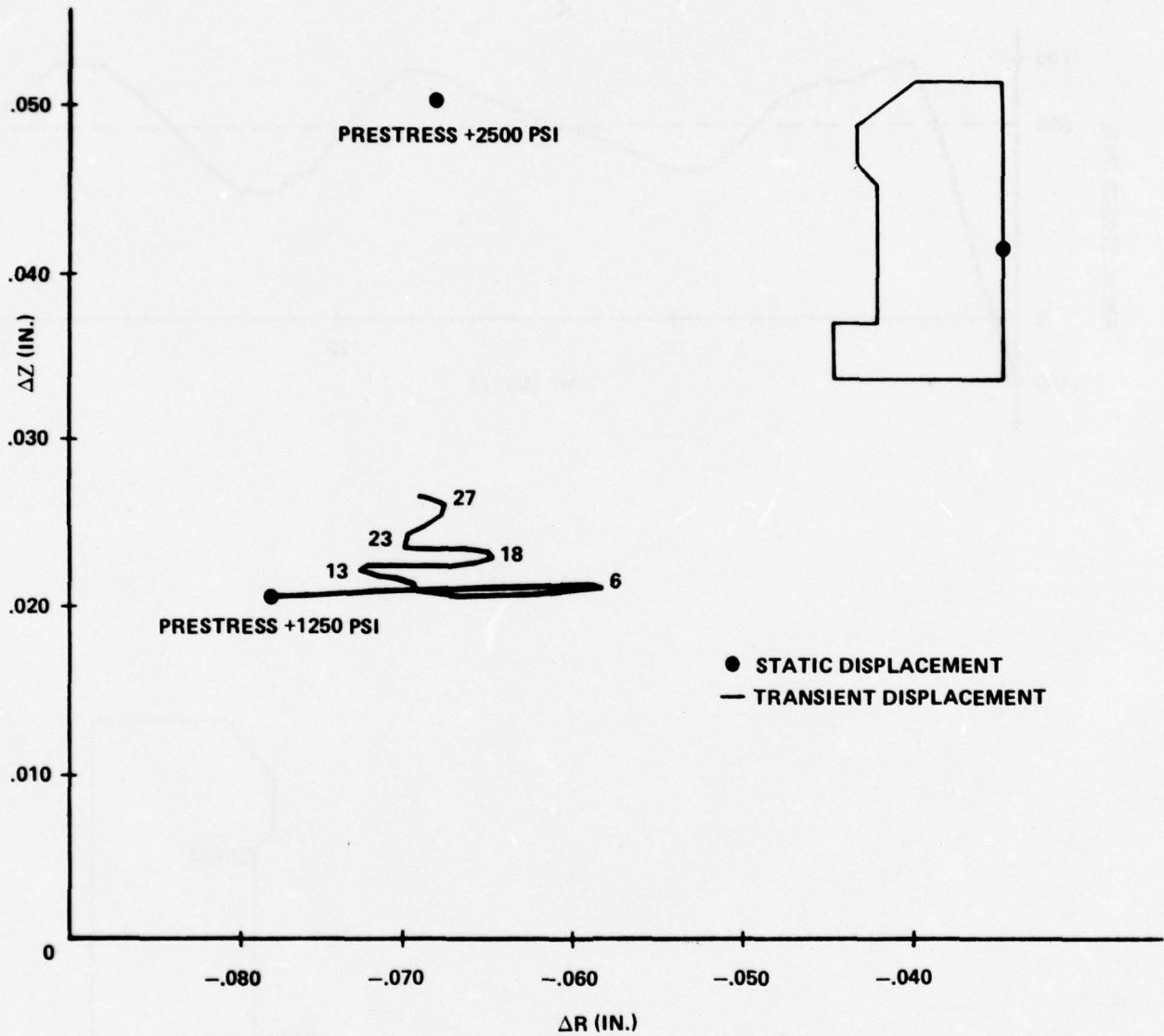


FIG. 3.10 DISPLACEMENT OF GRID POINT 519; TRANSIENT LOAD.

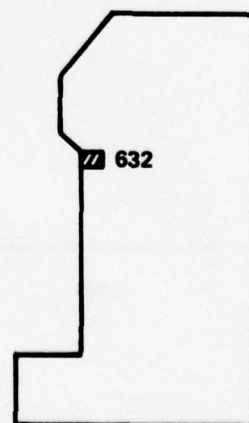
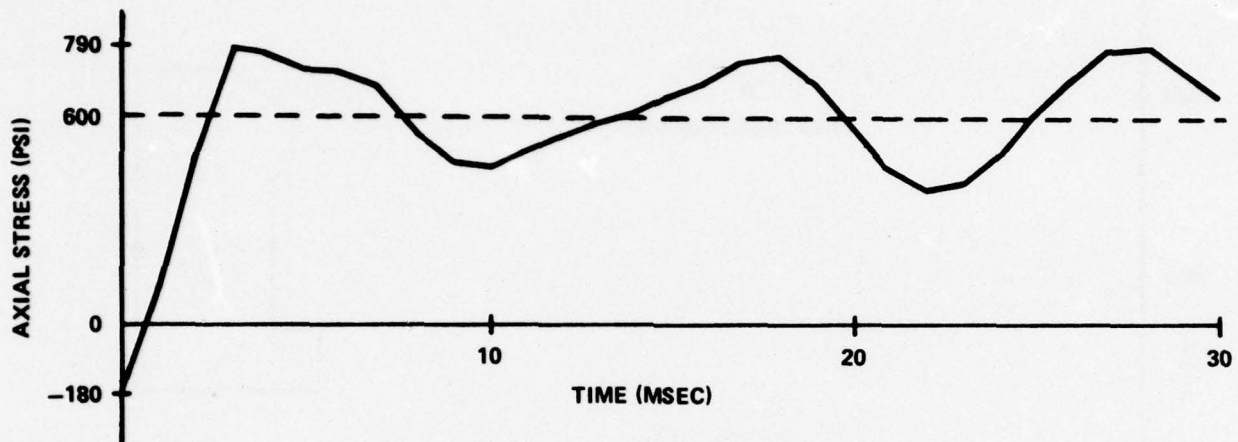


FIG. 3.11 STRESS VS. TIME, UPPER HAUNCH 1250 PSI 'STEP' LOAD.

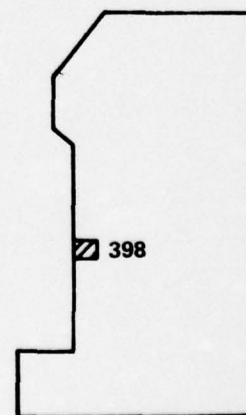
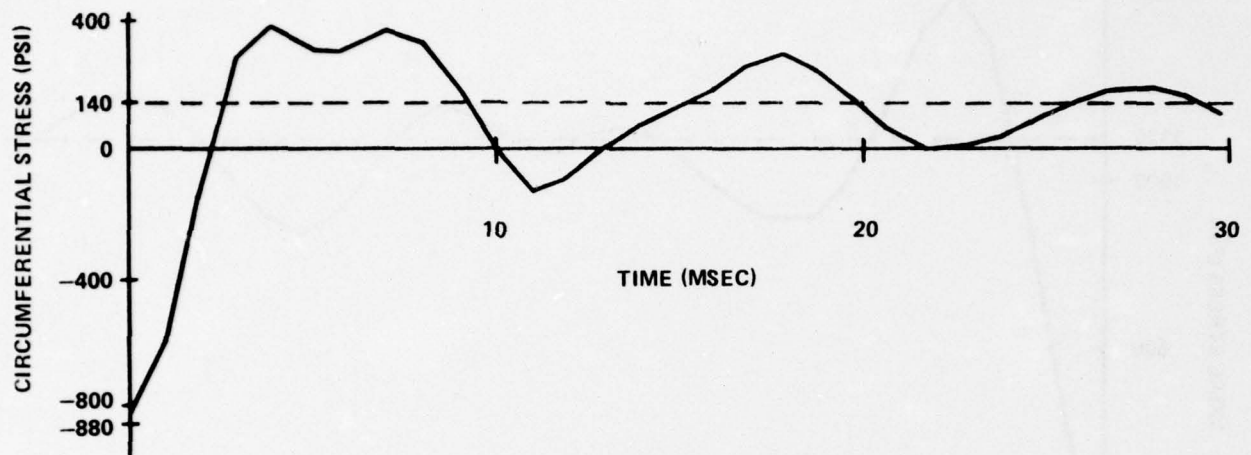


FIG. 3.12 STRESS VS. TIME, MID HEIGHT OF BARREL 1250 PSI 'STEP' LOAD.

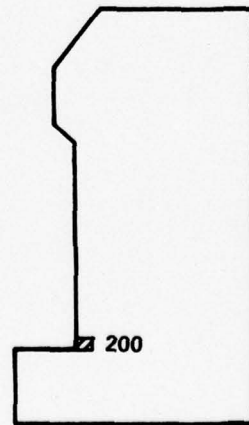
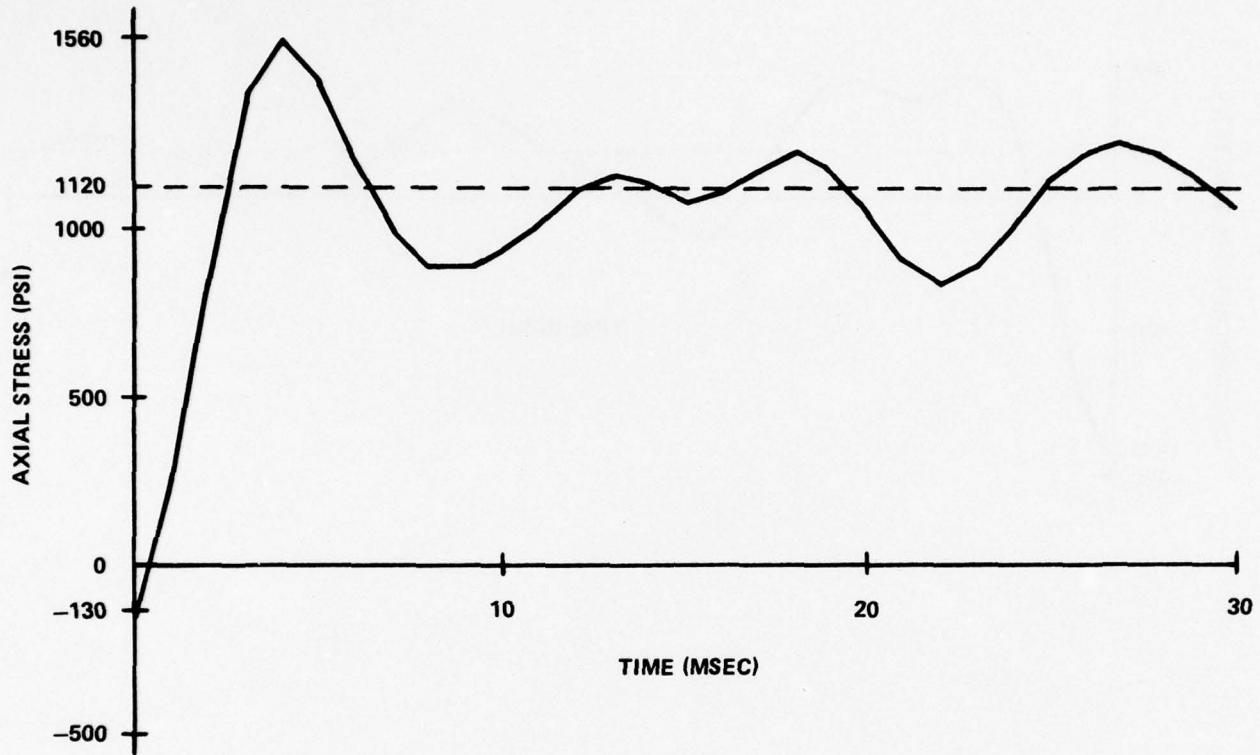


FIG. 3.13 STRESS VS. TIME, BARREL, BOTTOM HAUNCH 1250 PSI 'STEP' LOAD.

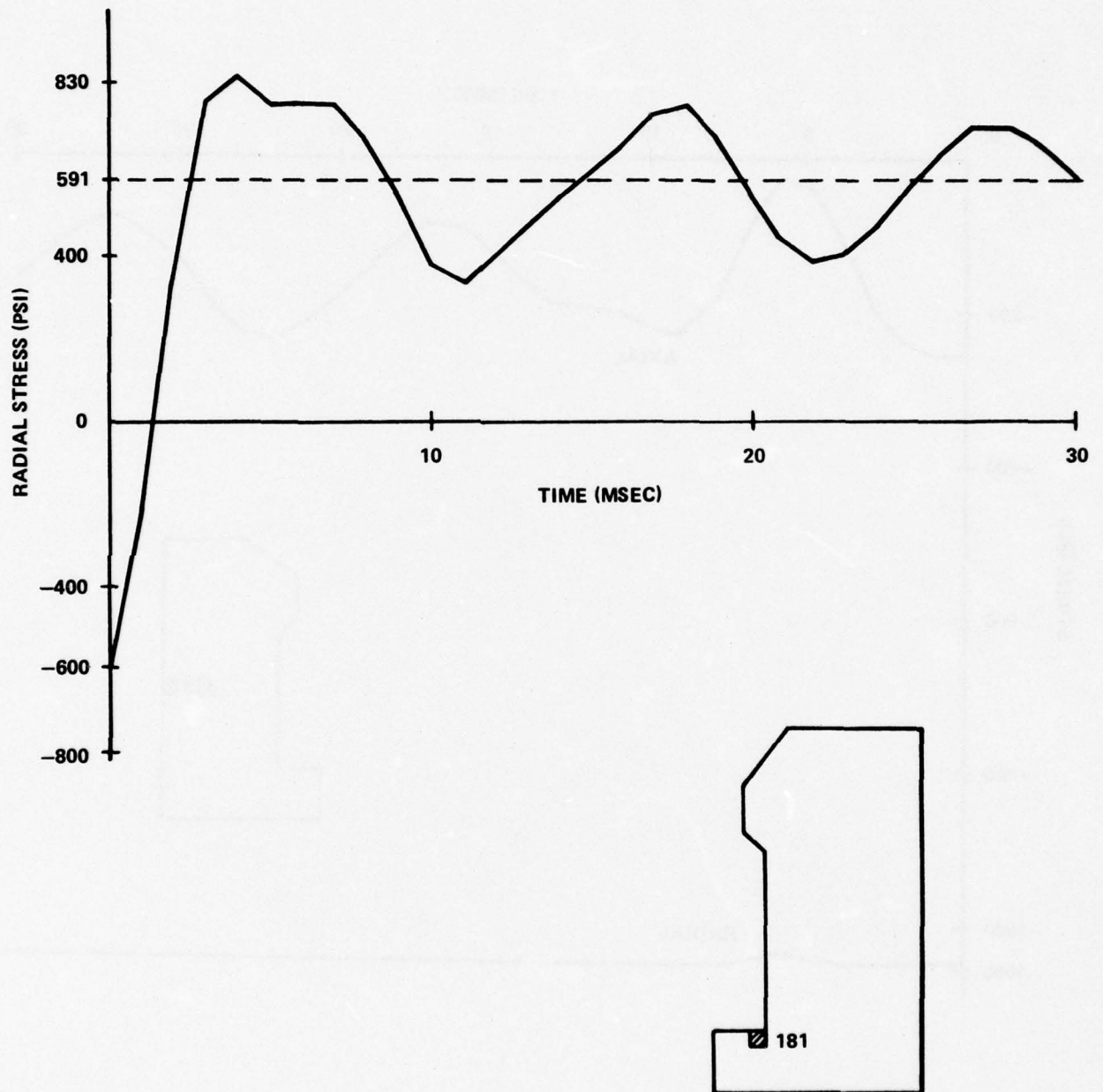


FIG. 3.14 STRESS VS. TIME, BOTTOM HEAD, HAUNCH 1250 PSI 'STEP' LOAD.

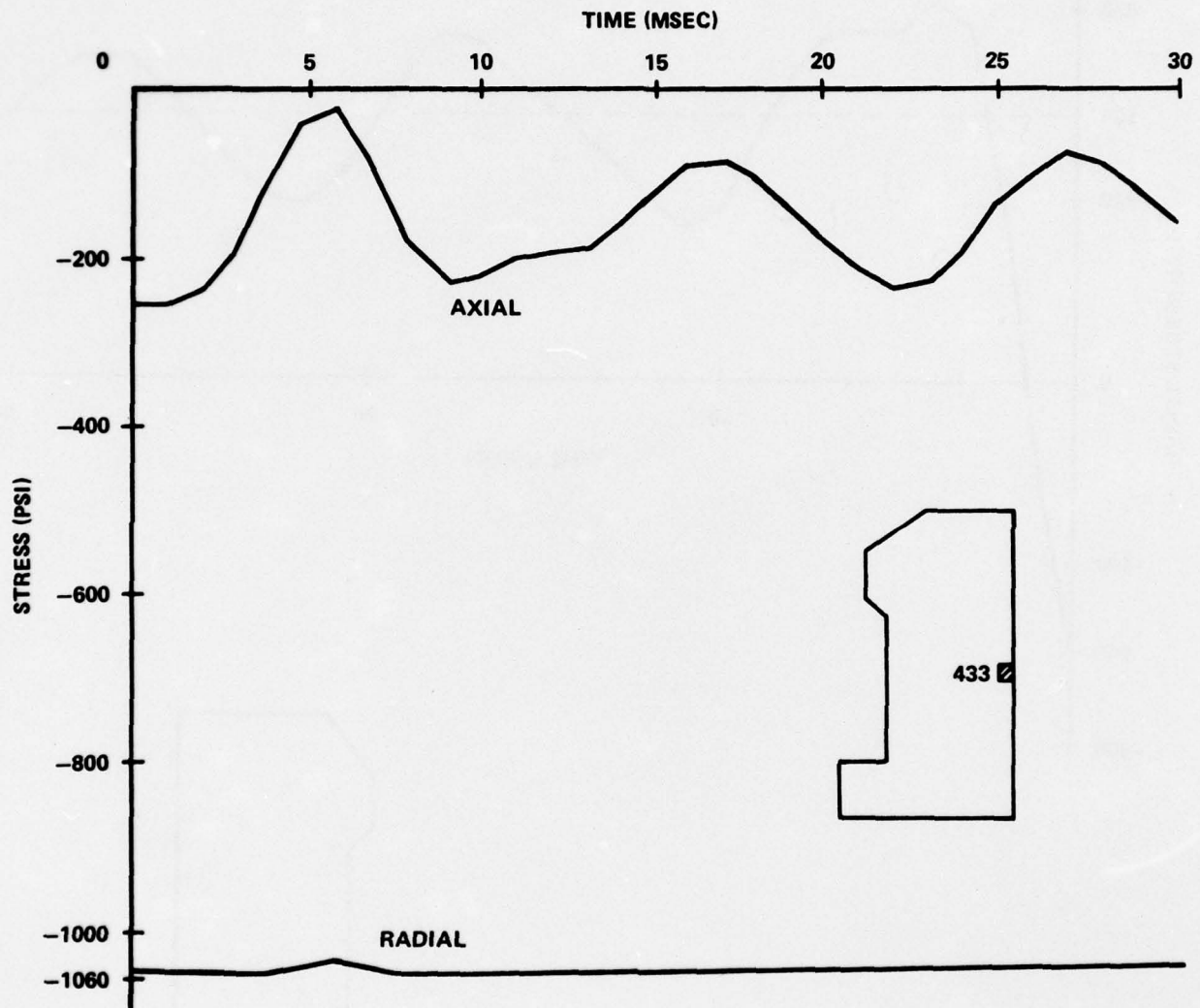


FIG. 3.15 AXIAL AND RADIAL STRESSES AT OUTER SURFACE.

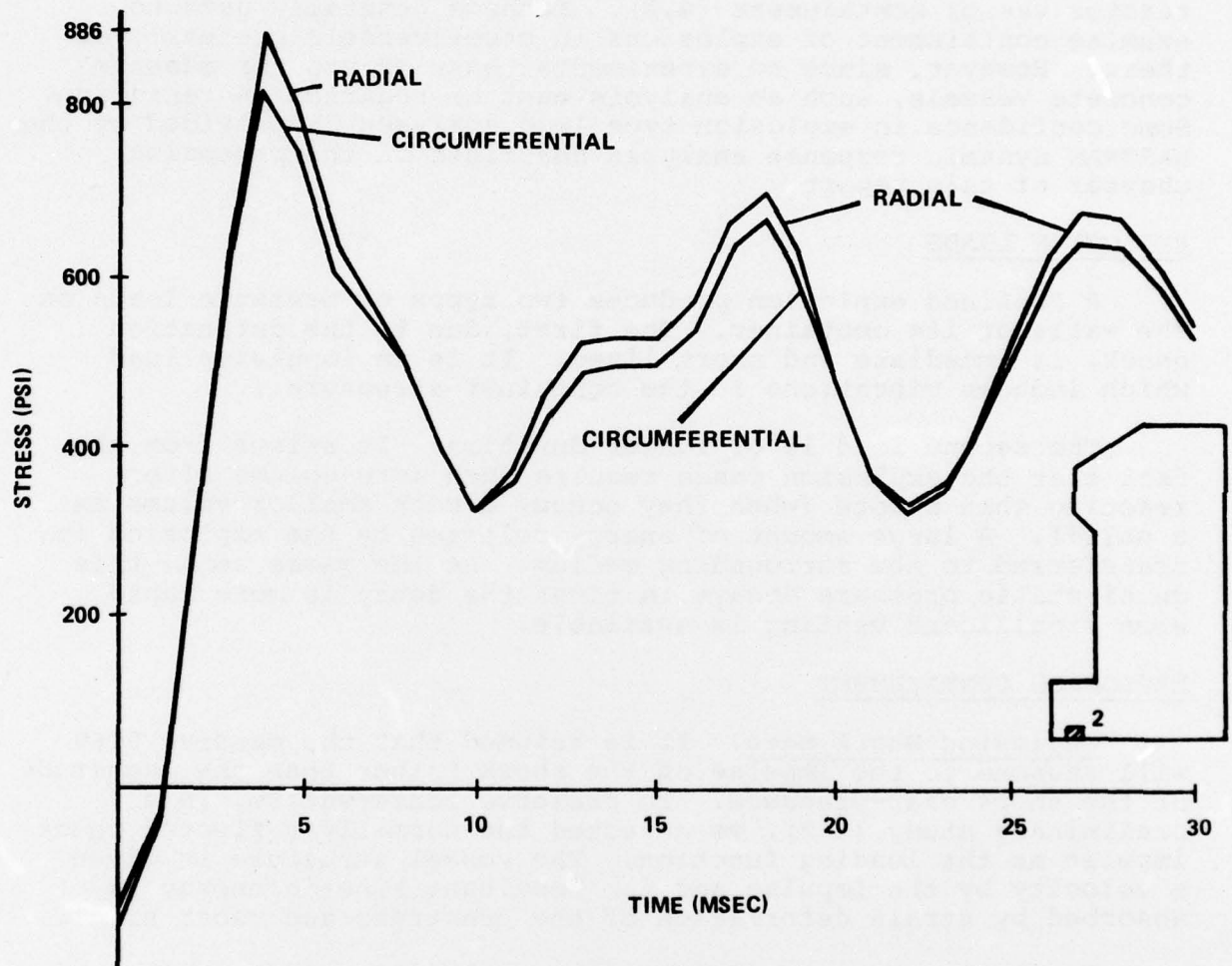


FIG. 3.16 RADIAL AND CIRCUMFERENTIAL STRESS IN BOTTOM HEAD.

IV. CONTAINMENT CAPABILITY

Because no postulated accident energy release has yet been established for the GCFR system, explosion releases become a conservative mechanism for estimating the containment potential of the PCRV. The conservatism of explosion-type releases in this application has been demonstrated in experimental work on reactor vessel containment (4.1). Methods generally used to examine containment of explosions in steel vessels are employed there. However, since no experimental base exists for massive concrete vessels, such an analysis must be regarded as tentative. Some confidence in explosion-type load analyses is provided by the NASTRAN dynamic response analysis described in the preceding chapter of this report.

EXPLOSION LOADS

A confined explosion produces two types of pressure loads on the walls of its container. The first, due to the detonation shock, is immediate and short lived. It is an impulsive load which induces vibrations in the container structure.

The second load is of longer duration. It arises from the fact that the explosion gases require much more volume after reacting than before (when they occupy a much smaller volume as a solid). A large amount of energy released by the explosion is transferred to the surrounding medium. As the gases cool, this quasi-static pressure decays in time; the decay is more rapid when significant venting is available.

EXPLOSION CONTAINMENT

Explosion Shock Wave. It is assumed that the massive PCRV will respond to the impulse of the shock rather than the magnitude of the shock over-pressure. To preserve conservatism, in a preliminary study (4.2), we selected the normally reflected shock impulse as the loading function. The vessel structure is given a velocity by the impulse and the resultant kinetic energy is absorbed by strain deformation of the prestress and rebar steel.

To obtain an upper limit on the explosive weight which, when detonated at the center of the reactor cavity, will produce failure, yielding of the prestress and rebar steel was defined as failure. In the cylindrical portion of the PCRV, the reflected

-
- (4.1) Wise, W. R., Jr. and Proctor, J. F., "Explosion Containment Laws for Nuclear Reactor Vessels," NOLTR 63-140 (Aug 1965).
 - (4.2) Atomic Energy Commission, "Preapplication Safety Evaluation of the Gas Cooled Fast Breeder Reactor," Directorate of Licensing, Project 456 (1 Aug 1974).

shock impulse from a 20,000 lb TNT charge would be required to bring the circumferential prestress to yield. On the bottom surface of the cavity, the reflected impulse from a 4000 lb TNT charge would be required to bring the vertical prestress tendons to yield (4.2).

Quasistatic Pressure. The over-pressure produced in the PCRV long after the reaction of various weights of TNT is shown in Figure 4.1. The curves are drawn through points calculated by INBLAST (4.3) for two cases: with and without venting to the circulator cavities from the main reactor cavity.

Assuming that the PCRV can withstand a quasistatic over-pressure equal to the operating pressure (that is, a total pressure equal to twice operating pressure, or 2500 psi), two charge sizes can be determined from these curves. If all the gases were contained within the reactor cavity, reaction of a 2000 lb TNT charge will produce an over-pressure of 1250 psi in the reactor cavity.

If the gaseous explosion products are allowed to vent into the six satellite cavities, then, reading from the lower curve in Figure 4.1, a 7500 lb TNT charge would be required to produce an over-pressure of 1250 psi throughout all the cavities.

DYNAMIC LOADS

NASTRAN calculations were described in the preceding chapter for a variety of load cases. In particular, a pulse from operating pressure of 1250 psi to 2500 psi, with 0.1 msec rise time and no decay, was applied to the inner walls of the main reactor cavity. Venting to the satellite circulator cavities was not included in the finite element model.

Elastic Limit. With this transient loading, the greatest peak tensile stress was found in element 200 at the lower haunch to be about 1560 psi in the axial direction. Since element stresses are directly proportional to load in an elastic structure, the load which would produce the limiting tensile stress (+600 psi) in this element can be determined by equating the ratios of stresses to loads for the two stress levels.

For a static 1250 psi operating pressure cavity load combined with the static prestress loads, the compressive axial stress in this element was -130 psi. When the transient 1250 psi load was

-
- (4.2) Atomic Energy Commission, "Preapplication Safety Evaluation of the Gas Cooled Fast Breeder Reactor," Directorate of Licensing, Project 456 (1 Aug 1974).
 - (4.3) Proctor, J. F., "Internal Blast Damage Mechanisms Computer Program," NOLTR 72-231 (Aug 1972).

applied (to the inner walls of the reactor cavity) the stress became +1560 psi. The transient pressure amplitude which would produce a +600 psi tensile stress in the same element is determined from the following linear proportion:

$$\frac{600 - (-130)}{1560 - (-130)} = \frac{\Delta P}{1250}$$

or:

$$\Delta P = 1250 \frac{730}{1690} = 540 \text{ psi}$$

Consulting Figure 4.1 we find that a TNT charge of 700 lb would produce this peak shock over-pressure.

Partial Cracking Limit. Figure 3.5 shows the principal stresses produced by a static 2500 psi cavity pressure load. From this Figure it is apparent that large stresses are found only at the PCRV cavity surfaces. Localized cracks occur which probably will not penetrate deeply into the concrete. Considering the elements in the second rows away from the cavity wall we find that the highest principal stress occurs in element 156 in the bottom head at the haunch. Unfortunately, the dynamic response stress for this element is unavailable. However, it is reasonable to assume that the peak radial stress in this element will be of the same order of magnitude as the maximum static principal stress found in the element. This is true for element 200 as discussed above.

So, if local cracking in the elements closest to the cavity is distributed by the rebar, then severe damage to the PCRV will not occur at least until the second layer of elements experiences stresses approaching the tensile strength of concrete: +600 psi. Considering element 156 specifically, the ratio used above for element 200 results in the following allowable cavity pressure:

$$\frac{600 - (-130)}{400 - (-130)} = \frac{\Delta P}{1250}$$

or:

$$\Delta P = 1250 \frac{730}{530} = 1722 \text{ psi.}$$

Again consulting Figure 4.1, we find that this peak over-pressure would be produced by detonation of a 2600 lb TNT charge at the center of the unvented reactor cavity.

ACCIDENT CONTAINMENT CAPABILITY

In the preceding section a number of limiting TNT charge weights were determined. Each is an estimate of the explosion

size which can be contained by the PCRV according to a particular failure criterion for a specific load condition. There remains the question of determining the largest among these charge weights which can be safely contained by the proposed PCRV. Further, once the charge weight is chosen it must be interpreted in terms of core disruptive accident severity.

Safe Explosive Weight. The many cases discussed in the preceding section are summarized in the following list:

Shock impulse --- circumferential prestress yield;
Limit: 20,000 lb TNT

Shock impulse --- vertical prestress tendon yield;
Limit: 4000 lb TNT

2500 psi quasistatic pressure, no venting;
Limit: 2000 lb TNT

2500 psi quasistatic pressure, venting to circulators;
Limit: 7500 lb TNT

Dynamic elastic limit: no concrete cracks;
Limit: 700 lb TNT

Dynamic limit: modest cracks at lower haunch;
Limit: 2600 lb TNT

It is obvious from this list that the PCRV will certainly contain the explosion of a 700 lb TNT charge while experiencing only elastic structural deformations. The vessel should remain intact under this loading --- no significant cracks should appear at any point.

However, if shallow cracks in the lower haunch region on the wall of the reactor cavity are allowed, then the PCRV will safely contain at least a 2000 lb TNT charge. None of the contents of the reactor will be vented to the atmosphere if a charge of this weight is detonated at the center of the main reactor cavity.

Equivalent Accident Severity. Expressing pounds of TNT in terms of reactor accident severity depends on the definition of energy release. If an accident is defined in terms of thermal energy release, 1 lb of TNT is equivalent to about 2 MWsec (4.4). If the accident is defined in terms of available work energy, the conversion is more like 1 lb of TNT representing 1 MWsec.

-
- (4.4) Proctor, J. F., "Adequacy of Explosion Response Data in Estimating Reactor Vessel Damage," Nuclear Safety 8 (6) 565 (1967).

Therefore, based on the NASTRAN and INBLAST calculations, it appears that the containment capability of the proposed GCFR PCRVR is probably in the vicinity of 4000 MWsec rapid thermal energy release with no venting of hot gases to the circulator cavities.

Venting will reduce the rise time of the initial pressure pulse, as well as the quasistatic pressure ultimately reached in the cavities. Rebar will prevent the spread of local cracks, further extending the capability of the PCRVR to contain a reactivity accident.

In addition, it should be noted that the reactor cavity is not completely empty in an operating reactor. The reactor core, thermal insulation blankets, fuel control rods, and other hardware will tend to lengthen the rise time of the shock pulse by diffracting it.

Thus, 4000 MWsec is a conservative estimate of the accident containment capability of this proposed PCRVR.

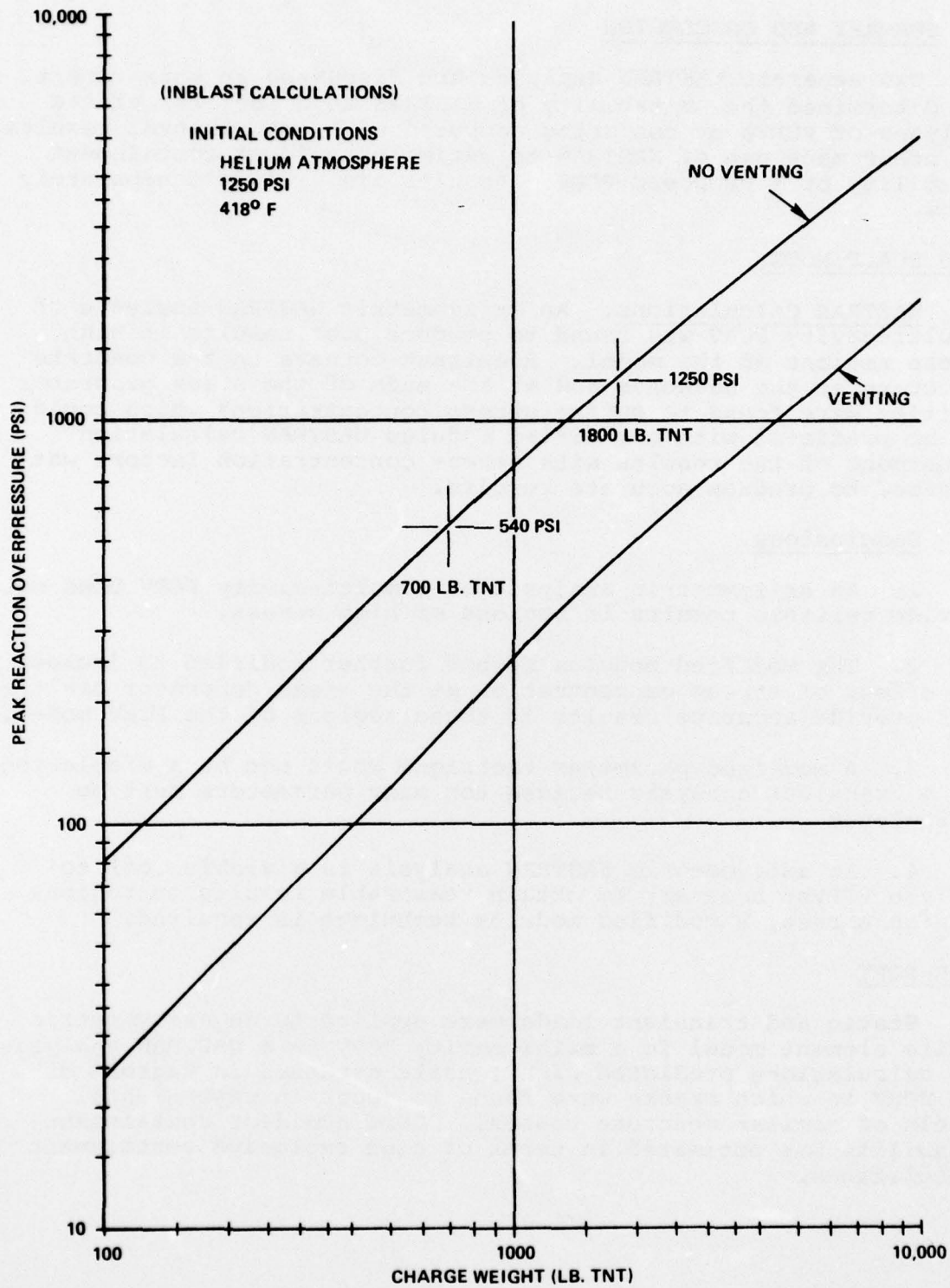


FIG. 4.1 PEAK REACTOR CAVITY OVERPRESSURE VS. TNT CHARGE WEIGHT.

V. SUMMARY AND CONCLUSION

Two separate NASTRAN analyses are discussed in this report. One determined the suitability of NASTRAN as a tool for static analyses of PCRVs by comparing computed with experimental results. The other made use of NASTRAN to estimate accident containment capability of a proposed PCRV. Results are discussed separately below.

1/20 SCALE MODEL

NASTRAN Calculations. An axisymmetric NASTRAN analysis of a multi-cavity PCRV was found to produce poor results in high stress regions of the model. Reentrant corners in the concrete structure at the haunches and at the ends of the steam generator cavities were found to suffer stress concentrations which could not be predicted with a modified modulus NASTRAN calculation. Adjustment of the results with stress concentration factors was required to produce accurate results.

Conclusions.

1. An axisymmetric analysis of a multi-cavity PCRV does not provide reliable results in regions of high stress.
2. The modified modulus method further modified to include the effect of stress concentration at the steam generator cavities does provide accurate results in those regions of the PCRV model.
3. A modified parameter technique would not be a viable tool for a transient analysis because too many parameters must be manipulated.
4. An axisymmetric NASTRAN analysis is a viable tool to analyze PCRVs; however, to obtain reasonable results in regions of high stress, a modified modulus technique is required.

GCFR-PCRv

Static and transient loads were applied to an axisymmetric finite element model for a multi-cavity PCRV in a NASTRAN analysis. The calculations predicted high tensile stresses in regions of the PCRV in which cracks were found to occur in experimental models of similar concrete vessels. Core accident containment capability was estimated in terms of high explosive containment calculations.

Conclusions.

NASTRAN Calculations. The two haunches and the bottom head are the regions of the vessel most likely to exhibit cracking when the PCRV is subjected to a static or transient cavity pressure load. High tensile stresses produced by static loads in these regions were exceeded by peak stresses produced by a transient cavity over-pressure step from operating pressure to twice operating pressure. Displacements of prestress tendon anchor points were intuitively acceptable, and not large enough to induce cracks or leaks around the cavity plug seals.

NASTRAN is an acceptable tool for determining threshold pressure levels and crack susceptible regions of a PCRV structure subjected to static and dynamic cavity over-pressure loads. However, at the present stage of development of NASTRAN it is impossible to include every detail of the construction of a PCRV in the finite element model.

Accident Containment. Explosion containment capacity of the PCRV was estimated on the basis of equilibrium calculations of quasistatic pressure in the closed vessel, with and without venting of the hot gases to the circulator cavities. The equivalent reactivity accident severity was then determined by taking 1 lb of TNT to be equivalent to an accidental thermal energy release of 2MWsec.

Allowing shallow crack penetration into the concrete at the lower haunch and requiring all gases to be contained in the reactor cavity, the PCRV should be able to withstand a 4000 MWsec accident (2000 lb TNT). This estimate is conservative because it is based on no venting of a transient pulse having a 0.1 msec rise time (much less than the rise time of a pulse associated with a reactor accident.)

If a longer rise time for the loading pulse is assumed, then containment capability will increase. For example, a rise time greater than about 3 msec (1/4 of the period of the lowest structural resonance) would cause a slow, near-static response with little or no overshoot to a large peak. Thus, peak stresses would be lower for a given energy release. The accident energy release for which damage occurs would be higher. We are confident that the PCRV will contain a 2000 lb TNT explosion (4000 MWsec) with only modest local cracking; if more severe damage is allowed, the PCRV may contain up to 15000 or 20000 lb of TNT. Experimental confirmation is required.

LIST OF REFERENCES

- 1.1 Penzien, J. and Hansen, R. J., "Static and Dynamic Elastic Behavior of Reinforced Concrete Beams", J. Am. Concrete Inst. 25 545 (Mar 1954).
- 1.2 Tan, C. P., "Prestressed Concrete in Nuclear Reactor Vessels: A Critical Review of Current Literature", Oak Ridge National Laboratory, ORNL 4227 (May 1968).
- 1.3 Corum, J. M. and Smith, J. E., "Use of Small Models in Design and Analysis of Prestressed Concrete Reactor Vessels", Oak Ridge National Laboratory, ORNL 4346 (May 1970).
- 1.4 Karlsson, B. I. and Sozen, M. A., "Shear strength of End Slabs with and without Penetrations in Prestressed Concrete Reactor Vessels", Univ. of Ill., ORNL Contract No. W-7405-eng-26, Subcontract No. 2906, (Jul 1971).
- 1.5 McCormick, C. W., "The NASTRAN User's Manual, Level 15", NASA SP-222(01) (Jun 1972).
- 1.6 Atomic Energy Commission, "Preapplication Safety Evaluation of the Gas Cooled Fast Breeder Reactor", Directorate of Licensing, Project 456 (1 Aug 1974).
- 2.1 Davies, I., Franklin, R. N. and Gotschall, H. L., "Model Studies of a Multicavity PCRV for 1000 MW(e) HTGR System", General Atomic Co., GA-P-1002-33 (Feb 1970).
- 2.2 Cheung, K. C., "PCRV Design Verification", General Atomic Company, San Diego, GA-A-12821 (GA-LTR-8) (Mar 1974).
- 2.3 Wistrom, J. D. and Bisset, J. R., "Simplified Elastic Analysis of Cylindrical Multicavity PCRVs", General Atomic Co., GA-B-12171 (Oct 1973).
- 2.4 Cornell, D. C., "SAFE-2D: A Computer Program for the Stress Analysis of Plane and Axisymmetric Composite Structures", Gulf General Atomic Report GA-9076 (12 Feb 1969).
- 3.1 General Atomic Company, "Preliminary Safety Information Document (PSID) for the Gas Cooled Fast Breeder Reactor (GCFR)", Volumes I and II, San Diego, CA, Ga 10928 (Feb 1971).
- 4.1 Wise, W. R., Jr. and Proctor, J. F., "Explosion Containment Laws for Nuclear Reactor Vessels", NOLTR 63-140 (Aug 1965).

REFERENCES (Cont.)

- 4.2 Atomic Energy Commission, "Preapplication Safety Evaluation of the Gas Cooled Fast Breeder Reactor", Directorate of Licensing, Project 456 (1 Aug 1974).
- 4.3 Proctor, J. F., "Internal Blast Damage Mechanisms Computer Program", NOLTR 72-231 (Aug 1972).
- 4.4 Proctor, J. F., "Adequacy of Explosion Response Data in Estimating Reactor Vessel Damage", Nuclear Safety 8 (6) 565 (1967).

NSWC/WOL/TR 77-42

DISTRIBUTION

Copies

Defense Documentation Center
Cameron Station
Alexandria, VA 22314

12

Oak Ridge National Laboratory
Oak Ridge, TN 37830
Attn: P. Callahan
W. Dodge
Technical Library

General Atomic Corporation
San Diego, CA 92112
Attn: D. Buttemer
Technical Library

Nuclear Regulatory Commission
Washington, D. C. 20555
Attn: P. M. Williams, DPM

40

Energy Research and Development Administration
Washington, D. C. 20545
Attn: Technical Library

TO AID IN UPDATING THE DISTRIBUTION LIST
FOR NAVAL SURFACE WEAPONS CENTER, WHITE
OAK LABORATORY TECHNICAL REPORTS PLEASE
COMPLETE THE FORM BELOW:

TO ALL HOLDERS OF NSWC/WOL/TR 77-42
by Joseph G. Connor, Jr., Code WR-15
DO NOT RETURN THIS FORM IF ALL INFORMATION IS CURRENT

A. FACILITY NAME AND ADDRESS (OLD) (Show Zip Code)

NEW ADDRESS (Show Zip Code)

B. ATTENTION LINE ADDRESSES:

C.

☐ REMOVE THIS FACILITY FROM THE DISTRIBUTION LIST FOR TECHNICAL REPORTS ON THIS SUBJECT.

D.

NUMBER OF COPIES DESIRED _____

DEPARTMENT OF THE NAVY
NAVAL SURFACE WEAPONS CENTER
WHITE OAK, SILVER SPRING, MD. 20910
OFFICIAL BUSINESS
PENALTY FOR PRIVATE USE, \$300

POSTAGE AND FEES PAID
DEPARTMENT OF THE NAVY
DOD 316



COMMANDER
NAVAL SURFACE WEAPONS CENTER
WHITE OAK, SILVER SPRING, MARYLAND 20910
ATTENTION: CODE WR-15